(12) INTERNATIONAL APPLICATION PUBLISHED UNDER THE PATENT COOPERATION TREATY (PCT)

(19) World Intellectual Property Organization
International Bureau

(43) International Publication Date
19 August 2010 (19.08.2010)

PCT

(10) International Publication Number
WO 2010/094022 A1

(51) International Patent Classification:
G05B 19/4099 (2006.01) *B23H 7/06* (2006.01)

(21) International Application Number:
PCT/US2010/024274

(22) International Filing Date:
16 February 2010 (16.02.2010)

(25) Filing Language: English

(26) Publication Language: English

(30) Priority Data:
61/152,756 16 February 2009 (16.02.2009) US
61/304,565 15 February 2010 (15.02.2010) US

(71) Applicant *(for all designated States except US)*: **THE PENN STATE RESEARCH FOUNDATION** [US/US]; 304 Old Main, University Park, Pennsylvania 16802-7000 (US).

(72) Inventors; and

(75) Inventors/Applicants *(for US only)*: **WYSK, Richard A.** [US/US]; 111 Meadow Lark Lane, Boalsburg, Pennsylvania 16827 (US). **YANG, Zhi** [CN/US]; 711 West Cherry Lane, Apt. 2, State College, Pennsylvania 16803 (US). **JOSHI, Sanjay** [US/US]; 120 Pinewood Place, Port Matilda, Pennsylvania 16870 (US).

(74) Agent: **FISCHER, Ralph G.**; Buchanan Ingersoll & Rooney PC, 301 Grant Street, 20th Floor, Pittsburgh, Pennsylvania 15219 (US).

(81) Designated States *(unless otherwise indicated, for every kind of national protection available)*: AE, AG, AL, AM, AO, AT, AU, AZ, BA, BB, BG, BH, BR, BW, BY, BZ, CA, CH, CL, CN, CO, CR, CU, CZ, DE, DK, DM, DO, DZ, EC, EE, EG, ES, FI, GB, GD, GE, GH, GM, GT, HN, HR, HU, ID, IL, IN, IS, JP, KE, KG, KM, KN, KP, KR, KZ, LA, LC, LK, LR, LS, LT, LU, LY, MA, MD, ME, MG, MK, MN, MW, MX, MY, MZ, NA, NG, NI, NO, NZ, OM, PE, PG, PH, PL, PT, RO, RS, RU, SC, SD, SE, SG, SK, SL, SM, ST, SV, SY, TH, TJ, TM, TN, TR, TT, TZ, UA, UG, US, UZ, VC, VN, ZA, ZM, ZW.

(84) Designated States *(unless otherwise indicated, for every kind of regional protection available)*: ARIPO (BW, GH, GM, KE, LS, MW, MZ, NA, SD, SL, SZ, TZ, UG, ZM, ZW), Eurasian (AM, AZ, BY, KG, KZ, MD, RU, TJ, TM), European (AT, BE, BG, CH, CY, CZ, DE, DK, EE, ES, FI, FR, GB, GR, HR, HU, IE, IS, IT, LT, LU, LV, MC, MK, MT, NL, NO, PL, PT, RO, SE, SI, SK, SM,

[Continued on next page]

(54) Title: METHOD FOR RAPID PROTOTYPING

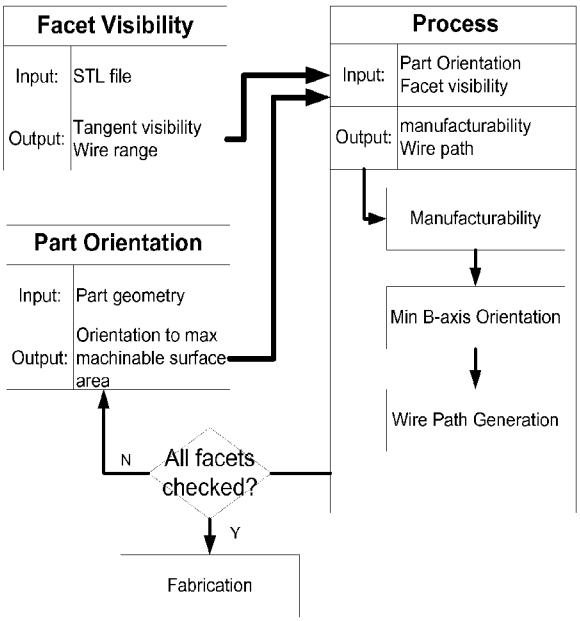

FIGURE 7

(57) Abstract: A method of rapid prototyping a product includes identifying a product geometry to prepare a geometric model, preparing a fabrication process, generating a cutting path; and fabricating the product using a linear cut process. Embodiments of the method may be embodied or practiced in rapid prototyping systems or computer systems. For example, a machining apparatus that includes at least one linear cutting mechanism, at least one input device, and at least one controller may be configured to implement one or more embodiments of the method.

WO 2010/094022 A1

TR), OAPI (BF, BJ, CF, CG, CI, CM, GA, GN, GQ, GW, ML, MR, NE, SN, TD, TG).

Declarations under Rule 4.17:

— *of inventorship (Rule 4.17(iv))*

Published:

— *with international search report (Art. 21(3))*

METHOD FOR RAPID PROTOTYPING

CROSS REFERENCE TO RELATED APPLICATION

The present application claims priority to U.S. Provisional Patent Application Serial No. 61/152,756, filed on February 16, 2009 and U.S. Provisional Patent Application Serial No. 61/304,565, filed on February 15, 2010. The entirety of U.S. Provisional Patent Application Serial No. 61/152,756 is incorporated herein by reference.

FIELD OF THE INVENTION

The present invention relates to rapid prototyping processes and manufacturing.

BACKGROUND OF THE INVENTION

Traditional rapid prototyping (RP) is also known as layered manufacturing or solid free form fabrication. RP is used for the physical modeling of a new product design where the object is obtained directly from computer aided design (CAD) model without the use of any special tooling or the need for costly process engineering. This rapid procedure reduces the lead time to produce a prototype of a product while improving the visualization ability due to its physical existence.

Even with the dramatic technology development during the last two decades, a majority of RP products cannot be used for producing end-use parts due to material limitations as well as manufacturing limitations such as surface finish, tolerances, process speed, repeatability, and cost effectiveness. The succeeding technologies, such as rapid tooling (RT) or rapid manufacturing (RM), intend to overcome the limitations that exist in production of end-use parts using rapid prototyping technologies. One of the major advantages of RP/RT/RM is the ability of the technologies to permit manufacture of an object, directly from CAD data input, without significant human intervention or skill. In order to overcome common limitations in RP/RT/RM,

researchers have focused on additive processes, those processes are considered as traditional RP processes, such as stereolithography, sheet lamination, laser sintering, adhesive bonding, drop deposition, etc. The generally used materials are powders, plastics, and paper, which are sufficient for concept models, but not for most mechanically functioning parts.

The fabrication of metallic parts using RP is still a challenge. Metallic materials, considered advanced materials for ready-to-use products, have caused difficulties in traditional RP processes. For instance, commonly used sintering processes often cannot produce fully dense parts; advanced systems like LENS and EBM have significantly higher costs than others and suffer from poor geometric accuracy and surface finish. Therefore, post-processing (typically using machining) is common, in order to provide better surface finishes and/or tight tolerances on critical features. It appears that significant attention has been given to the research and development of additive RP processes and very little attention has been given to conventional subtractive processes, such as milling process and wire electrical discharge machining (WEDM) for RP, even though conventional processes can handle wide variety of materials and produce end-use product with high accuracy.

There are no dominating processes for making rapid prototyped parts. From the nature of the manufacturing processes, irrespective of whether it is subtractive or additive, different processes may have their own innate advantages and disadvantages. Figure 1A and Figure 1B illustrates an example of two parts with different mass volume. The part in Figure 1A would require an excessive amount of machining to remove the material. This part however would be a reasonably efficient candidate for an additive RP process. On the other hand, for the part in Figure 1B an additive RP process will spend an excessive amount of time stacking simple layers, whereas the subtractive process would finish the part very quickly from a block of material.

RP technologies may be divided generally into additive processes and subtractive processes. The majority of RP research has focused on additive processes, and little effort has gone into subtractive techniques. RM technologies are introduced to ensure the long-term consistent component use for the entire production life cycle, one of the biggest chances and efforts are focused in the direct manufacture of long-term consistent metal parts. Six different RP principles are contending in direct metal parts fabrication. Figure 2 illustrate the basic technologies for metal components production relative to traditional manufacturing options. The cutting methodology and layer manufacturing, or in other word, the subtractive methodologies, occupies a large portion of the graph when quantity is relative low.

Conventional subtractive processes have been developed for years. The advantages of conventional subtractive processes are the accuracy and ability to handle diversity of materials, especially metallic materials, along with the low production time and cost associated with these methods.

The standard approach to plan parts for conventional machining is to define the "features" on the part, and match these features and tolerances to a set of processes that can create the required geometry to the specified accuracy. The current generation of CAD/CAM software has the ability to generate tool path automatically for simple geometries, and several software packages have made NC programming much easier and less labor-intensive. However, software still needs the user to select surfaces, features on the part and specify tool path strategies one by one. In most cases, the time required for planning the part, kitting the required tooling, design fixturing and setting up the machine has limited the use of CNC for RP parts.

U.S. Patent No. 6,021,358 to Sachs discloses traditional subtractive processes as rapid prototyping tools. Sachs describes a method of fabricating complex parts using CNC milling

machines. The part is divided into layers and each layer cut separately and then glued together to fabricate based on a computer generated model.

To achieve maximum utilization of the subtractive RP process and overcome the limitations associated with tool path generation, fixture design and tooling, research focusing on point contact mode has been investigated for years. However, some materials, such as titanium, stainless steel and cobalt alloy, e.g., materials that work hardened, are difficult to machine on milling process. To handle hard-to-mill metallic materials, new subtractive processes need to be investigated. As a non-traditional linear cutting process, Electrical Discharge Machining (EDM) is used to machine electrically conductive materials. It cuts by using precisely controlled sparks that occur between an electrode and a work piece in the presence of dielectric fluid, regardless of the hardness of the material. Wire EDM (WEDM) is one such process where a wire is used to produce the spark between the material and wire and perform the cutting operation. Processing on wire EDM is a forceless process and makes WEDM a strong candidate for RP applications. Like other linear cut manufacturing systems, such as abrasive water jet and laser material processing, WEDM has a noticeable line contact characteristic with the part being produced. Unlike traditional manufacturing processes which involve point contact between the tool and the work piece, the contact mode in wire cutting processes is a linear edge. Figures 3A and 3B illustrates the contact models for traditional machining processes and linear cut manufacturing systems. Generally, metal material fabrication is not performed using traditional RP additive processes. Even though well developed CNC machining can process a variety of materials with high accuracy as a subtractive RP process, this method has its own problems associated with tool path generation, tooling, and fixturing. Laser based processes suffer either low density of the finished part or poor surface finish and accuracy. Even though some post-processes, such as

metal casting, can make a traditional RP product with high accuracy, it is not fit for mass customization type metal RP applications. A new rapid prototyping manufacturing process is needed to overcome the shortcomings of traditional RP processes for metal products and fit the mass customization requirement with low cost and short lead time.

Using wire electric discharge machining as a rapid prototyping tool is discussed in U.S. Pat. No. 6,627,835, which discloses cutting a three dimensional object into slices, using a wire electric discharge machine to fabricate each slice, and assembling the slices into a final product. This application analyzes the geometry of the object, and generates the numerical control code to fabricate the object together. However, the individual layers cut with WEDM still need to be stacked and held together. Such a WEDM can process any electrical conductive part regardless of the hardness of the material. It normally produces 2D or 2½-D parts with reasonable complexity. Unfortunately, WEDM process engineering for complex 3-D geometries has not become suitable for RP.

A WEDM processing method is needed for complex geometries suitable for rapid prototyping. Such a process preferably permits utilization of known WEDM processing tools.

SUMMARY OF THE INVENTION

One embodiment of our method of rapid prototyping a product may include identifying a product geometry to prepare a geometric model, determining fabrication setup orientation, preparing a fabrication process, generating a cutting path based NC code and fabricating the product using a linear cut process. The NC code is numerical control code such as Step-NC code or NC G-code.

The cutting path may include one or more paths that require a wire to move along one or more cutting paths or perform one or more cutting passes along a part for fabricating the part into a product.

The linear cut process may be wire electrical discharge machining, water jet cutting, laser machining or hot wire machining. Preferably, the linear cut process is conducted by a wire electrical discharge machine (WEDM) that utilizes a five axis or a six axis electrical discharge machining (EDM) machine. The linear cut process may also be conducted by a four, five or six axis laser machine.

Another embodiment of our method of rapid prototyping may include identifying a product geometry, selecting a rapid prototyping system, preparing a first model for fabrication, preparing a first fabrication process that takes input and generates tangent visibility for each facet identified in the input, identifying a part orientation, generating a modeling process for fabricating the product from stock material, generating at least one cutting path and fabricating the product using a linear cutting mechanism.

Preferably, the input is one or more STL files that provide part or product geometry data. For example, any polygonal part data may also be used. Eventually, even the direct boundary representation may be used. The generation of the modeling process can include determining

tangent visibility and wire range based on the input and determining part orientation based on product geometry and information provided in the input for each facet of the product. A three dimensional tool path or wire path will be generated based on tangent visibility results to prepare the first fabrication process or any additional fabrication processes.

The first fabrication process is preferably the only process needed to be run to fabricate the product.

It should be appreciated that the preparing of the first model can include adding at least one support to the first model prior to tool path planning for the first fabrication process. The fabrication process may also be run such that the one or more supports are severed to fabricate the part.

Embodiments of the method may also include preparing one or more visibility methods to determine if an axis of rotation of the product is feasible.

It should be understood that the one or more cutting paths may include multiple wire paths that include convex edges of the product that are generated to minimize the number of setups and number of B-axis orientations for fabrication of the product.

Embodiments of the methods may be incorporated in a machining apparatus, such as a machining apparatus configured for rapid prototyping. That apparatus may include one or more linear cutting mechanisms, one or more input devices and one or more controllers. The one or more controllers may include a computer or may include one or more processors operatively connected to memory that has software stored thereon for running by the one or more processors. The input device may be a scanner, keyboard, or other device configured to provide data, such as one or more STL files that may be utilized by the software run by the one or more processors.

The one or more controllers are connected to the at least one input device and at least one linear cutting mechanism. The one or more controllers are configured to control the at least one cutting mechanism. The one or more controllers are also configured to identify a geometry of a product, prepare a first model for fabrication; prepare a first fabrication process that takes input received from the at least one input device and generates tangent visibility for each facet identified in the input; identify a product orientation, generate a modeling process for fabricating the product from stock material, generate at least one cutting path, and actuate the cutting mechanism to move along the at least one cutting path to fabricate the product.

Preferably, the input is comprised of at least one STL file. The at least one cutting path may include a plurality of wire paths. The wire paths may include convex edges of the product and may be generated to minimze B axis orientation for the fabrication of a part or product.

Other details, objects, and advantages of the invention will become apparent as the following description of certain present preferred embodiments thereof and certain present preferred methods of practicing the same proceeds.

BRIEF DESCRIPTION OF THE DRAWINGS

Present preferred embodiments of the rapid prototyping method are shown in the accompanying drawings in which:

Figure 1A is a perspective view of a part illustrating a part with a mass volume.

Figure 1B is a perspective view of a part that has a second mass volume.

Figure 2 is a chart illustrating a qualitative situation of the direct metal components production relative to usual options.

Figure 3A is a schematic illustrating a contact model of a traditional machining process.

Figure 3B is a schematic illustrating contact model for a linear cut process.

Figure 4 is a flow chart illustrating examples of a general approach for using conventional machining as a rapid prototype tool.

Figure 5 is a perspective view of a six axis wire electrical discharge machine.

Figure 6A is a perspective view of a toll illustrating conventional visibility from a point.

Figure 6B is a perspective view illustrating WEDM visibility.

Figure 7 is a flow chart illustrating a present preferred embodiment of a method for rapid prototyping.

Figure 8 is a perspective view of an embodiment of a model pagoda.

Figure 9A is a perspective view illustrating raw material on an indexer.

Figure 9B is a view similar to Figure 9A illustrating a present preferred initial fabrication setup step of a present preferred method of rapid prototyping.

Figure 9C is a view similar to Figures 9A and 9B illustrating a present preferred part after a first cut path has been run along the part in accordance with a present preferred method of rapid prototyping.

Figure 9D is a view similar to Figures 9A, 9B and 9C illustrating the present preferred part after several rotations on an indexer.

Figure 9E is a view similar to Figures 9A, 9B, 9C and 9D illustrating a finished part made by a present preferred method of rapid prototyping.

Figure 10 is a flow chart illustrating a present preferred method for data preparation for use in a present preferred method of rapid prototyping.

Figure 11 is a flow chart illustrating a present preferred method of rapid prototyping.

Figure 12 is a perspective view of a part being fabricated by a present preferred method of rapid prototyping.

Figure 13 is a schematic view illustrating relations between cylinder center line l and rotational norm R_N and rotational orientation R_o.

Figure 14 is a flow chart illustrating a present preferred method of generating a wire path that may be utilized in a present preferred method of rapid prototyping.

Figure 15 is a graph illustrating a comparison between production cost of selective laser sintering (SLS) and WEDM prototyping.

Figure 16 is a present preferred embodiment of a computer apparatus that may implement an embodiment of our method for rapid prototyping.

Figure 17 is a coordinate system defined in this research

Figure 18 is a demonstration of rotational Norm R_{N_N} and rotational orientation R_O on a six-axis WEDM machine

Figure 19 is the flowchart to calculate the optimal set of intermediate coordinate systems

Figure 20 is the flowchart to calculate initial R_N.

Figure 21 is the flowchart to calculate initial R_O.

Figure 22 is an example of a present preferred intersection graph for a polygon.

Figure 23 is a flow chart illustrating a present preferred method for computing the tangent visibility percentage

Figure 24 is a fragmentary view of a present preferred cutting path generated for cutting a part using a linear cutting mechanism.

Figure 25 is a graph illustrating a present preferred method of determining edges based on a center of mass.

Figure 26 is a schematic view illustrating all coverable edges for a given rotational norm are shown in Figure 26

Figure 27 is a schematic view illustrating how a rotational norm of a cutting mechanism may be capable of covering certain degree of edges for a part.

Figure 28 is a graph illustrating a valid wire orientation perpendicular to a facet norm.

Figure 29 a graphical view illustrating coverable polygon norms for a particular orientation product.

Figure 30 is a flow chart illustrating a present preferred method for determining an intermediate coordinate system by determining a rotational norm and a rotational orientation.

Figure 31 is a graphical illustration of a plurality of rotational norms determined based on a determined rotational orientation.

Figure 32 is a graphical illustration of a plurality of rotational orientations determined based on a determined rotational norm.

Figure 33 is a flow chart illustrating a present preferred method for calculating an initial rotational norm.

Figure 34 is a flowchart of a present preferred method for calculating an initial rotational orientation.

Figure 35 is a flowchart showing a present preferred method for classifying tangent visibility results into different coordinate systems.

Figure 36 is a flowchart of a present preferred method for determining the intermediate coordinate system for a given edge.

Figure 37 illustrates an example of a cutting wire in its intermediate coordinate system.

Figure 38 is a flowchart showing a present preferred method of wire path generation.

Figure 39 is a flowchart illustrating a present preferred method for determining the intermediate coordinate system for triangle results.

Figure 40 is a schematic view illustrating straight lines parallel to a vector orientation product that may be used as a rectangle boundary.

Figure 41 is a schematic view illustrating a present preferred manufacturing coordinate system.

Figure 42 is a flowchart representing a present preferred method for the generation of the cutting sequence.

Figure 43 is a schematic view illustrating Six defined surfaces.

Figure 44 is a flowchart representing a present preferred method for a "GOTOZero" function.

Figure 45 is a schematic or graphical view illustrating a first present preferred wire path generation process.

Figure 46 is a schematic or graphical view illustrating a second present preferred wire path generation process.

Figure 47 is a schematic or graphical view illustrating a third present preferred wire path generation process.

Figure 48 illustrates an example of a cut off plane for a present preferred part.

Figure 49 is a block diagram illustrating a present preferred software structure for the WEDM-RP system.

Figure 50 illustrates a present preferred slotted part that may be fabricated via a rapid prototyping process.

Figure 51 is a schematic view illustrating setup orientation and rotational orientation results for the slot part shown in Figure 50.

Figure 52 is a schematic view illustrating the wire trajectory result for a determined coordinate.

Figure 53 illustrates a present preferred inner feature part that may be fabricated via a present preferred rapid prototyping process.

Figure 54 is a schematic view illustrating setup orientation and rotational orientation results for the inner feature part of Figure 53.

Figure 55 illustrates a present preferred pagoda part that may be fabricated via a present preferred rapid prototyping process.

Figure 56 is a schematic view illustrating setup orientation and rotational orientation results for the pagoda of Figure 55.

Figure 57 illustrates a present preferred hourglass part that may be fabricated via a present preferred rapid prototyping process.

DETAILED DESCRIPTION OF PRESENT PREFERRED EMBODIMENTS

As conventional subtractive processes, WEDM has some similarity in general approaches as a rapid prototyping process. This process requires a product geometry model, analysis of the product model for producibility, tool path generation and fabrication preparation, and fabrication of the final product.

WEDM removes material using line contact. Figure 5 illustrates the design of a six-axis WEDM. The electric wire in Figure 5 is the cutting tool for WEDM; the electric wire will be kept straight in a line during fabrication. Due to the uncommon fabrication approach of WEDM, the tool path planning for WEDM-RP is not a layer-based approach (neither additive nor subtractive).

One flow chart of the entire process for WEDM-RP is illustrated in Figure 7 and can be summarized by the following important contents:

1. Input for the proposed system is a CAD file. One embodiment of this CAD file is in STL format, where the boundary of the part is represented by triangular facets.

2. *Tangent Visibility*: Because of the uncommon fabrication approach of WEDM, the visibility problem is different from the normal visibility problem. Figures 6A and 6B illustrate the difference between conventional visibility and WEDM visibility. This step can use input such as an STL file, and generates tangent visibility for each facet in the STL file.

3. *Part Orientation*: This part of the problem intends to seek an orientation such that maximum the machinable surface area. This step can also take tangent visibility result and STL file as input and generate the fabrication orientation.

4. *Model Process and wire path generation*: Based on tangent visibility and part orientation results, the manufacturability of the given part can be analyzed and a wire path generated.

5. *Fabrication*: After analysis all the facets in the STL file, the wire path, setup plan can be sent to a six-axis WEDM machine for fabrication the prototyping model.

An example part to fabricate on six-axis WEDM is a small statue of a pagoda, which is illustrated in Figure 8. The pagoda is a symmetric part without cavities in the geometry and can be fully fabricated on six-axis WEDM in one setup with multiple rotation orientations.

Figure 8 illustrates one embodiment of a pagoda product made by a WEDM-RP rapid prototype process that utilizes a method such as the method shown in Figure 7.

The process illustrated in Figures 9A through 9E requires the development of algorithms to perform all the steps in an automatic manner. The algorithms may be applied by software configured to be processed by one or more processors for controlling the actions of a machine, such as a WEDM. One approach to performing these tasks is described in the following section:

The input of the WEDM-RP is any geometric model. Preferably, the input is formatted as Stereolithography (STL) files. Data preparation can prepare the data for the whole method. The

STL file will be translated in to labeled triangles, vertices, concave edges, and convex edges. The steps in one present preferred method of data preparation are presented in Figure 10.

The tangent visibility problem is not the same as the traditional visibility problem of CNC RP and needs to be solved in order to determine if the geometric shape can be produced using any linear process. Figures 6A and 6B illustrate the difference between regular visibility and WEDM's visibility. The regular visibility is a natural phenomenon in everyday life. Seeing an object means identifying the portions of the object visible from the current position. A point is visible from the current position if the line segment connecting the point and the current position does not intersect with any other part of the same object.

In Figure 6A, the regular visibility problem is illustrated. The points on the pagoda are visible from the current position because the line segments connecting them to the current position do not intersect with any other objects. On the other hand, the visibility problem for WEDM requires tangent visibility. A point is tangent visible if a straight line can cross the point without intersecting with any other objects.

In Figure 6B, the tangent visibility is illustrated. Tangent visibility intends to solve the tangent visibility problem for WEDM. A Stereolithography (STL) file, the common RP input, may be used as input for our process. The fundamental elements in the STL file are triangle facets. The tangent visibility will be tested for each triangle facet in the given STL file. The detail flowchart for tangent visibility is presented in Figure 11. This tangent visibility could also be applied to other linear cutting processes, such as a gamma knife operation or laser cutting, to determine the reachable region for those linear cutting processes.

There are two problems associated with fabrication orientation -- setup and rotational orientation. Rotational orientation R_O and rotational norm R_N are illustrated in Figure 13. Different

rotational norm R_N represents different setups. The orientation is preferably chosen such that it maximizes the machinable surface area under the rotational norm R_N. The wire needs to move only within the wire movement range in order to fabricate the facet, and straight lines in the range will be produced as a result of the cutting wire orientations for fabricating the facet. A part will be fabricated by completing fabrication of each facet. Furthermore, for each setup, not all facets can be fabricated in one rotational orientation for a given setup and given rotational orientation; the location of the wire will vary in a two cones, as illustrated in Figure 13. The center line of the cones is located on the vector $R_O \times R_N$ passing the center of mass of the input geometry. The relationships of cylinder center line O_P, rotation norm R_O, and rotational orientation R_N are illustrated in Figure 13. If the orientations of straight lines for some facets lie in the cones, those triangle facets could be fabricated under given rational orientation R_O and the setup.

In order to cover the tangent visible regions from the tangent visibility result, the cutting wire needs to rotate and translate following the orientations obtained from the visibility results. However, due to many machines' physical limitations, the cutting wire movement range is restricted. Some wire orientations may require the rotation of the workpiece on WEDM instead of rotating cutting wire. Note that the coordinate system for global tangent visibility results is based on the coordinate system of the input STL geometry. Consequently, the cutting wire orientation is also based on the coordinate system of the input geometry. The rotation of the workpiece will change the cutting wire orientation in the coordinate system. Furthermore, the coordinates required to manufacture the part should be based on the WEDM machines instead of the input part geometry. In order to solve this coordinate system problem, a series of manufacturing coordinates are defined to classify the tangent visibility results into several

categories. Under each set of manufacturing coordinates, the cutting wire can access all tangent visible regions without the movement of the rotational axis on WEDM. Each coordinate system, named as *intermediate coordinate system*, is defined by three vectors: (1) rotational norm R_N, the physical meaning of rotational norm is the setup orientation for the given geometry; (2) rotational orientation R_O and (3) orientation product O_P. The origin of the coordinate system is the center of mass of the input geometry. These intermediate coordinates can be translated into final manufacturing coordinates. The transformation matrix can be then used to transform cutting wire orientations under each intermediate coordinate into the final manufacturing coordinates.

Figure 17 illustrates the relationships among rotational norm R_N, rotational orientation R_O, and orientation product O_N. Each of these vectors has a physical meaning. Rotational Norm R_N is same as the rotational axis on a six-axis WEDM or other rotary axis. The direction of the rotation is defined using right hand rule: the fingers of the right hand are curled to match the rotation motion, and the thumb indicates the direction of the vector. For example, Figure 18 illustrates an example of a rotational norm. For each given rotational norm R_N, a series of R'_{OS} is defined, as illustrated Figure 18. Each rotational orientation R_O is used to indicate the current position of the rotary axis under a certain coordinate. Orientation product O_P represents the neutral position of the cutting wire. Based on the physical limitations of a WEDM machine, the cutting wire can only rotate in a restricted area around the orientation product O_P.

In order to find the optimal set of intermediate coordinates, the most important vectors to define are the rotational norm R_{NS}. With properly defined R_{NS}, all possible cutting wire orientations in 3D space can be covered. Based on the definitions of rotational norm, rotational orientation, and orientation product, an intermediate coordinate system requires at least two out of the three vectors, and the third vector is the cross product resulting from the two known

vectors. An overall flowchart on how to determine the intermediate coordinate system by determining the rotational norm R_N and rotational orientation R_O is presented. The flowchart is illustrated in Figure 19. Each rotational norm obtained from the algorithm results represents a setup orientation for six-axis WEDM. A greedy algorithm is used to classify all visibility result in to all necessary coordinate systems and generate two important vectors: initial R_N and initial R_O. The intermediate coordinates formed by initial R_N and initial R_O will cover most of the tangent visible areas of the given geometry. A series of R_Ns will be generated by rotating initial R_N around initial R_O. Each rotational norm R_N represents one required setup orientations to fabricate the input geometry. Furthermore, under each rotational norm R_N, a series of rotational orientation R_O will be calculated. Those rotational orientations will be used to guide the rotational axis movement on six-axis WEDM. The flowchart to calculate initial R_N is illustrated in Figure 20. The flowchart to calculate initial R_O is illustrated in Figure 21.

The manufacturability result can provide wire movement information for each triangle facet in the given STL file. Because the cutting wire can be moved within the machine physical limitation, a number of B-axis orientations R_O can be calculated based on machine physical limitation and manufacturability result. If the taper angle of the WEDM machine is α, $\lceil 90 \div \alpha \rceil$ number of rotational orientation R_O will be able to cover all necessary tangent visible regions.

The wire path generation flowchart is illustrated in Figure 14. For each rotational norm R_N, a fixture can be designed to hold the part. Because WEDM has the characteristic of a zero cutting force, the function of those fixtures will be clamping the part. Sacrificial fixtures can also be used. Because the part can be fixed on B-axis indexer for each setup, the fixture is preferably located as close to the rotation center as possible. Furthermore, some other issues can be considered:

- The sacrificial fixture is preferably not an obstacle for fabrication
- Simplification of the cut-off surface is preferred. For instance, a planar surface is much easier for cut off than a curved surface.

Global Tangent Visibility Calculations

A global tangent visibility problem for a polyhedral model can be simplified into a 2D problem. In order to find the global tangent visibility information, each planar surface of a product geometry or part geometry must be expanded to obtain an intersection plane with the given geometry. Because the geometry is a polyhedral model, the intersection plane is on a tangent surface of each planar surface. Based on the intersection plane results, a tangent visibility analysis may then be performed and the tangent visible percentage for the planar surface may then be calculated.

The first step to computing tangent visibility is to calculate the polygon plane intersection graph. The convex-concave edge property plays of a particular part may play a key role in the tangent visibility definition. In order to compute the tangent visibility, the edge property must be correctly assigned. Before providing the rules for assigning the edge property, several important definitions are presented first.

Definition —original edges: original edges are the edges in the original geometry $\mathbb{G} = \{\mathbb{F}, \mathbb{E}, \mathbf{P}\}$, where $\mathbb{F}$ is the set of surfaces in geometry $\mathbb{G}$, $\mathbb{E}$ is the set of edges in geometry $\mathbb{G}$, and $\mathbf{P}$ is the set of points in geometry $\mathbb{G}$. These edges are shared by connected polygons in the given geometry. The set of original edges is noted as $\mathbb{E}_O$.

$$\mathbb{E}_o = \{e: e \in \mathbb{E}, e = P_1 \cap P_2, P_1, P_2 \in \mathbb{F}\}$$

Definition —extended surface for the polygon: The extended surface is used to calculate the intersection graph for the polygon. Polygon $P = \{norm, \mathbf{P}\}$, where norm is the polygon norm, $\mathbf{P}$ is the set of points on the polygon boundary. The extended surface for the polygon is noted as F_e and can be expressed as:

$$norm \cdot v + d_0 = 0$$

where $v = [x, y, z]$

$$d_0 = -norm \cdot v_i, \; v_i \in \mathbf{P}$$

Definition —intersection graph for the polygon: the intersection graph for polygon P is denoted as $\mathbb{G}_{PI}$. $\mathbb{G}_{PI} = \{\mathbb{E}, V(\mathbb{E})\}$. Where $\mathbb{E}$ is the set of all edges of the geometry.

Definition —Non-original edges: Non-original edges are the edges that are not the original geometry $\mathbb{G} = \{\mathbb{F}, \mathbb{E}, \mathbf{P}\}$. It is the intersection result of the extended surface F_e and the other polygons. The set of non-original edges is noted as $\mathbb{E}_N$:

$$\mathbb{E}_o = \{e: e \notin \mathbb{E}, e = F_e \cap P_2, P_1 \cap P_2 = \Phi, P_1, P_2 \in \mathbb{F}\}$$

Definition —special original edges: special original edges are the edges in the original geometry $\mathbb{G} = \{\mathbb{F}, \mathbb{E}, \mathbf{P}\}$. However, it is not shared directly by the polygons. It is the intersection result of the extended surface F_e of P_1 and the other polygon P_2. The set of non-original edges is noted as $\mathbb{E}_{sp}$:

$$\mathbb{E}_{sp} = \{e : e \in \mathbb{E}, e = F_e \cap P_2, P_1 \cap P_2 = \Phi, P_1, P_2 \in \mathbb{F}\}$$

Figure 22 illustrates an example of an intersection graph for polygon P_1. Edge e_1 is shared by polygon P_1 and P_2, and it is an original edge. According to the relationship of P_1 and P_2, e_1 is a convex edge. Edge e_2 is shared by Polygon P_5 and P_1, and the relationship between P_5 and P_1 is concave, so that e_2 is a concave edge. Edge e_3 is the intersection result of the extended surface F_e and the polygon P_4. Edge e_4 is the intersection result of F_e and polygon P_3. Both edge e_3 and edge e_4 are original edges; therefore, they are special original edges considering that they do not belong to polygon P_1. A non-original edge, edge e_5 is the intersection result of polygon P_6 and extended surface F_e and it is a non-original edge.

The following rules may be used to assign the property of the edges:

1. The convex concave property of the original edge is defined by the edge definition presented in Section 3.3.
2. All non-original edges are treated as concave edges.
3. Special original edges need further inspection to determine the convex concave property. Assume that the special edge is shared by polygon P_{s1} and polygon P_{s2}, and the original polygon is P_1:

a. If P_1 locates on the same plane with P_{s1} or P_{s2}, the convex concave property of the special edge is the same as the convex concave property of the original edge. In Figure 22, edge e_3 is a special edge, and because polygon P_4 and polygon P_1 are located on the same plane, edge e_3 is a convex edge.

b. If P_1 is not co-plane with P_{s1} and P_{s2}, the convex concave property is determine as following:

i. Except the points on shared edge between P_{s1} and P_{s2}, all points on P_{s1} is located on different side of P_1 with P_{s2}, the edge is assigned as a concave edge. In Figure 22, edge e_4 is shared by polygon P_3 and polygon P_5. Point v_2 on polygon P_5 is located on positive side of polygon P_1. Point v_1 on polygon P_3 is located on negative side of polygon P_1, so the edge e_4 is a concave edge on the intersection graph for polygon P_5.

ii. Except the points on shared edge between P_{s1} and P_{s2}, all points on P_{s1} is located on same side of P_1 with P_{s2}, the edge is a convex edge.

A present preferred algorithm that may be used for calculating the intersection graphs is illustrated in the below Table 1:.

Table 1 - Present Preferred Algorithm for Computing Intersection Graphs

For (each polygon F_i in the given Geometry $\mathbb{G}$) {
    $\mathbb{E}_i = \Phi$
For (each polygon $F_j \neq F_i$ in the given Geometry $\mathbb{G}$) {
        $e = F_i \cap F_j$
        Assign edge property to e /* convex or concave */
        $\mathbb{E}_i = \mathbb{E}_i \cup \{e\}$
    }
}
/* $\mathbb{E}_i$ are used to compute the tangent visibility for each polygon*/

An algorithm that may be used to calculate a tangent visibility percentage for a part to be rapid prototyped mat be determined from the result of the intersection graph and the properly defined edge properties, which may be used as input for this algorithm.

The input of a present preferred algorithm for use to calculate a tangent visibility percentage may include the following definitions:

1. **Intersection Polygon** P_1 is the polygon we are interested in.
2. **Intersection graph:** $\mathbb{G}_{PI}$ is the intersection graph for polygon P_1. $\mathbb{G}_{PI} = \{\mathbb{E}, V(\mathbb{E})\}$.
3. **Convex edge sets:** $\mathbb{E}_{vex}$ is all convex edges in the intersection graph $\mathbb{E}_{vex} \subseteq \mathbb{E}$.
4. **Concave edge sets:** $\mathbb{E}_{cave}$ is all concave edges in the intersection graph $\mathbb{E}_{cave} \subseteq \mathbb{E}$.

The algorithm for computing the tangent visibility percentage may be appreciated from Figure 23 and may be described as follows:

Step1: Determine whether the edges in $\mathbb{G}_{PI}$ intersect with any concave edges.

Step2: If all edges in $\mathbb{G}_{in}$ are convex edges, then use convex edges to form rectangle with points in $\mathbb{G}_{in}$ in order to cover the intersection polygon P_1.

Step 3: If $\mathbb{E}_{vex} \neq \Phi$ and $\mathbb{E}_{cave} \neq \Phi$, then form rectangles and triangles to cover the polygon P_1.

Table 2 illustrates a present preferred algorithm to calculate tangent visibility. The sub-functions of the tangent visibility algorithms are illustrated in Tables 3-8

Table 2; Present Preferred Algorithm for Compute Tangent Visibility

$Vis_{List} = \Phi$ /*tangent visibility */
For (each intersection graph $\mathbb{G}_{PI} = \{\mathbb{E}, V(\mathbb{E})\}$ for polygon P) {
$TVC = \Phi$ /* the tangent visible region*/
For (each edge $e \in \mathbb{E}$) {
If ($Edge_{IntersectTest(e,\mathbb{E})}$) {
$v = ClosestPoint(e, V(\mathbb{E}))$

$TVC = TVC \cup Form_{Region(e,v,P)}$ /*polygon clipping*/
}
If ($e \in \mathbb{E}_{cave}$) {
$TVC = TVC \cup Form_{Cones(e,V(\mathbb{E}),P)}$ /*polygon clipping*/
$TVC = TVC \cup Form_{Rects(e,V(\mathbb{E}),P)}$ /*polygon clipping*/
}
}
$vis = Area(TVC) \div Area(P)$
$Vis_{List} = Vis_{List} + \{(P, vis)\}$
}

Table 3; Present Preferred Sub-function: Edge_Intersect_Test ($e, \mathbb{E}$)

L is the straight line that is coincident with edge e
For (each edge $e_i \in \mathbb{E}$ and $e_i \neq e$){
Flag = true
$v = L \cap e_i$
If ($v \neq \Phi$) and ($e \in \mathbb{E}_1 cave$) {
If ($v \notin V(\mathbb{E})$ {
/*intersects with concave edge in the middle*/
Flag = false
}**else** {
If ($v \in V(\mathbb{E}_{vex})$) {
/*intersect at convex concave point*/
$\mathbb{E}_v = \{e : e \in \mathbb{E}, v = e.v(0)\ or\ v = e.v(1)\}$
If ($V(\mathbb{E}_v)$ *is located on same side of* L) {
/*intersects at convex concave point*/
/*Line L runs into solid */
Flag = false
}
} **else** {
/*intersects with the concave point*/
Flag = false
}
}
}
}
return Flag

Table 4; Present Preferred Sub-function: Form_Region (e, v, P)

$INF = 10^6$
/*build a "large enough" rectangle $R = *(*v_1, v_2, v_3, v_4*)*$ */
/* it has an edge that is coincident to edge e */
/* the other edge passes point v and is parallel to edge e */
$v_1 = e.v(0) - INF * (e.v(0) - e.v(1))$
$v_2 = e.v(0) + INF * (e.v(1) - e.v(0))$
$v_3 = v + INF * (e.v(1) - e.v(0))$
$v_4 = v - INF * (e.v(0) - e.v(1))$
$Region = P \cap R$ /*get the intersection of the original polygon P and the rectangle R */
return $Region$

Table 5; Present Preferred Sub-function: Form_Rects ($e, V(\mathbb{E}), P$)

$Region = \Phi$
For $(each\ v \in V(\mathbb{E}))$ {
/*build edge e_1 passes the point v and parallel to edge e */
$e_1.v(0) = v + (e.v(1) - e.v(0))$
$e_1.v(1) = v + (e.v(0) - e.v(1))$
If ($Edge_{Intersect_{Test}(e_1, \Xi)}$){
$v' = ClosestPoint(e_1, V(\mathbb{E}))$
$Region = Region \cup Form_{Region(e_1, v', P)}$ /*polygon clipping*/
}
/*build edge e_2 start at the point v and end at point $e.v(0)$ */
$e_2.v(0) = v$
$e_2.v(1) = e.v(0)$
If ($Edge_{Intersect_{Test}(e_2, \Xi)}$){
$v' = ClosestPoint(e_2, V(\mathbb{E}))$
$Region = Region \cup Form_{Region(e_2, v', P)}$ /*polygon clipping*/
}
/*build edge e_3 start at the point v and end at point $e.v(1)$ */
$e_3.v(0) = v$
$e_3.v(1) = e.v(1)$
If ($Edge_{Intersect_{Test}(e_3, \Xi)}$){
$v' = ClosestPoint(e_3, V(\mathbb{E}))$
$Region = Region \cup Form_{Region(e_3, v', P)}$ /*polygon clipping*/
}
}
return $Region$

Table 6; Present Preferred Sub-function: Form_Triangle ($v_1, v_2, v_3, V(\mathbb{E}), P$)

$Region = \Phi$
$INF = 10^6$
/*build a "large enough" triangle $Tr_1 = \{v_a, v_b, v_c\}$ */
$v_b = v_1 + INF * (v_2 - v_1)$
$v_c = v_1 + INF * (v_3 - v_1)$
$v_a = v_1$
/*build a "large enough" triangle $Tr_2 = \{v'_a, v'_b, v'_c\}$ */
$v'_b = v_1 + INF * (v_1 - v_2)$
$v'_c = v_1 + INF * (v_1 - v_3)$
$v'_a = v_1$
/*Triangle Tr_1 and Tr_2 share a vertex, they are vertical angle triangles*/
Flag = false
For $(each\ v_p \in \mathbb{E}_{cave})$ {
If $((v_1P\ inside\ Tr_1 1)\ or (v_1P\ inside\ Tr_1 2))$ {

```
                Flag = true
                Break
}
}
If (! Flag) {
        Region = P ∩ (Tr1 ∪ Tr2)
}
return Region
```

Table 7; Present Preferred Sub-function : Form_Cones $(e, V(\mathbb{E}), P)$

```
Region = Φ
For (each v ∈ V(E)) {
        Region = Region ∪ Form_Triangle(e.v(0),e.v(1),v,V(Ξ),P)
        Region = Region ∪ Form_Triangle(e.v(1),e.v(0),v,V(Ξ),P)
        Region = Region ∪ Form_Triangle(v,e.v(1),e.v(0),V(Ξ),P)
}
Return Region
```

The present preferred global tangent visibility algorithm includes three major steps, as illustrated in Table 2. The input intersection graph $\mathbb{G}_{PI} = \{\mathbb{E}, V(\mathbb{E})\}$ may have m concave edges, n convex edges, and k points, where $k \leq 2(m+n)$. The first major step is the edge intersection test. In this step, an intersection test is performed for the edges in the intersection graph $\mathbb{G}_{PI}$ with all concave edges. The complexity of this operation is $O(m \times (m+n))$. The second step in the global tangent visibility algorithm of Table 2 is that of performing the polygon-clipping operations for polygons without concave edges. In this research, the polygon-clipping operation is finished using the third-party open source package, Computational Geometry Algorithms Library (CGAL). The general polygon-clipping operation has the complexity $O(xy)$ with x and y being the edge numbers of the arbitrary polygons. Consequently, the complexity of the second step is $O(n^2)$, given that these polygons do not have concave edges. The third step in the present preferred tangent visibility algorithm of Table 2 is that of forming visible regions and performing polygon clippings. The complexity is $O((m+n) \times (k + (m+n)^2))$.

Because $k \leq 2(m+n)$, $O((m+n) \times (k + (m+n)^2)) = O((m+n)^3)$. The second and third steps

in the algorithm are not executed simultaneously; therefore, when polygons contain both convex and concave edges, the worst case size complexity is $O((m+n)^3)$ when polygons contain both convex and concave edges. Let the total number of polygons be p : there are p intersection graphs to perform tangent visibility analysis. Therefore, the overall complexity of the tangent visibility algorithm is $O(p \times (m+n)^3)$.

Classification of Edges

Global tangent visibility results may contain only triangle and rectangle shapes. Due to the fact that the coordinates of the tangent visibility result are based partly on geometry coordinates, those shapes may be classified into intermediate coordinate systems before they are translated into manufacturing coordinates. Present preferred methods of classifying edges and facets into different intermediate coordinate systems are discussed below.

Triangle or rectangle shapes usually require edges to cover them. For example, each triangle shape, as illustrated in Figure 24, requires two edges to cover the whole triangle. The two edges are the starting cutting edge and the end cutting edge. Several lemmas may be used to classify those edges under a certain intermediate coordinate system.

Lemma 1 : An edge is coverable for a certain R_N if the edge forms an angle with R_N between $[90-\alpha, 90+\alpha]$, where α is the taper angle limitation for WEDM machines.

Due to the physical limitation of WEDM machines, the maximum angle between the edge and the neutral wire position is α . Under a certain intermediate coordinate system, the angle range between the vector Orientation Product O_P and the edge is $[-\alpha, \alpha]$. If the edges are normalized and the start point of the edges are moved to center of the mass (as illustrated in Figure 25), all edges that are located in the cone space are coverable under the current intermediate coordinate system. Because $O_P = R_N \times R_O$, O_P

is perpendicular to R_N. As the result, if any edge forms an angle between $[90-\alpha, 90+\alpha]$ with R_N, then the edge is coverable under the current intermediate coordinate system.

Lemma 2: In 3D space, only $\lceil 90 \div \alpha \rceil$ number of R_Ns are required to cover all possible edges in 3D space, where α is taper angle limitation for WEDM machines.

If all edges are normalized and translated for their starting point to center of mass, then all edges in 3D will form a unit globe with center at center of mass. According to Lemma 1, all coverable edges for a given R_N are shown in Figure 26. Each R_N is capable of covering 2α degree of edges, as illustrated in Figure 27. If a whole globe of edges is required to cover, we only need $\lceil 360 \div (2 \times 2 \times \alpha) \rceil = \lceil 90 \div \alpha \rceil$ number of R_Ns.

A certain edge orientation for the rectangle shape may need to be determined in order to translate the tangent visibility result into manufacturing information. Several lemmas are introduced in order to classify those polygons without concave edges under a certain intermediate coordinate system.

Lemma 3: A polygon without concave edges is coverable for a certain R_N R_O intermediate coordinate system if the polygon norm forms an angle with $O_N = R_N \times R_O$ between $[90-\alpha, 90+\alpha]$, where α is the taper angle limitation for WEDM machines.

For a given polygon norm, a valid wire orientation is perpendicular to the facet norm. So, if the angle between the polygon norm and the orientation product O_P is between $[-\alpha, \alpha]$, then as illustrated in Figure 28, the polygon is reachable under the current intermediate coordinate system.

Lemma 4. Only $\lceil 90 \div \alpha \rceil$ number of R_Os under the any R_N is required to cover all possible polygons in 3D space, where α is the taper angle limitation for WEDM machines.

In 3D, if all polygon norms are normalized and their starting points are translated to the center of a mass, then all polygon norms will form a unit globe with its center at the center of that mass. According to Lemma 3, all coverable polygon norms for a given O_P are shown in Figure 29. Each O_P is capable of covering 2α degrees of an edge. If covering a whole globe of edges is required, then we only need $\lceil 360 \div (2 \times 2 \times \alpha) \rceil = \lceil 90 \div \alpha \rceil$ number of O_Ps.

Present Preferred Method For Determining Intermediate Coordinates For a WEDM-RP

Tangent visibility results may be classified into several intermediate coordinates and then translated into manufacturing coordinates. Based on Lemma 1 and Lemma 2, discussed above, $\lceil 90 \div \alpha \rceil$ number of R_Ns are capable of covering all possible edges in 3D space. Based on Lemma 3 and Lemma 4, $\lceil 90 \div \alpha \rceil$ number of O_Ps under any R_N is enough to cover all polygons without concave edges. However, even though any set of intermediate coordinate systems can be a feasible solution for WEDM-RP, finding the optimal solution for setup is not guaranteed. In this section, an algorithm to determine the optimal set of intermediate coordinate systems is presented such that the number of trial setups is minimized.

In order to find an optimal set of intermediate coordinates, vectors that define the rotational norm R_Ns may be determined. With properly defined R_Ns, all possible edges in 3D space and polygons without concave edges can be covered. Based on the definitions of rotational norm, rotational orientation, and orientation product, an intermediate coordinate system requires at least two out of the three vectors, and the third vector is the cross product resulting from the two known vectors. An overall flowchart on how to determine the intermediate coordinate system by determining the rotational norm R_N and rotational orientation R_O is presented. The flowchart is illustrated in Figure 30.

In this calculation procedure, an algorithm may be applied to calculate two initial vectors, initial R_N and initial R_O. The intermediate coordinates formed by initial R_N and initial R_O will cover most of the tangent visible areas of the given geometry. Based on the two initial vectors, $\lceil 90 \div \alpha \rceil$ norms are calculated by rotating initial R_N around initial R_O. Each rotational norm forms a 2α angle with its neighbor rotational norms. For example, in Figure 31, the taper angle $\alpha = 20^0$, $\lceil 90 \div \alpha \rceil = \lceil 90 \div 20 \rceil = 5$ $R'_N s$ is defined around the initial R_O. Each R_N forms a 40^0 angle with its neighbor $R'_N s$.

Based on above discussed Lemma 4, for any given R_N, only $\lceil 90 \div \alpha \rceil$ intermediate coordinate systems are required to cover all polygons without concave edges. Consequently, we build $\lceil 90 \div \alpha \rceil$ R_O evenly distributed vectors around initial R_N. Each rotational orientation R_O forms a 2α angle with its neighbor rotational orientations. For example, in Figure 32, the taper angle $\alpha = 20^0$, $\lceil 90 \div \alpha \rceil = \lceil 90 \div 20 \rceil = 5$ $R'_O s$ is defined around the initial R_N. Each R_O forms a 40^0 angle with its neighbor $R'_O s$.

A flowchart for a present preferred method of calculating an initial R_N is illustrated in Figure 33. In this procedure, a list of initial R_N candidates is generated. For each facet or polygon with concave edges, the facet or polygon norm is used as a potential initial R_N and saved into the $RnList$. The total area that is reachable under each initial R_N candidate is calculated, and the final initial R_N is the one that has the maximum reachable total area. Furthermore, the initial R_N affects the cut off plane, as discussed in Chapter 6. Consequently, any initial R_N candidate must have at least one polygon without a concave edge that is perpendicular to the initial R_N. This perpendicular polygon is used as the cut off plane.

The initial rotational orientation R_O is a unit vector that is perpendicular to the initial R_N. The flowchart for calculating initial R_O is presented in Figure 34. In this procedure, all polygon

norms which are perpendicular to the initial R_N, are candidates for initial R_O. Those candidates are grouped together if the norms coincide. For each group of polygons, the total area is calculated. The final initial R_O is the group norm with the maximum total area. If no polygon has a norm that is perpendicular to the initial R_N, the initial R_O will be an arbitrary vector that is perpendicular to the initial R_N.

After calculating $\lceil 90 \div \alpha \rceil$ number of $R'_N s$ and $\lceil 90 \div \alpha \rceil$ number of $R'_O s$ under initial R_N, the resulting intermediate coordinate systems are able to cover all polygons without concave edges. More intermediate coordinate systems may need to be defined using the $\lceil 90 \div \alpha \rceil$ number of R_Ns calculation in order to cover all possible edges from the tangent visibility results. A classification procedure is used to classify the tangent visibility results under different intermediate coordinate systems. Figure 35 illustrates a flowchart of a present preferred method for classifying tangent visibility results into different coordinate systems.

There may be three types of target visibility results. For a rectangle result, if the edge defines the rectangle shape it can be covered under a certain intermediate coordinate; the whole rectangle shape can be covered under the intermediate coordinate. For a triangle result, each shape is formed by two edges, and an intermediate coordinate can be determined for each edge. A procedure called FindRnRoEdge is defined to determine the intermediate coordinate system for a given edge. A flowchart of a present preferred method of finding the RnRoEdge is illustrated in Figure 36.

A third type of tangent visibility result is a polygon without concave edges. There may be an infinite number of feasible solutions to cover these polygons. Based on Lemma 3, only one intermediate coordinate system for these polygons may be found. Due to the fact that any $\lceil 90 \div \alpha \rceil$ number of R_O under any given R_N is capable of covering all polygons without concave

edges, the initial R_N and its first pre-defined $\lceil 90 \div \alpha \rceil$ number of R_O will be used to cover all polygons without concave edges. A function named "FindRnRoFct" is defined to classify the polygon without concave edges into different intermediate coordinates.

In "FindRnRoEdge" procedure, the angle between the input edge and pre-defined R_N are calculated. Based on Lemma 1, the R_N forms an angle with the input edge between $[90 - \alpha, 90 + \alpha]$ will be selected. The angle between the input edge and existing orientation product O_N under the current R_N is calculated; the O_N that forms an angle with the input edge between $(0, \alpha)$ or $(180 - \alpha, 180)$ is select. In case no existing O_N satisfies this requirement, a new O_N is calculated by the cross-product of the input edge and the rotational norm R_N. This procedure returns the R_N and R_O that form the intermediate coordinate system to cover the edge.

In "FindRnRoFct" procedure, the angle between the input polygon norm and pre-defined O_P under initial R_N is calculated. Based on Lemma 3, the O_P forms an angle with the input edge between $[90 - \alpha, 90 + \alpha]$ will be selected. The detailed information of the procedure is shown in Table 8.

Table 8; Present Preferred FindRnRoFct Procedure

Input: initial R_N, all pre-defined R_O under initial R_N, the polygon P
Output: intermediate coordinate system R_{N-out} R_{O-out}

$R_{N-out} = initial\ R_N$

find an $O_P(i) = R_N(i) \times R_O(i)$, *forming an angle with norm of* P *between* $[90 - \alpha, 90 + \alpha]$

$R_{O-out} = R_O(i)$

Result is R_{N-out} R_{O-out}

Present Preferred Method For Wire Path Generation and Transformation Wire Path Generation

Tangent visibility results may be classified into several intermediate coordinate systems. Under each intermediate coordinate system, the tangent visibility results are stored as rectangle shapes, triangle shapes and polygons without concave edges.

Figure 37 illustrates an example of a cutting wire in its intermediate coordinate system. In this example, the UV plane and the XY plane are perpendicular to vector O_P in the intermediate coordinate system. The distance between the UV plane and the XY plane is D, which is a parameter related to the physical restrictions of a WEDM machine. The distance D represents the physical distance between the upper wire guide and lower wire guide on a WEDM machine. The distances from the origin of the intermediate coordinate system to the UV plane and the XY plane are both equal to $\frac{D}{2}$. In Figure 37, the cutting edge from the tangent visibility result is an edge which covers the polygon in the graph. The extension of the cutting edge will intersect with the UV plane and the XY plane to create the cutting wire trajectory points.

A flowchart for a present preferred method of wire path generation is shown in Figure 38. The tangent visibility results are classified into rectangle results, triangle results, and results for polygons without concave edges. For each result, corresponding intermediate coordinate systems and wire path trajectories are found.

A rectangle result may have two cutting edges that have the exact same orientation. Consequently, the rectangle result can be finished using the same intermediate coordinate system. The cutting wire trajectories on the XY plane and the UV plane are used to guide the cutting wire and finish the rectangle coverage.

A triangle result may have two cutting wire orientations; the orientation differences may result in a need for different intermediate coordinate systems to cover the triangle result. There are three possible scenarios for the intermediate coordinate system for triangle coverage: the cutting wires are in the same coordinate system; the two cutting wires share the same rotational orientation R_N ; or the two cutting wires share different rotational orientations R_{NS} . A flowchart illustrating a present preferred method for determining the intermediate coordinate system for triangle results is illustrated in Figure 39. Based on the result, one or multiple intermediate coordinate systems may be generated to cover the whole triangle area.

A polygon without concave edges can be covered using an infinite number of rectangle regions. The straight lines parallel to vector O_P are used as the rectangle boundary, as illustrated in Figure 40. Because the straight lines covering the polygon have the exact same orientation, the coverage for a polygon without concave edges can be finished using the same intermediate coordinate system as well.

Present Preferred Methods For Wire Path Transformation

After wire path trajectories are generated for each tangent visibility result, those trajectories may be transformed into a manufacturing coordinate system. The manufacturing coordinate system may be appreciated from Figure 5 and Figure 41:

1) The origin of the manufacturing system is at the rotational center of the B-axis on a six-axis WEDM machine.

2) The UV plane and the XY plane are perpendicular to the Z-axis

In order to transform the intermediate coordinate system into the final manufacturing coordinates, the center of mass (the origin of the intermediate coordinates), may be translated. The rotational norm R_N needs to be translated to the X-axis. Assuming that the center of mass

is P_{CM}, the trajectory point in the intermediate coordinate is P, the rotational norm of the intermediate coordinate is R_N, and the rotational orientation is R_O. The new trajectory point P_{new} in the manufacturing coordinate can be calculated by:

$$P_{new} = P \times T - P_{CM}$$

where T is the transformation matrix and can be calculated by:

$$T = \begin{bmatrix} cos\theta + \omega_x^2(1-cos\theta) & \omega_x\omega_y(1-cos\theta) - \omega_z sin\theta & \omega_x\omega_z(1-cos\theta) + \omega_y sin\theta \\ \omega_z sin\theta + \omega_x\omega_y(1-cos\theta) & cos\theta + \omega_y^2(1-cos\theta) & \omega_z\omega_y(1-cos\theta) - \omega_x sin\theta \\ \omega_x\omega_z(1-cos\theta) - \omega_y sin\theta & \omega_x sin\theta + \omega_z\omega_y(1-cos\theta) & cos\theta + \omega_z^2(1-cos\theta) \end{bmatrix}$$

where $\omega = R_N \times [1,0,0]$, $\theta = \text{acos}(R_N \cdot [1,0,0])$

Each shape in the tangent visibility result may have a trajectory segment on the UV plane and the XY plane. The wire path generated by this method may be isolated. In order to minimize the rapid movement between the cutting segments, the separate trajectories should be translated into one connected trajectory. In this section, a method is presented to combine separate trajectories into one trajectory and generating the wire path plan automatically. A flowchart representing a present preferred method for the generation of the cutting sequence is illustrated in Figure 42. In this operation, the wire trajectories are classified into trajectories generated by triangle coverage and trajectories generated by rectangle coverage. For all trajectories generated by triangle coverage, a function named "GOTOZero" is used to generate the lead-in wire path before the trajectory and lead-out wire path after the trajectory. For all rectangle coverage generated trajectories, the connected trajectories form one cutting chain, and the "GOTOZero" function is used to generate the lead-in wire path before the newly-formed cutting chain and the lead-out wire path after the cutting chain.

Before presenting the detailed methodologies related to generating lead-in/lead-out wire paths and cutting chain trajectories generated for rectangle coverage, several definitions used in those methods are presented. Six surfaces are defined as follows and illustrated in Figure 43:

UV plane is a plane parallel to $R_N R_O$ plane, and in the area corresponding to negative direction of vector O_P. The distance from the origin to the UV plane is $\frac{D}{2}$. This plane is used for wire path projection.

XY plane is a plane parallel to $R_N R_O$ plane, and in the area corresponding to the positive direction of vector O_P. The distance from the origin to the UV plane is $\frac{D}{2}$. This plane is used for wire path projection.

Right Plane is a plane parallel to $O_P R_N$ plane, and in an area corresponding to the positive direction of vector R_O. The distance from origin to the right plane is $\frac{width}{2}$.

Left Plane is a plane parallel to $O_P R_N$ plane, and in an area corresponding to the negative direction of vector R_O. The distance from the origin to the left plane is $\frac{width}{2}$.

Top plane is a plane parallel to $R_O O_P$ plane, and in an area corresponding to the positive direction of vector R_N. The distance from the origin to the top plane is $\frac{height}{2}$.

Bottom plane is a plane parallel to $R_O O_P$ plane, and in an area corresponding to the negative direction of vector R_N. The distance from the origin to the top plane is $\frac{height}{2}$.

For these definitions, parameter D is the fixed distance from the UV plane to the XY plane. This is a distance related to machine dimensions. Parameter $height$ and $width$ are related to input machine dimension limitations. In addition, four edges are defined and illustrated in Figure 43: (1) **Top Right Edge** is the intersection edge of the top plane and right

plane; (2) **Top Left Edge** is the intersection edge of the top plane and left plane; (3) **Bottom Right Edge** is the intersection edge of the bottom plane and right plane; (4) **Bottom Left Edge** is the intersection edge of the bottom plane and left plane.

A flowchart representing a present preferred method for a "GOTOZero" function is illustrated in Figure 44. This function intends to create a lead-in for the wire path from an idle position to the initial cutting point or to create the lead-out for the wire path from the last cutting point to an idle position.

There are at least three possible scenarios for this wire path generation process:

Scenario 1: When the starting point of the cutting chain trajectory is formed by coverage of a polygon without concave edges, the last segment in the cutting chain will be extended to intersect with one of the six surfaces defined above. When the starting point of the cutting chain trajectory is not formed by coverage of a polygon without concave edges, the last segment on the cutting chain will also be extended to test any intersection with the six surfaces defined above or any existing cutting chain trajectory.

Scenario 2: If the intersection with the surfaces is closer than the intersection with the cutting chain trajectory, then the lead-in/lead-out wire path will follow the rules used for Scenario 1.

Scenario 3: If the intersection with the cutting chain trajectory is closer than the intersection with the surfaces, the lead-in/lead-out wire path will follow the intersected cutting chain trajectory.

Figure 45 illustrates an example of Scenario 1. The cutting chain "Chain 1" and "Chain 2" are on the UV plane. The extension of the first segment of "Chain 1" intersects with *Right Plane* on edge $E1$. The extension of the last segment of "Chain 1" intersects with *Right Plane* on

edge $E2$. The extension of the first segment of "Chain 2" intersects with *Left Plane* on edge *E3*. The extension of the last segment of "Chain 2" intersects with *Left Plane* on edge *E4*. Consequently, the cutting chain sequence for "Chain 1" is: Top Right Edge→E1→Chain 1→E2→Top Right Edge. The cutting chain sequence for "Chain 2" is Top Left Edge→E3→Chain 2→E4→Top Left Edge.

Figure 46 illustrates an example of Scenario 2. The projection of a cutting chain, "Chain 1", is on the UV plane. The projection of the first segment of "Chain 1" intersects with *Top Plane* on edge $E1$. The projection of the last segment of "Chain 1" intersects with *Top Plane* on edge $E2$. Consequently, the cutting chain sequence for "Chain 1" is: Top Right Edge→ E1→Chain 1→ E2 → Bottom Left Edge → Top Right Edge.

Figure 47 illustrates an example of Scenario 3.

The last operation of wire cutting may be to cut off the part or product that is rapid prototyped or fabricated by a rapid prototype process. In order to accomplish this automatically, a cut off plane is required. During the process of finding the initial rotational norm R_N, the cut off plane is the plane that is perpendicular to the initial R_N and is a polygon without concave edges. Because the rotational norm is the initial R_N and the cut off plane is a polygon without concave edges, the intermediate coordinate could be formed by initial R_N and initial R_O. The cut off plane coverage is rectangle coverage.

Figure 48 illustrates the example of a cut off plane for a model pagoda. Because the cut off plane is obtained from a polygon without concave edges, initial R_N and initial R_O are used to build the intermediate coordinate system. The bottom part of the pagoda is perpendicular to the initial R_N and is a polygon without concave edges; it is selected as the cut off plane, as

illustrated in Figure 48. The cutting wire orientations will be exactly same with the vector $O_P = initial\ R_N \times initial\ R_O$.

It should be understood that embodiments of our method may be implement on a computer 1 or computer system as shown in Figure 16. For example, software may be configured to be stored on memory 2 and run by a processor 3 that implements an embodiment of our method for rapid prototyping. The software may be configured to receive input from one or more input devices 4 connected to the processor and may send output data via the processor to one or more output devices 5. The input devices may be, for example, scanners, measurement devices, sensors, detectors, keyboards, key pads, or a computer mouse. Output devices may be, for example, speakers, monitors or displays. An example of a computer system that may utilize an embodiment of our method is shown in Figure 16. The processor 3 may be configured to communicate with and control the actions of a WEDM to control rapid prototyping of a part or device. Alternatively, the computer system may be a component of a WEDM system or WEDM.

For example, a WEDM-RP algorithms may be implemented in VC++.net 2005 and tested on an Inter® Core™2 Duo 2.60GHZ processor personal computer, running Windows XP operating software. The software accepts ASCII STL files as input and outputs the Numerical Control (NC) code. The following are also considered as input parameters for the six-axis WEDM: taper angle, the distance between UV and XY planes, STL file accuracy level, maximum height and maximum width, and wire path incremental accuracy. The taper angle may be the maximum angle to which the cutting wire can rotate from its neutral position. The STL file accuracy level is used to deal with round-up errors in the co-planar triangle combination procedure. The distance between the UV and XY planes, and the maximum height and maximum width of the six-axis WEDM are the parameters used to generate wire path.

Due to the requirement of a polygon-clipping operation in a tangent visibility algorithm, the polygon libraries in Computational Geometry Algorithms Library (CGAL) may be used to improve computation speed. Figure 49 illustrates a present preferred software structure for the WEDM-RP system. Seven major modules were implemented for this WEDM-RP. The file organization module was used to organize the input ACSII STL file into the data structure used in WEDM-RP. The AAG simplification module was used to simplify the input polyhedral geometry into planar polygons. The intersection graph module was used to calculate the intersection graph for each planar polygon in the input geometry. The tangent visibility module solved the global tangent visibility problem based on the intersection graphs generated from the intersection graph module. In this module, CGAL libraries were used to finish the polygon-clipping operations. The manufacturing orientation module determines the optimal manufacturing orientation for the input geometry. NC codes drive the WEDM machines to fabricate the final product. The visualization module was built to help visualize the intermediate and final result in the WEDM-RP system. This module generated Visual Basic for Application (VBA) codes, which were then executed in Solidwork® 2008 software to generate drawings automatically. For example, the drawings for the intersection graphs and tangent visibility results were all generated automatically by the VBA codes produced by the WEDM-RP system. This visualization function is used to help the user understand and verify the algorithms' output.

Several CAD models were created and STL files generated to verify the algorithms of a WEDM-RP system. The tangent visibility algorithms were verified by a group of similar geometries.

Part orientation algorithms may be used to determine the optimal setup orientations for the given geometry and calculate number of setup required to finish the final product. Figure 50

illustrates a slot part with its coordinate system. The part orientation algorithm may be configured to determine that this slot part requires one setup and two rotational operations. Recall that the number of rotational norms represents the number of setups, and under each rotational norm, the number of rotational orientations indicates the rotational axis movement (see Chapter 5 for detailed information). Figure 51 provides the setup orientation and rotational orientation results for the slot part. The slot part will be setup along $R_N(1)$, and the rotational axis will have two positions, $R_O(1)$ and $R_O(2)$ to finish all fabrication operations. Figure 52 illustrates the wire trajectory result for $R_N(1)R_O(1)$ coordinate. The wire trajectory information will be transformed into final manufacturing coordinates in NC generation module.

Figure 53 illustrates an inner feature part with its coordinate system. The part orientation algorithm determined that this part required one setup and two rotational operations. Figure 54 provides the setup orientation and rotational orientation results for the inner feature part. The part was set up along $R_N(1)$, and the rotational axis had two positions, $R_O(1)$ and $R_O(2)$, whereby all the fabrication operations were finished.

Figure 55 illustrates a model pagoda, a more complex part, with its coordinate system. The part orientation algorithm determined that this part required one setup and four rotational operations. Figure 59 provides the setup orientation and rotational orientation results for the pagoda. The pagoda was set up along $R_N(1)$, and the rotational axis had four positions, $R_O(1)$, $R_O(2)$, $R_O(3)$ and $R_O(4)$, whereby all the fabrication operations were finished. Note that though the pagoda as designed along the X-axis in its design coordinate and the NC code generation required the part to rotate around the Y-axis, the WEDM-RP program found the correct design orientation and found the good setup orientation corresponding to the rotational orientations for fabricating the pagoda.

Non-prismatic geometries were also examined. Figure 57 illustrates a model hourglass. The global tangent visibility analysis shows that all triangles on the model hourglass are globally tangent visible. However, due to existence of the incorrectness in edge convexity in the input STL file, it required 17 setups to finish manufacturing the whole hourglass model. A complex pagoda was also evaluated similarly to the hourglass model of Figure 57.

Table 9 shows the total computation time for different model geometries. The prismatic geometries require less unit computation per facet than non-prismatic geometries. Because the prismatic geometries do not require the error elimination procedure to deal with incorrectness in edge convexity error in STL file, the unit computation time is much less than non-prismatic geometries.

Table 9; Computation results of five CAD models

	Model	Number of facets	Computation Time	Unit Time
Prismatic geometries	The slot part	28	6 sec	0.2143 sec/facet
	Inner feature example	44	13 sec	0.2955 sec/facet
	Model pagoda	140	35 sec	0.2500 sec/facet
Non-Prismatic geometries	Hourglass	228	694 sec	3.0439 sec/facet
	Complex model pagoda	1382	2218 sec	2.8640 sec/facet

The advantages of conventional processes are the well developed methodology and low material and manufacturing cost. High process engineering cost consumes the cost efficiency of conventional processes when facing with low volume production. We have determined that our method of WEDM-RP solves this problem by creating automatic process plans and production setup plans and decreasing human or worker involvement. A general conventional process cost model was used to identify the cost savings that may be made by using embodiments of our rapid prototyping methods. A general unit cost model for RM is presented as follows:

$$Unit\ Cost = \frac{Engineering\ Cost}{N} + Material\ Cost + \frac{Manufacturing\ Cost}{N}$$

Where $$Manufacturing\ Cost = \left(\frac{C_{machine}}{8}^{1} + C_{maintain} + C_{labor} \right) \times \frac{t_{proc}}{t_{total}} + C_{tool} \frac{t_{proc}}{t_{tool}}$$

1: assume the machine depreciate rate is $\frac{C_{machine}}{8}$

$C_{machine}$ is the machine cost

$C_{maintain}$ is the maintenance cost

C_{labor} is the labor cost

t_{proc} is process time

t_{total} total available time $= 24\ {}^{hr}/_{day} \times 5\ {}^{day}/_{week} \times 50\ {}^{week}/_{year} \times u$

u is machine utilization

C_{tool} is tool cost (if applicable)

t_{tool} is tool life

$Engineering\ Cost = C_{eng} \times t_{eng}$ (if applicable)

N is the batch size

This unit cost model is applicable for both additive processes and subtractive processes. The unit cost related with machine and labor will be a portion ($\frac{t_{proc}}{t_{total}}$) of the total machine and labor cost. Looking closely at the cost equation, $\frac{Engineering\ Cost}{N}$ is the portion of the cost that WEDM-RP intends to decrease. WEDM-RP provides methodologies to create tooling plan, tool path and fixtures, and very little to no human interaction is necessary. As a result, the engineering time is trivial .

Figure 8 illustrates the selected part for a cost analysis. Two processes are evaluated for producing the pagoda, selective laser sintering, and an embodiment of our WEDM-RP. The main assumptions are provided in Table 10.

Table 10; Main cost assumptions used in this research

Activity	SLS	WEDM-RP
Machine	$525,000	$150,000[1]
Machine Maintenance	$31,500	$2,000
Labor Cost	$31,430	$40,000
Machine utilization	33%	33%
Material Cost	$84/Kg	$2.1[3]
Density of material g/cm^3	0.5	2.82
Engineering Cost ($/hr)	0	41.53
Engineering time (hr)	0	0.1hr[4]
Tool Cost	NA[2]	$163[5]
Tool Life (hour)	NA	100[5]
Process Time	1.78 hr[6]	3.28 hr[7]

Notes:
1. Mitsubishi FA-10S
2. Not applicable
3. The bar is Alloy 6061 round bar $2"(dia) \times 3"(long)$
4. Estimation time
5. 0.014" Brass wire, tool life =100 hr.
6. Process time from calculation based on Ruffo's model
7. Process time from Estimated cutting area

We collected data from an industry website to estimate the fabrication cost of the pagoda using SLS process. Furthermore, we calculated the SLS process cost based on Ruffo's model and calculated the process cost for WEDM as well. Figure 15 illustrates the cost comparison between several sources. The result in Figure 15 shows that WEDM process has cost advantages when the fabrication volume is small, for this pagoda example, the volume is less than 15.

Total cost is the only consideration in Figure 15, the finish product quality, such as accuracy and material issue are not included. Table 11 summarized the RP process accuracy from different processes. It should be understood that the conventional subtractive processes, such as CNC milling and WEDM, have the highest accuracy.

Table 11; A comparison of RP processes.

	Material	Cutting Velocity	Accuracy
Stereolithography	Resin Plastic	0~40 in/sec	±0.004 in
Laser Sintering	Plastic, Metal powder	0.4 in/hr ~0.3 in^3/hr	± 0.006 in
Layer Laminated Manufacturing	Thin paper	0.07~0.47 in/hr	± 0.01 in
Three-dimensional printer	Chemical , stainless steel powder	1.5 in^3/hr or higher	± 0.002 in
Laser Generation	Plastic, metal powder	2.5 in^3/hr	± 0.01 in
CNC Milling	Machinable materials	Depends on material	± 0.001 in
WEDM RP	Electric conductive material	Depends on material	± 0.001 in

It should be understood that the advantages obtained by utilizing embodiments of our method include permitting conventional processes to be profitable even while making small volume product. Embodiment of our WEDM-RP method provides a possibility for applying conventional process, such as WEDM, as rapid prototyping tools. Use of such embodiments can decrease the total engineering time by automatically generating process plan and decreasing human interaction. Cost comparison results also show that WEDM has cost advantages when production volume is less than 15. Furthermore, WEDM can provide higher accuracy product than normal additive rapid prototyping processes.

It should be understood that other variations to the present preferred methods for rapid prototyping and embodiments of rapid prototyping mechanisms discussed above may be made, as may be appreciated by those of at least ordinary skill in the art. For example, other examples of present preferred methods for rapid prototyping and present preferred embodiments of rapid prototype machine apparatuses may be appreciated from , *Wire Electrical Discharge Machining*

(WEDM) As A Subtractive Rapid Manufacturing Tool, filed as U.S. Provisional Patent Application Serial No. 61/304,565. The entirety U.S. Provisional Patent Application Serial No. 61/304,565 is incorporated by reference herein as illustrating and describing present preferred embodiments of the above discussed methods and rapid prototype machines.

While certain present preferred methods of prototyping parts have been discussed and illustrated herein, it is to be distinctly understood that the invention is not limited thereto but may be otherwise variously embodied and practiced within the scope of the following claims.

We claim:

1. A method of rapid prototyping a product comprising:

identifying a product geometry to prepare a geometric model;

preparing a fabrication process;

generating a cutting path based on NC code; and

fabricating the product using a linear cut process.

2. The method of claim 1 wherein the linear cut process is conducted by a Wire Electrical Discharge Machining (WEDM) machine that is a five axis Electrical Discharge Machining (EDM) machine or six or more axis wire EDM machine.

3. The method of claim 1 wherein the linear cut process is a process selected from the group consisting of wire electrical discharge machining , water jet cutting, laser machining, and hot wire machining.

4. A method of rapid prototyping a product comprising:

identifying a product geometry;

selecting a rapid prototyping system;

preparing a first model for fabrication;

preparing a first fabrication process that takes input and generates tangent visibility for each facet identified in the input

identifying a part orientation;

generating a modeling process for fabricating the product from stock material;

generating at least one cutting path; and

fabricating the product using a linear cutting mechanism.

5. The method of claim 4 wherein the linear cutting mechanism is a five axis wire electrical discharge machining (WEDM) machine, a siz axis WEDM machine or a multiple axis WEDM machine.

6. The method of claim 4 wherein the input is at least one STL file or wherein the input is at least one faceted CAD model file or a boundary model, facets in the CAD model file being any polygonal facets used to create a polygonal model, the at least one faceted CAD model generated from a boundary model.

7. The method of claim 4 wherein the generation of the modeling process is comprised of determining the tangent visibility and wire range based on the input and determining the product orientation based on product geometry information provided in the input for each facet of the product.

8. The method of claim 4 wherein the first fabrication process is the only process needed to be run to fabricate the product.

9. The method of claim 4 wherein the linear cutting mechanism is a four, five or six axis laser CNC machine.

10. The method of claim 4 wherein the linear cutting mechanism is a water jet cutting mechanism, a laser machining mechanism, a hot wire machining mechanism or a gamma knife mechanism.

11. The method of claim 4 further comprising utilizing a three dimension tool paths to prepare at least one of the first fabrication process and the second fabrication process.

12. The method of claim 4 further comprising decomposing part geometries for the product for at least one of the prepared fabrication processes.

13. The method of claim 4 wherein preparing the first model comprises adding at least one support to the first model prior to tool path planning for the first fabrication process.

14. The method of claim 4 further comprising severing at least one support.

15. The method of claim 4 further comprising preparing at least one visibility method to determine if an axis of rotation is feasible.

16. The method of claim 4 wherein the rapid prototyping system is a wire electrical discharge machining rapid prototyping system.

17. The method of claim 4 wherein the at least one cutting path is comprised of a plurality of wire paths and wherein the wire paths include convex edges of the part and are generated to minimize B-axis orientations for fabrication of the product.

18. A machinating apparatus configured for rapid prototyping comprising:

at least one linear cutting mechanism;

at least one input device;

at least one controller, the at least one controller comprised of at least one processor connected to at least one memory, the at least one controller connected to the at least one cutting mechanism and the at least one input device; and

the at least one controller configured to control the at least one cutting mechanism, the at least one controller configured to identify a geometry of a product, prepare a first model for fabrication; prepare a first fabrication process that takes input received from the at least one input device and generates tangent visibility for each facet identified in the input; identify a part orientation, generate a modeling process for fabricating the product from stock material, generate at least one cutting path, and actuate the cutting mechanism to move along the at least one cutting path to fabricate the product.

19. The machining apparatus configured for rapid prototyping of claim 18 wherein the at least one linear cutting mechanism is a water jet cutting mechanism, a laser machining mechanism, a hot wire machining mechanism or a gamma knife mechanism.

20. The machining apparatus configured for rapid prototyping of claim 18 wherein the input is comprised of at least one STL file and the at least one cutting path is comprised of a plurality of wire paths and wherein the wire paths include convex edges of the product and are generated to minimize B-axis orientations for fabrication of the product.

21. The machining apparatus of claim 18, wherein the at least one controller is configured to generate a an optimal setup procedure, the setup procedure comprised of a plurality of setup orientations, each setup procedure configured such that a minimum number of B-axis orientations are identical to rotational orientations R_{OS} under a determined rotational norm R_N.

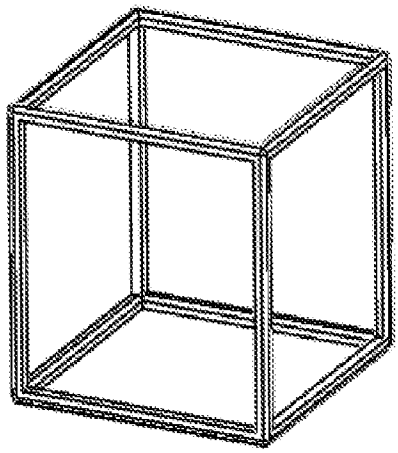

FIGURE 1A

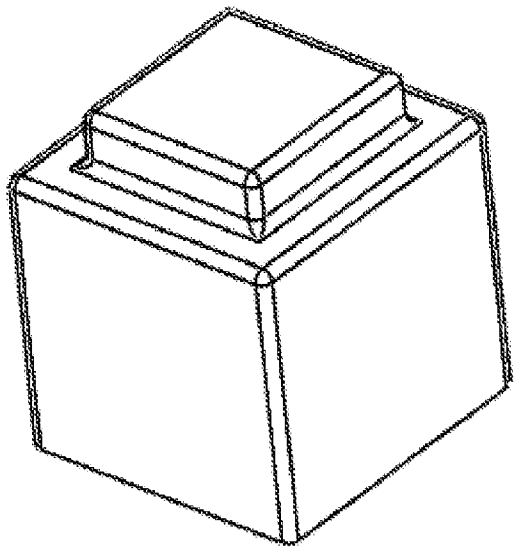

FIGURE 1B

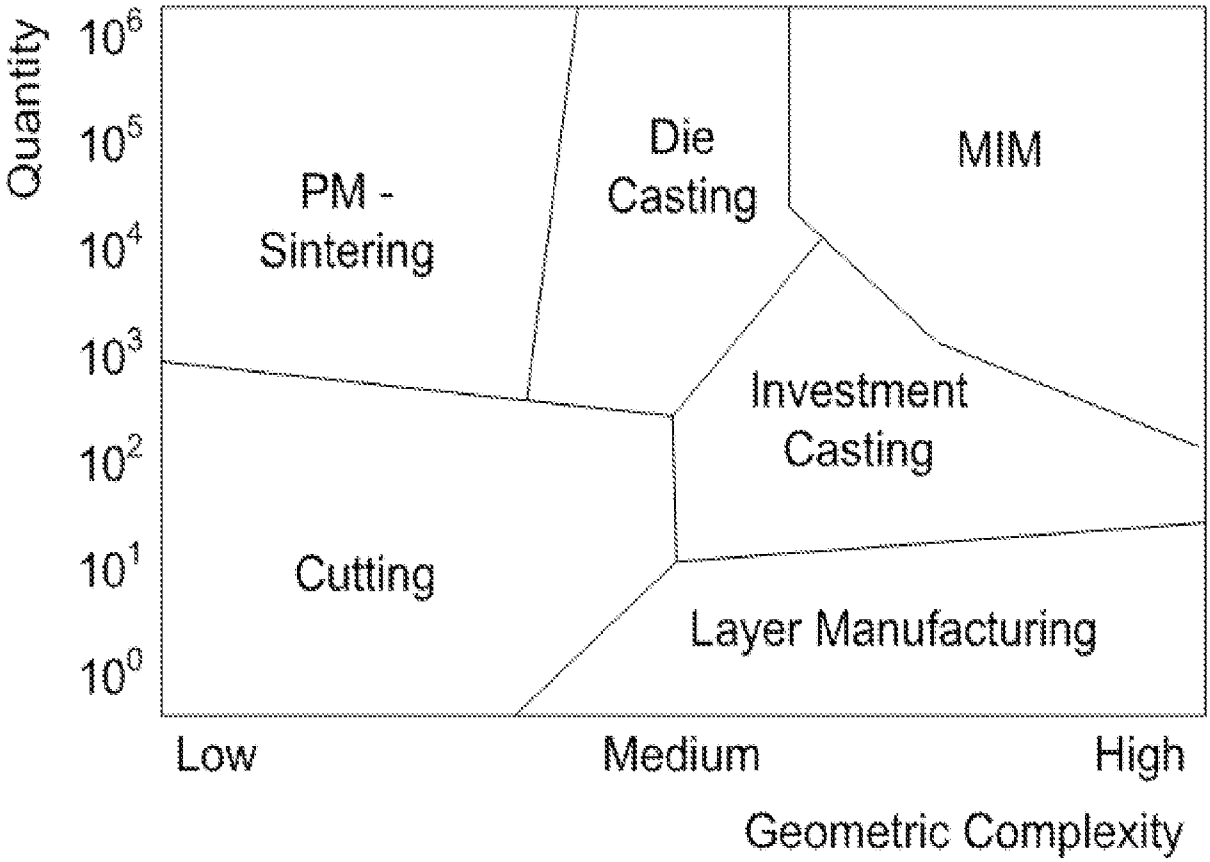
Quantity
10^6
10^5
10^4
10^3
10^2
10^1
10^0
PM - Sintering
Die Casting
MIM
Investment Casting
Cutting
Layer Manufacturing
Low
Medium
High
Geometric Complexity

FIGURE 2

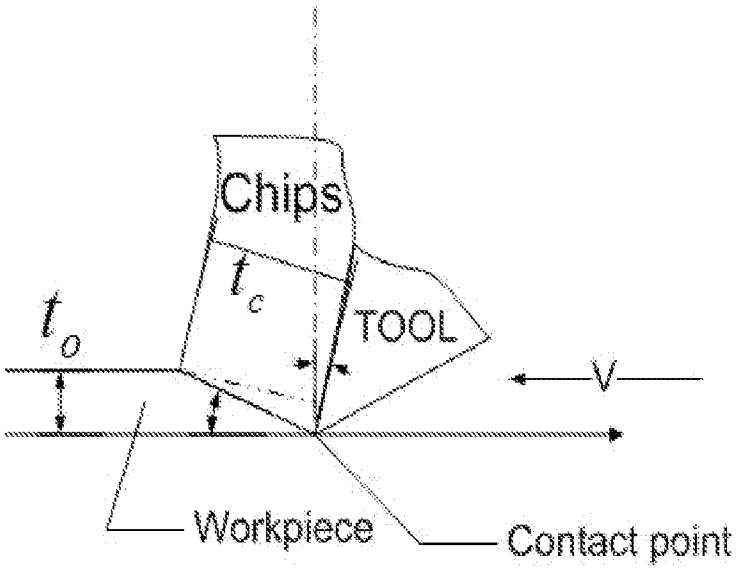

Traditional machining process

FIGURE 3A

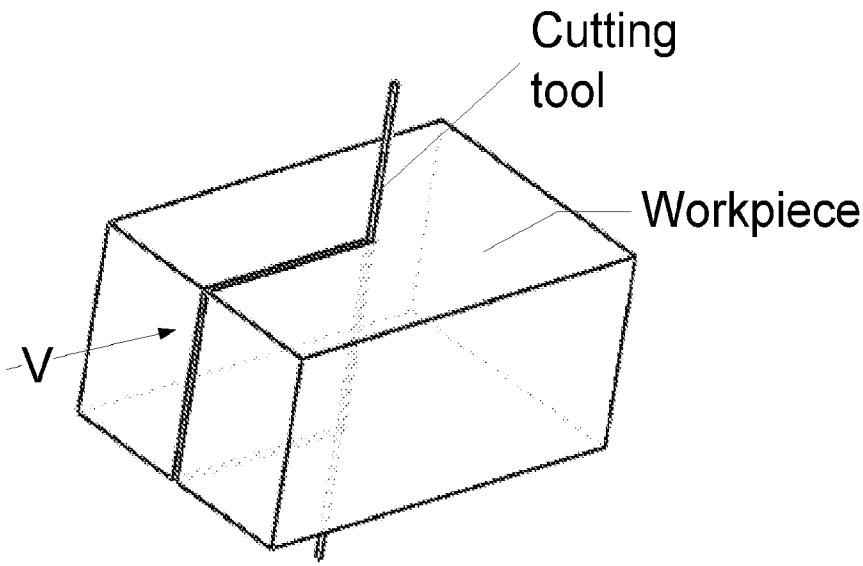

Linear cut process

FIGURE 3B

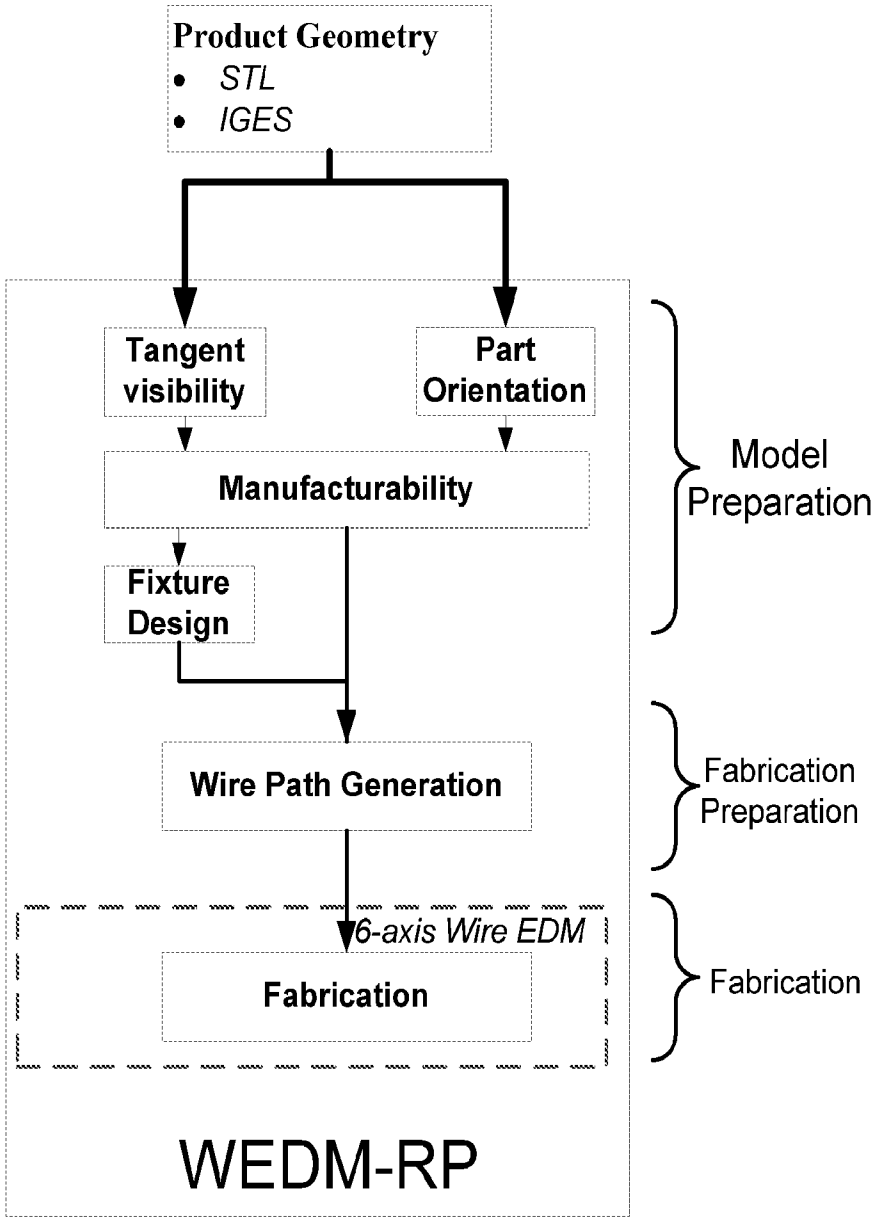
Product Geometry
• STL
• IGES
Tangent visibility
Part Orientation
Manufacturability
Fixture Design
Wire Path Generation
6-axis Wire EDM
Fabrication
Model Preparation
Fabrication Preparation
Fabrication
WEDM-RP

FIGURE 4

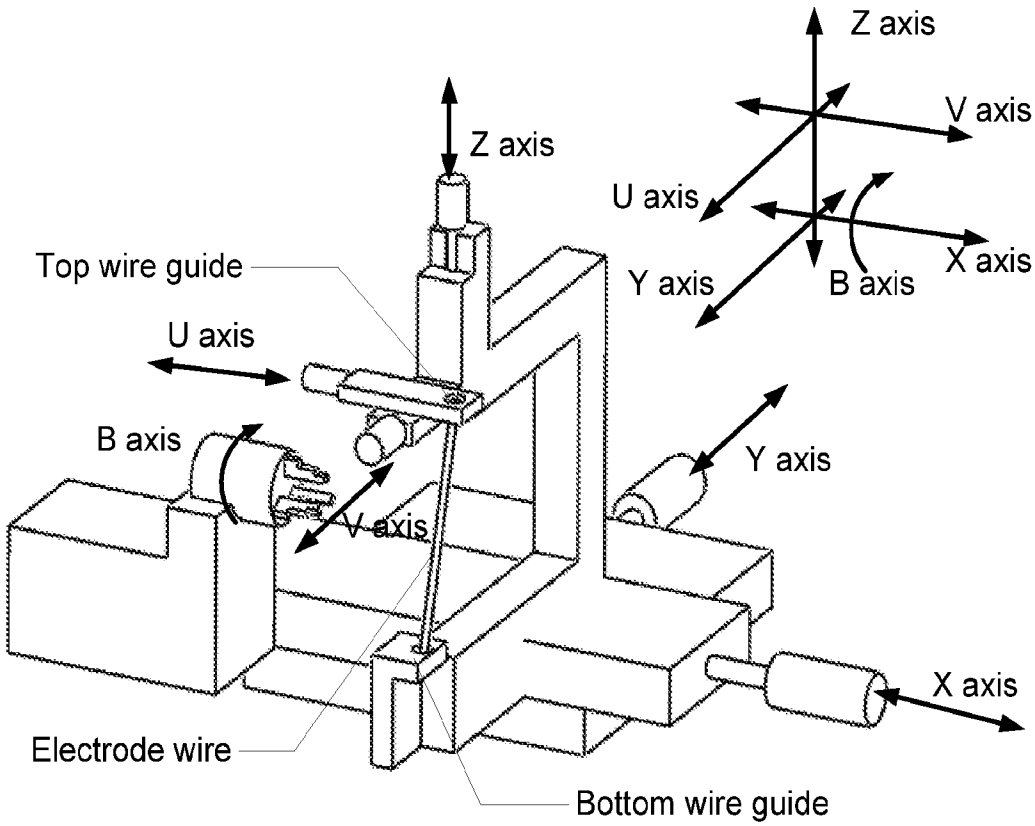
Z axis
V axis
U axis
X axis
Y axis
B axis
Z axis
Top wire guide
U axis
B axis
V axis
Y axis
X axis
Electrode wire
Bottom wire guide

FIGURE 5

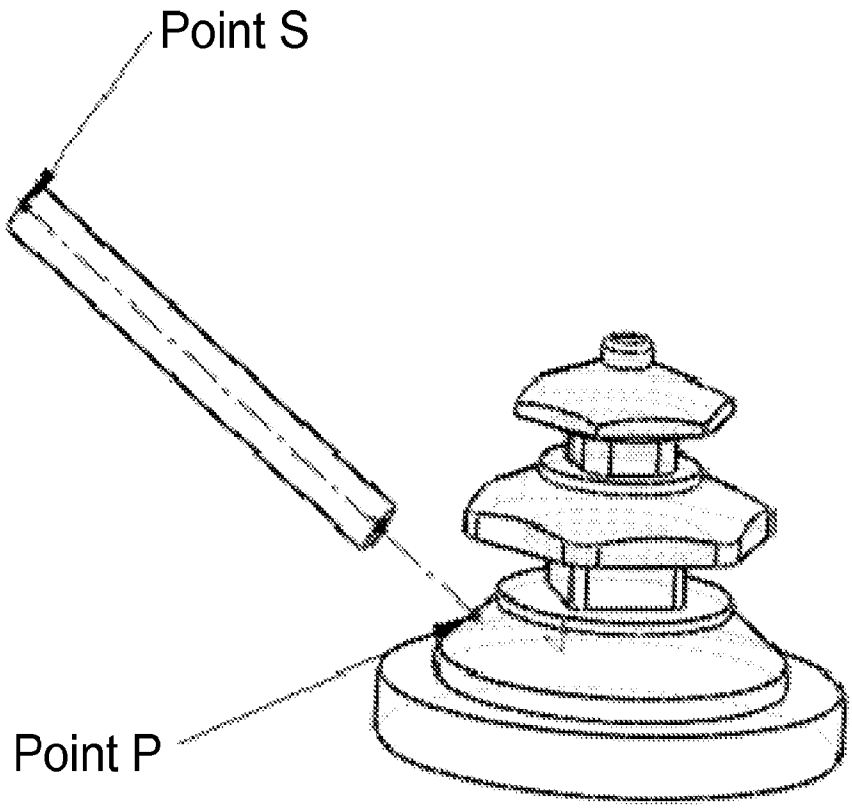

FIGURE 6A

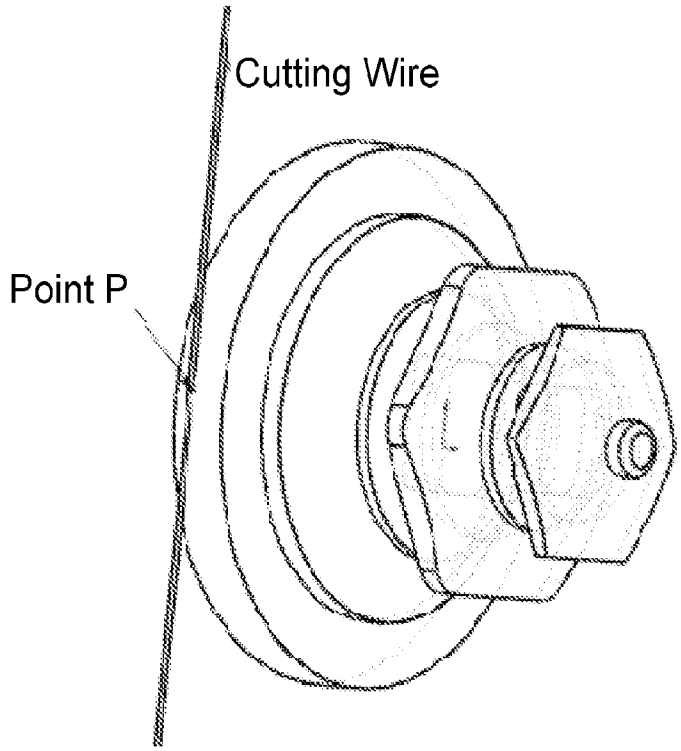

FIGURE 6B

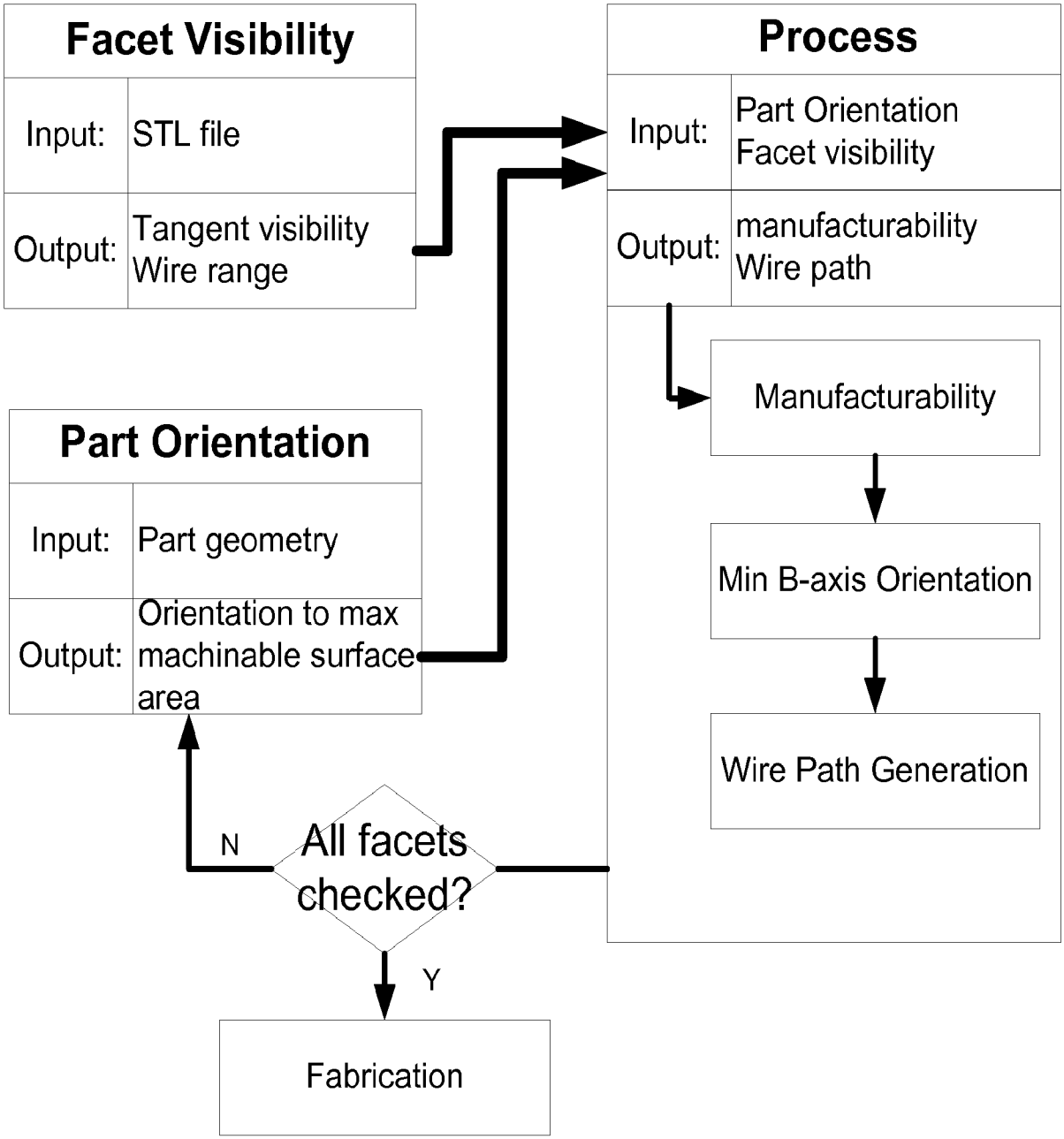
Facet Visibility
Input:
STL file
Output:
Tangent visibility
Wire range
Process
Input:
Part Orientation
Facet visibility
Output:
manufacturability
Wire path
Manufacturability
Min B-axis Orientation
Wire Path Generation
Part Orientation
Input:
Part geometry
Output:
Orientation to max machinable surface area
N
All facets checked?
Y
Fabrication

FIGURE 7

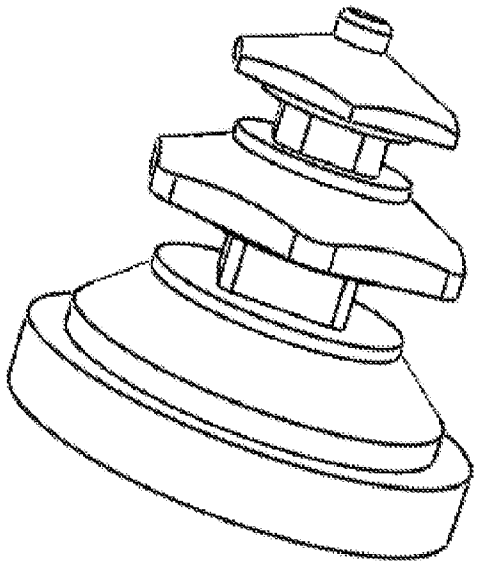

FIGURE 8

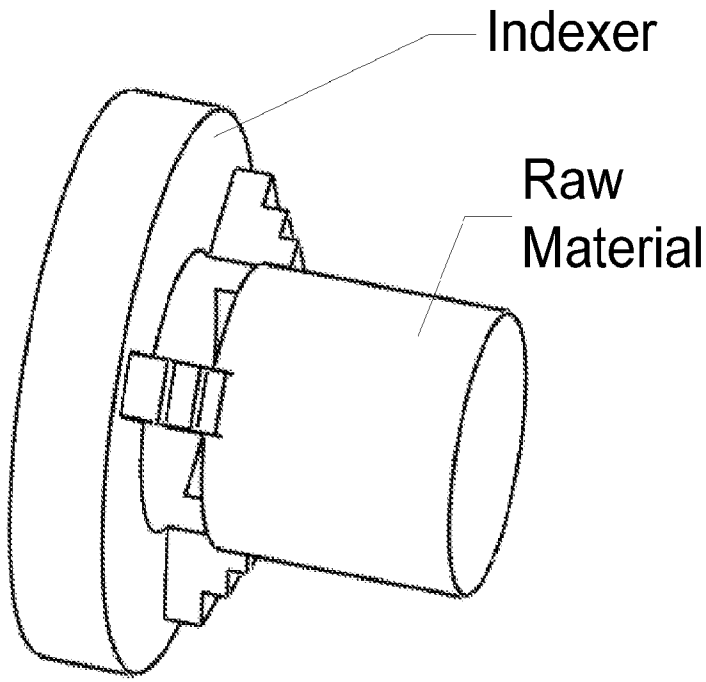

FIGURE 9A

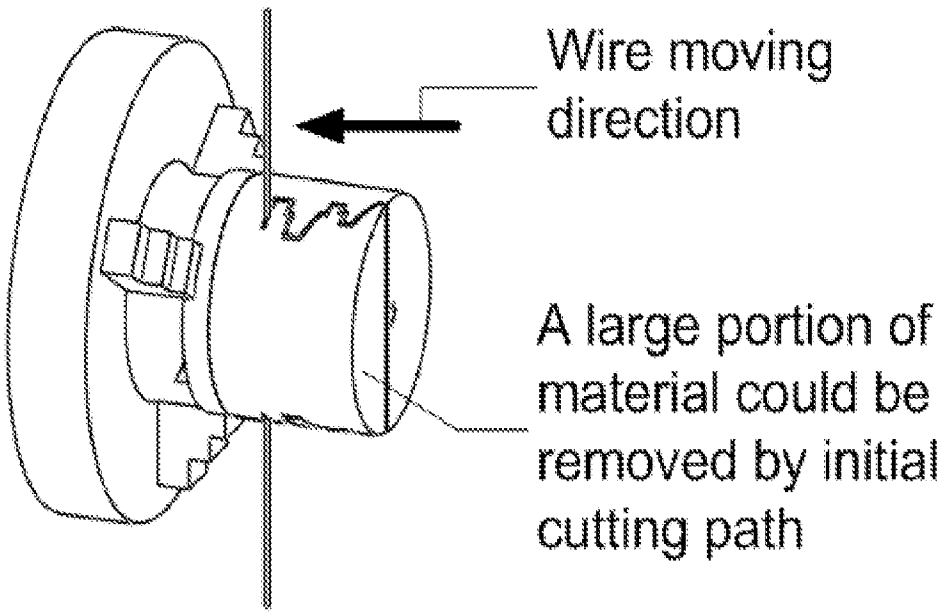

FIGURE 9B

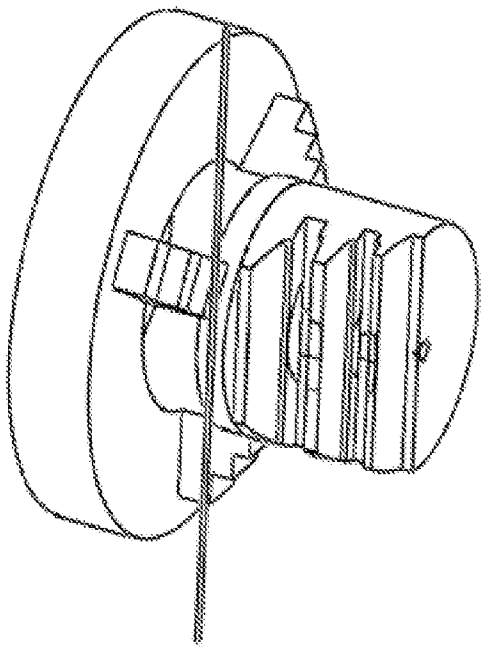

FIGURE 9C

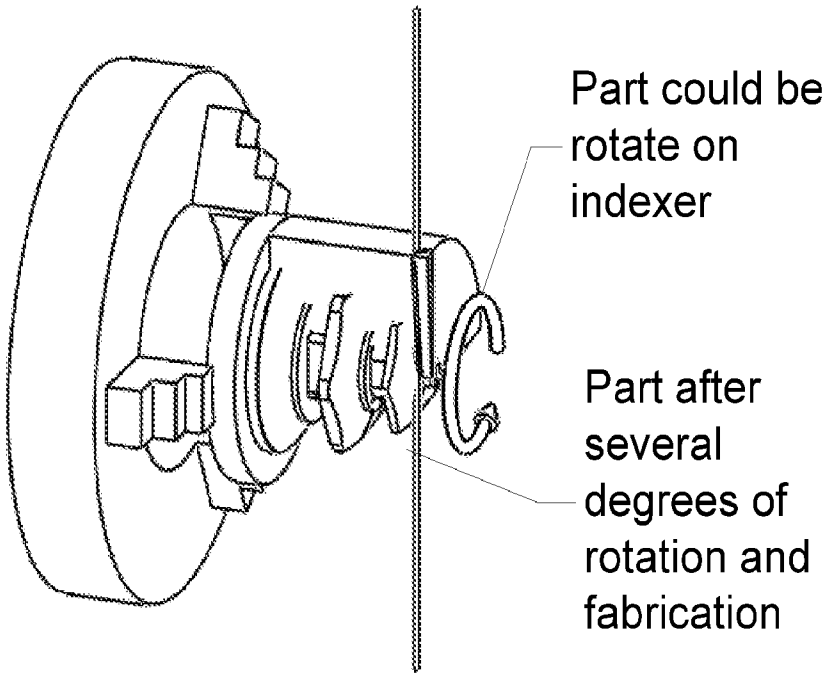

FIGURE 9D

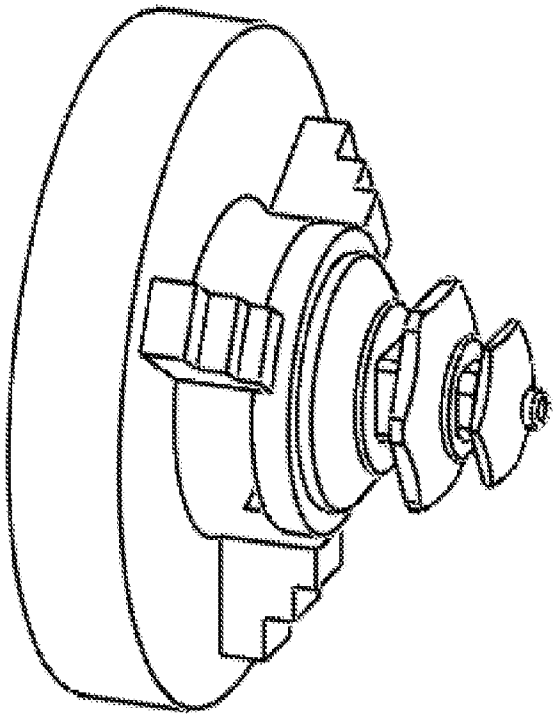

FIGURE 9E

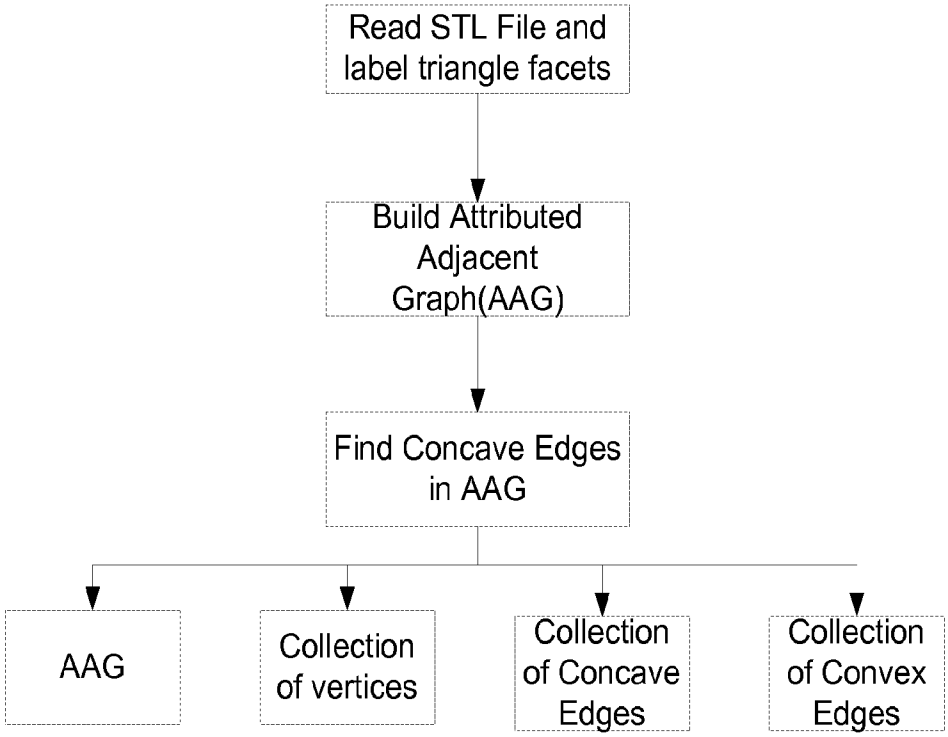
Read STL File and label triangle facets
Build Attributed Adjacent Graph(AAG)
Find Concave Edges in AAG
AAG
Collection of vertices
Collection of Concave Edges
Collection of Convex Edges

FIGURE 10

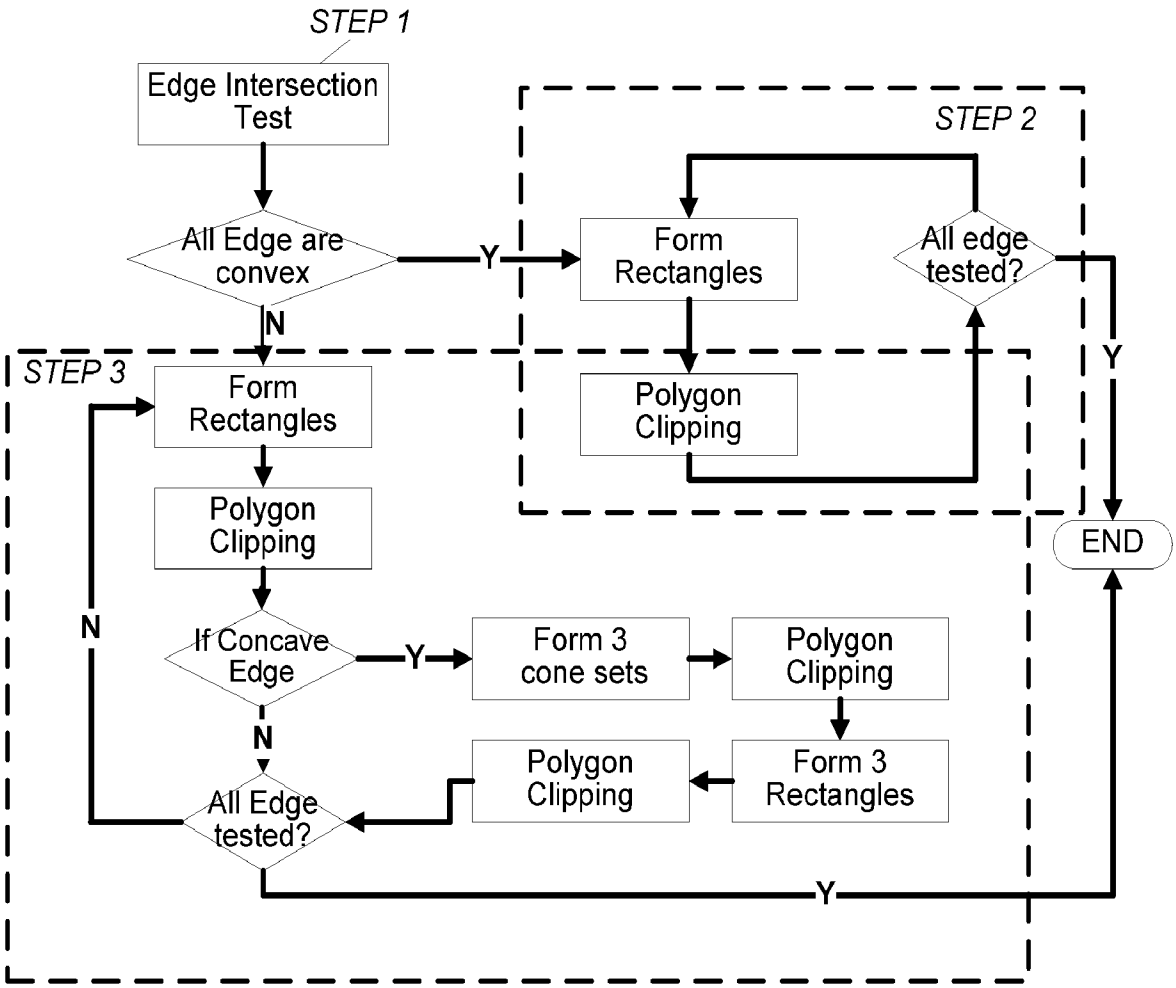
STEP 1
Edge Intersection Test
All Edge are convex
Y
N
STEP 2
Form Rectangles
Polygon Clipping
All edge tested?
Y
END
STEP 3
Form Rectangles
Polygon Clipping
If Concave Edge
Y
Form 3 cone sets
Polygon Clipping
Form 3 Rectangles
Polygon Clipping
All Edge tested?
N
N
Y

FIGURE 11

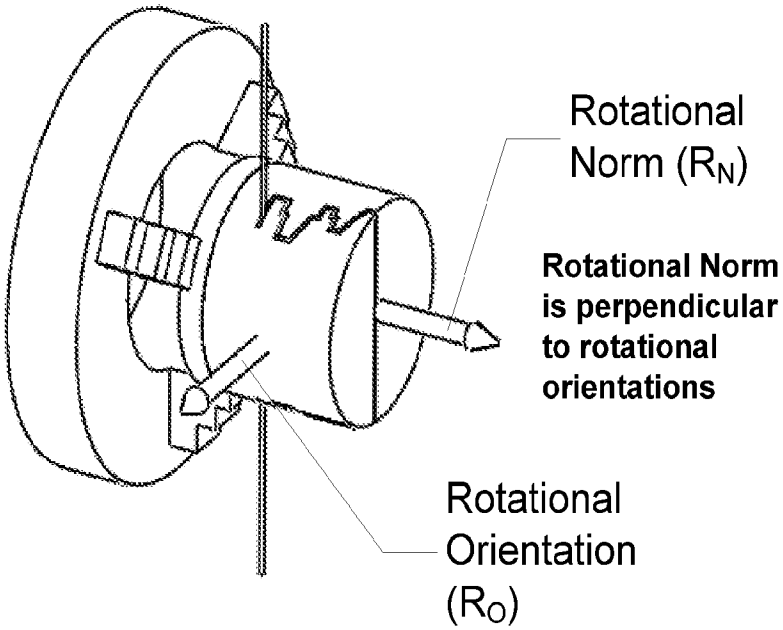
Rotational Norm (R_N)
Rotational Norm is perpendicular to rotational orientations
Rotational Orientation (R_O)

FIGURE 12

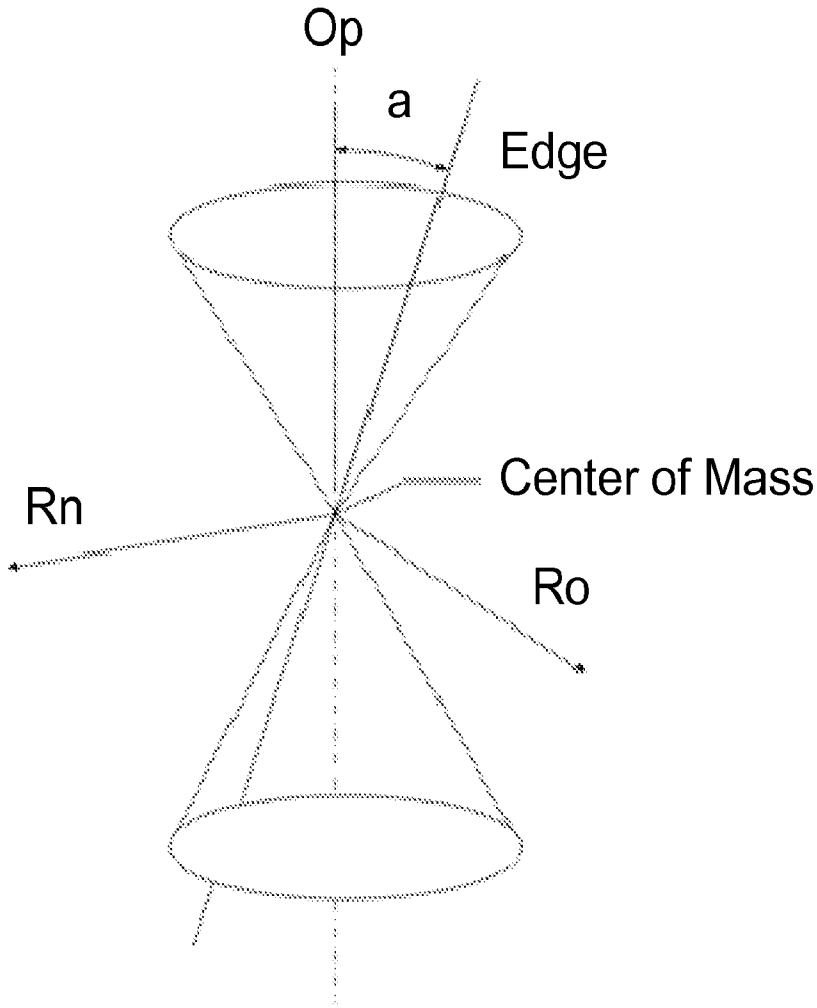

FIGURE 13

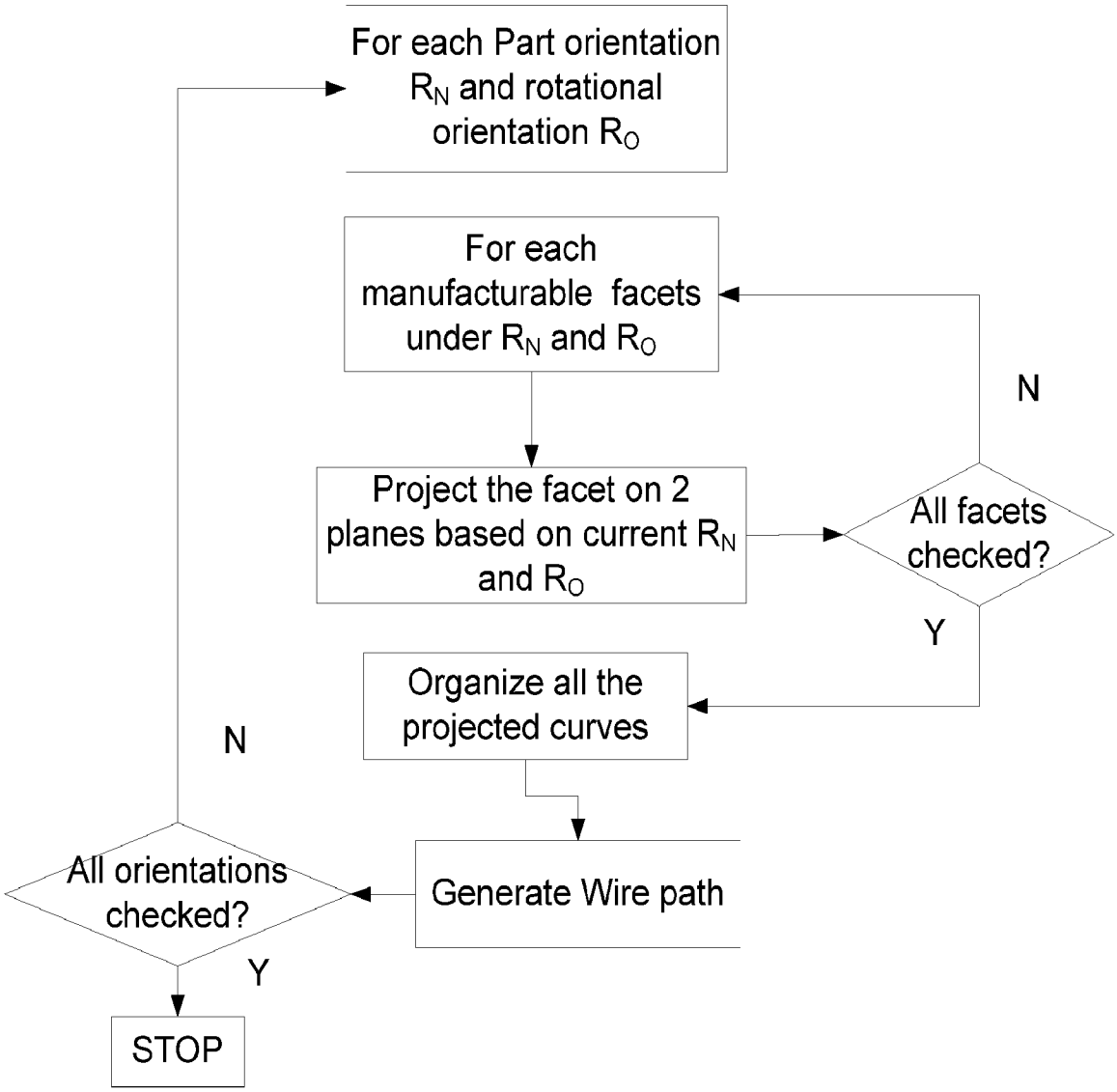
For each Part orientation R_N and rotational orientation R_O
For each manufacturable facets under R_N and R_O
Project the facet on 2 planes based on current R_N and R_O
All facets checked?
N
Y
Organize all the projected curves
Generate Wire path
All orientations checked?
N
Y
STOP

FIGURE 14

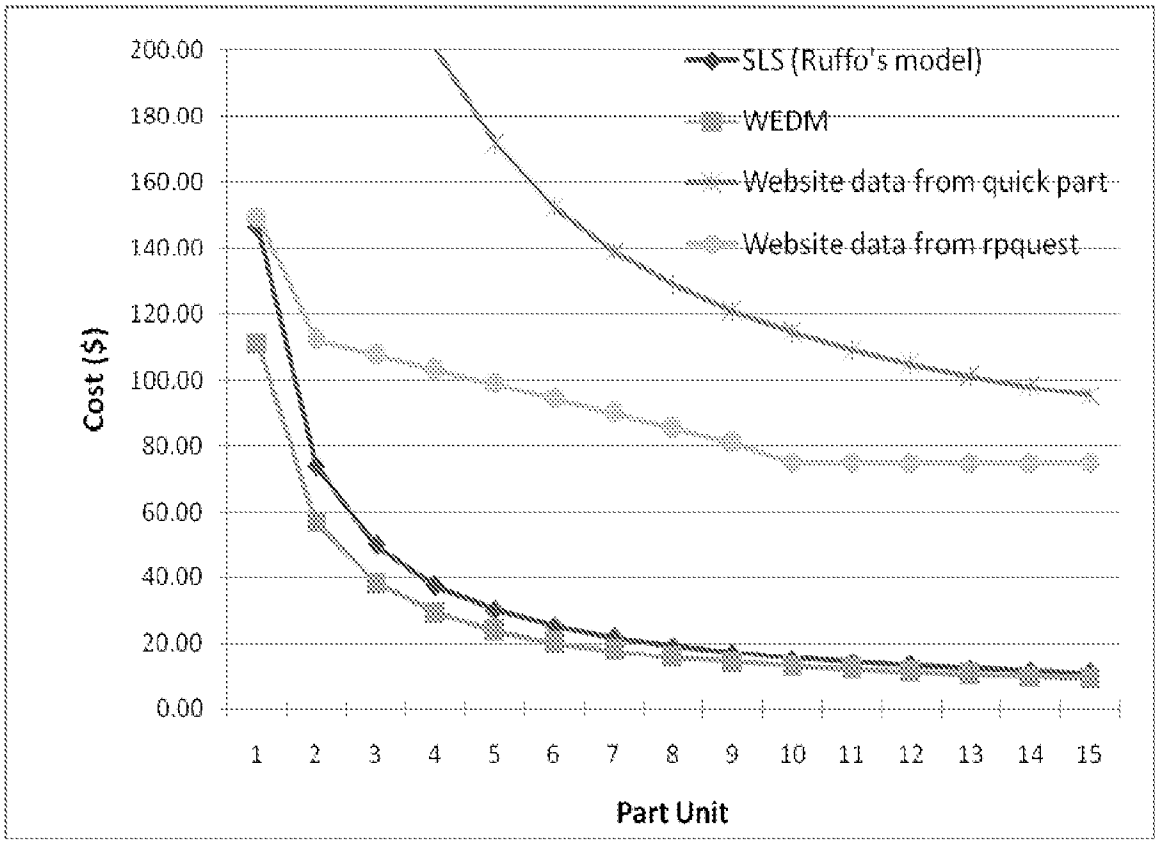
200.00
180.00
160.00
140.00
120.00
100.00
80.00
60.00
40.00
20.00
0.00
Cost ($)
1
2
3
4
5
6
7
8
9
10
11
12
13
14
15
Part Unit
SLS (Ruffo's model)
WEDM
Website data from quick part
Website data from rpquest

FIGURE 15

FIGURE 16

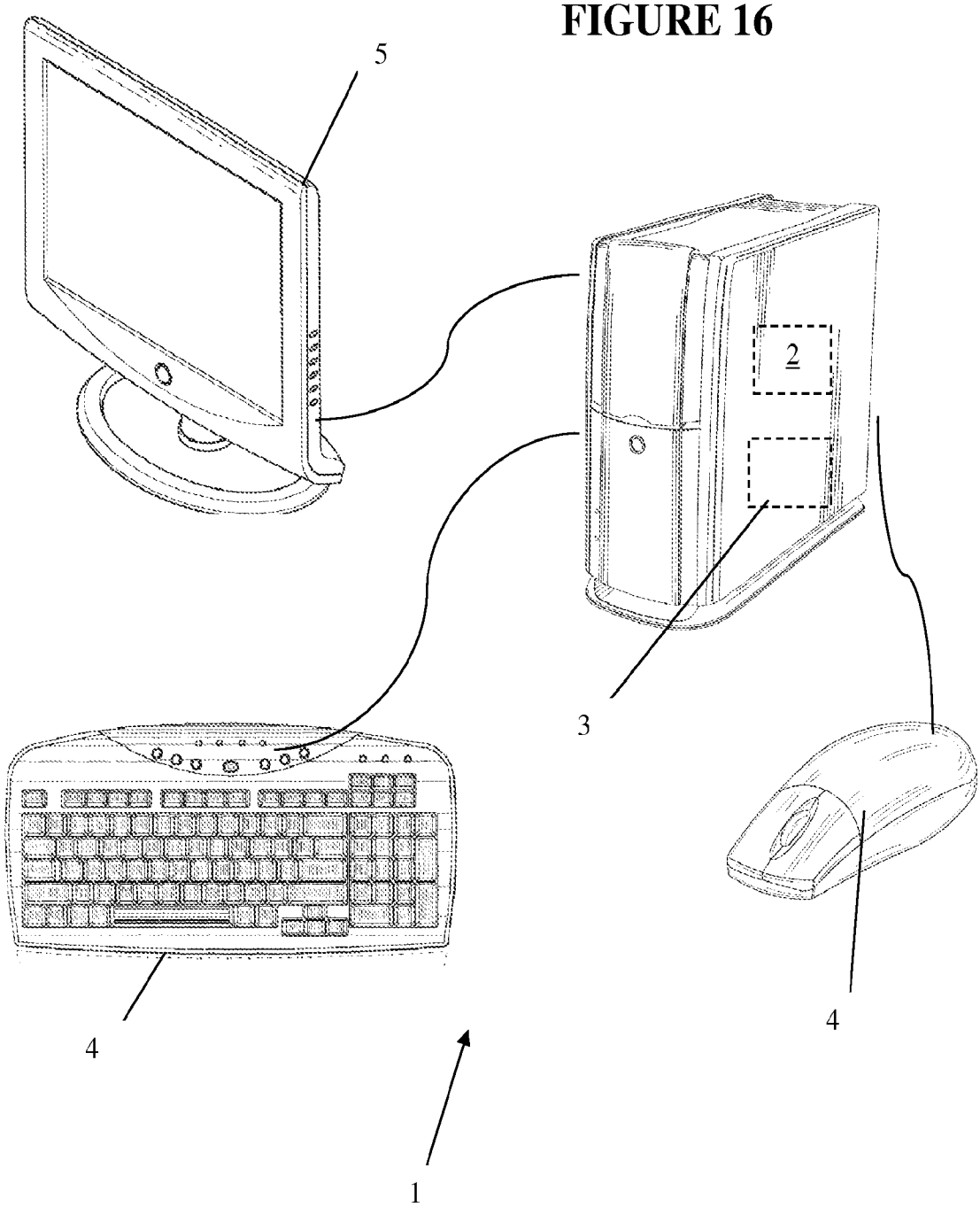

FIGURE 17

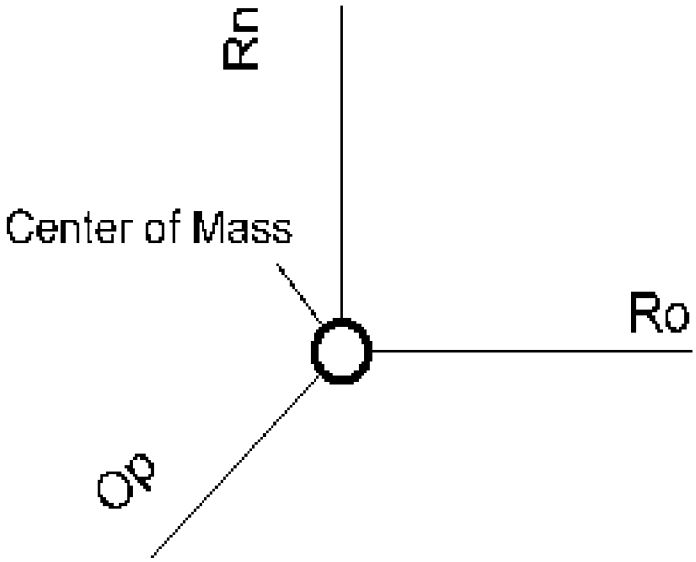

FIGURE 18

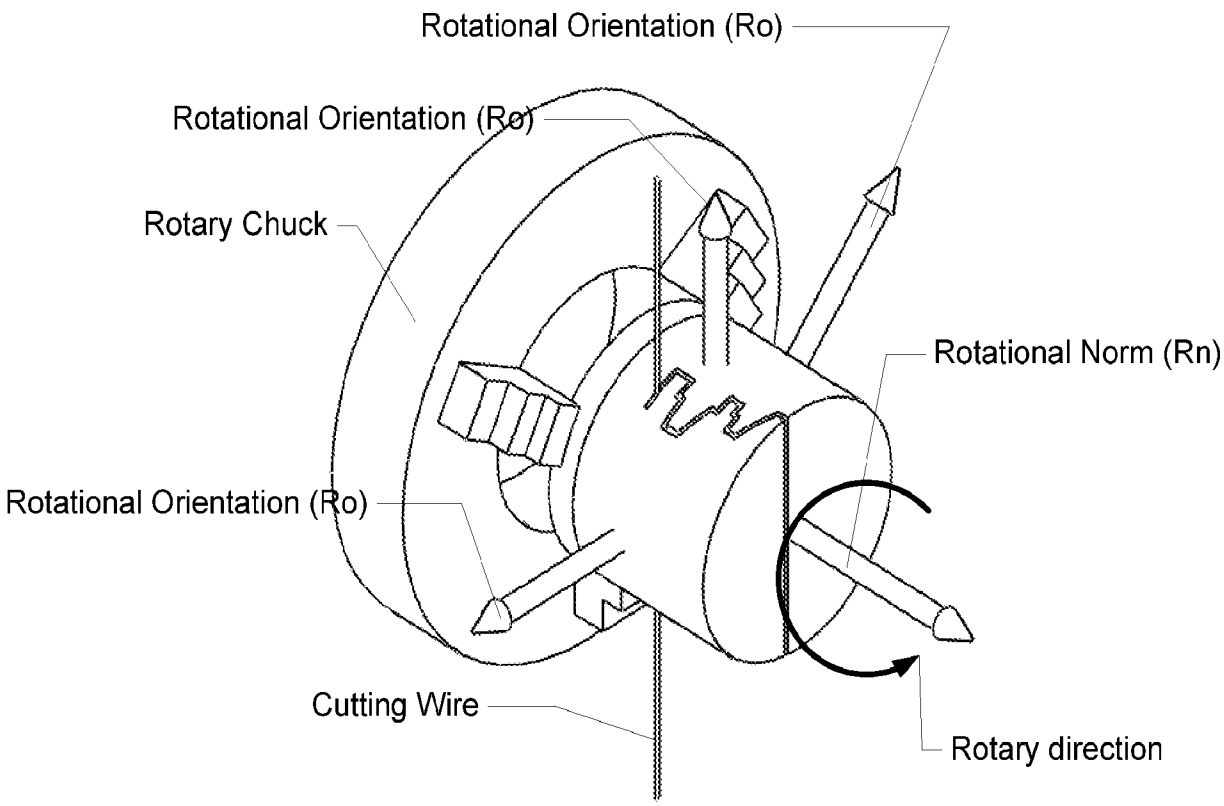

FIGURE 19

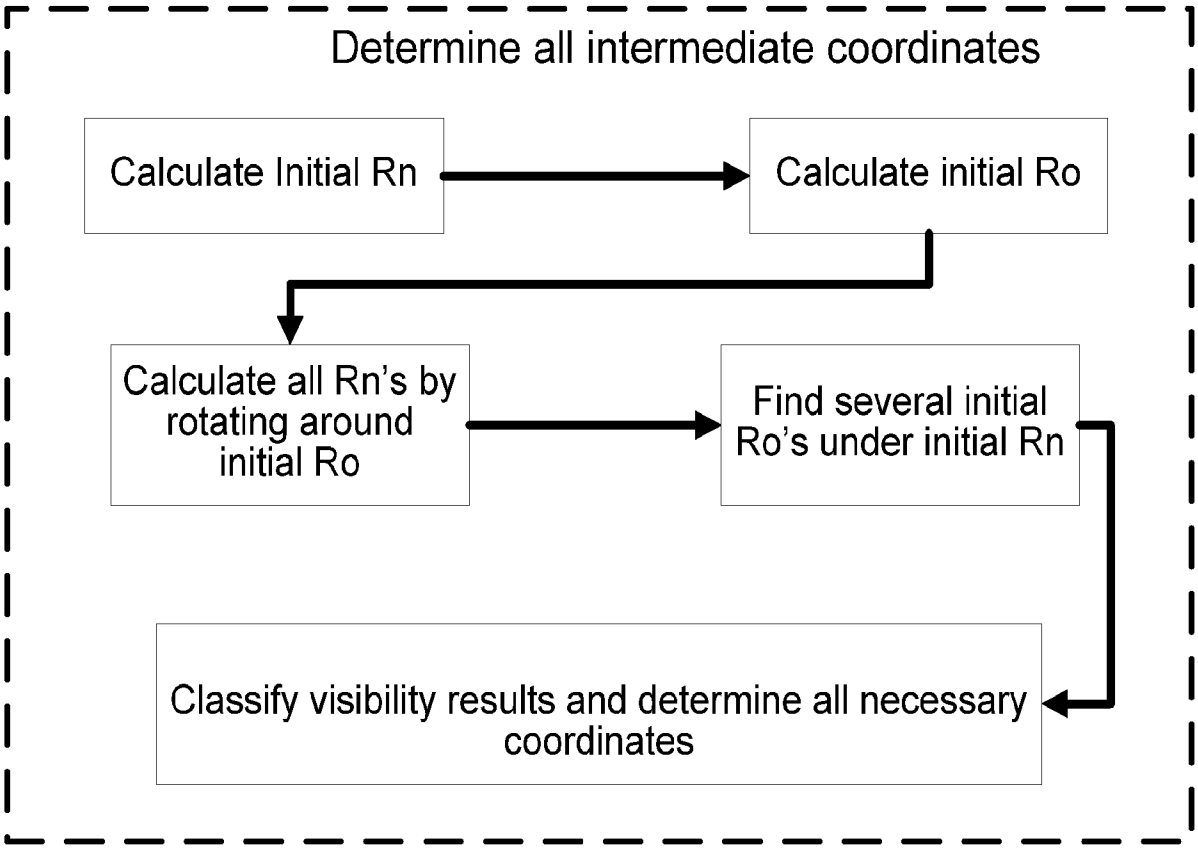
Determine all intermediate coordinates
Calculate Initial Rn
Calculate initial Ro
Calculate all Rn's by rotating around initial Ro
Find several initial Ro's under initial Rn
Classify visibility results and determine all necessary coordinates

FIGURE 20

Calculate Initial Rn

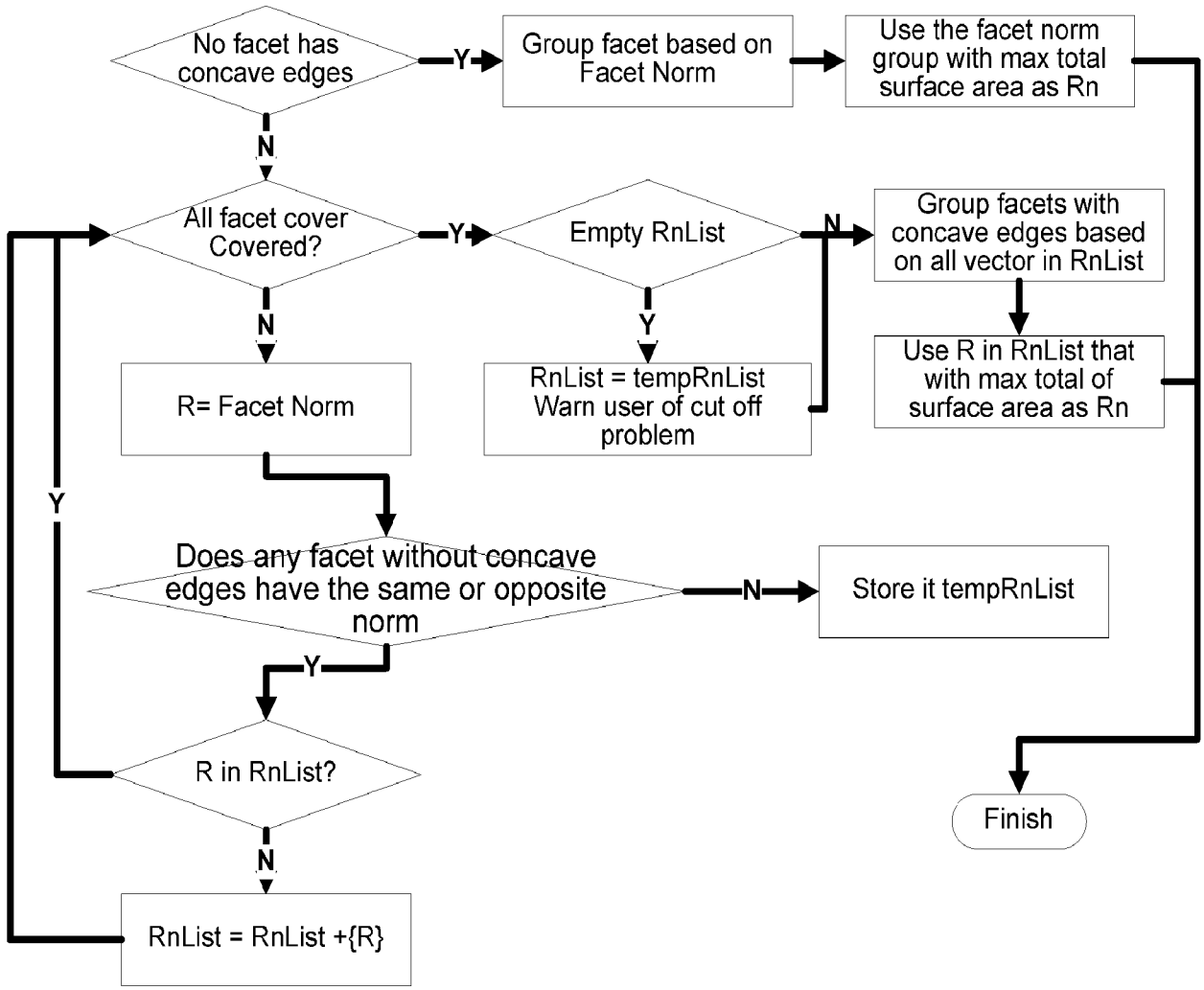

FIGURE 21

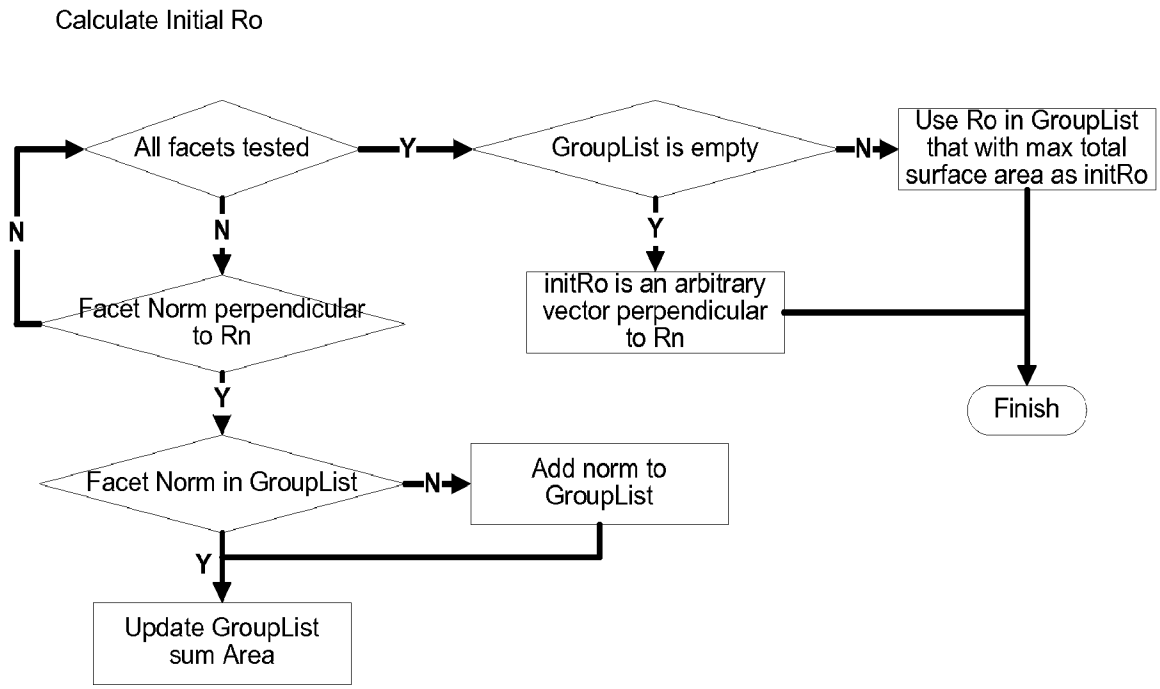
Calculate Initial Ro
All facets tested
Y
GroupList is empty
N
Use Ro in GroupList that with max total surface area as initRo
N
N
Y
Facet Norm perpendicular to Rn
initRo is an arbitrary vector perpendicular to Rn
Finish
Y
Facet Norm in GroupList
N
Add norm to GroupList
Y
Update GroupList sum Area

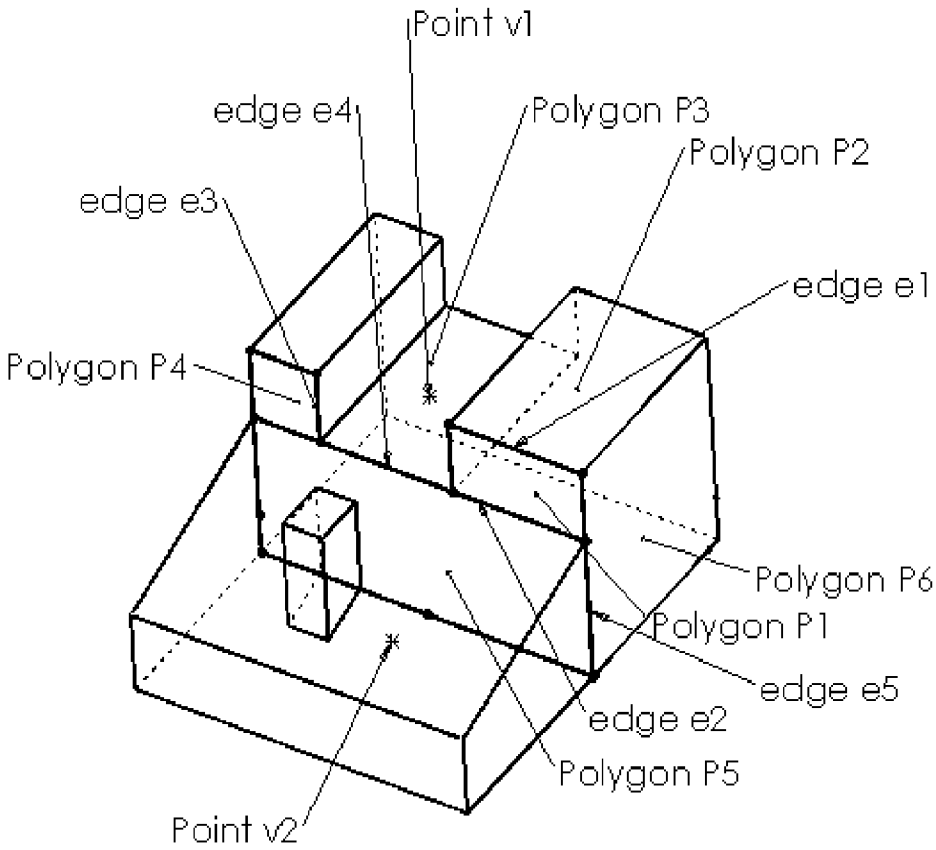
Point v1
edge e4
Polygon P3
Polygon P2
edge e3
edge e1
Polygon P4
Polygon P6
Polygon P1
edge e5
edge e2
Polygon P5
Point v2

FIGURE 22

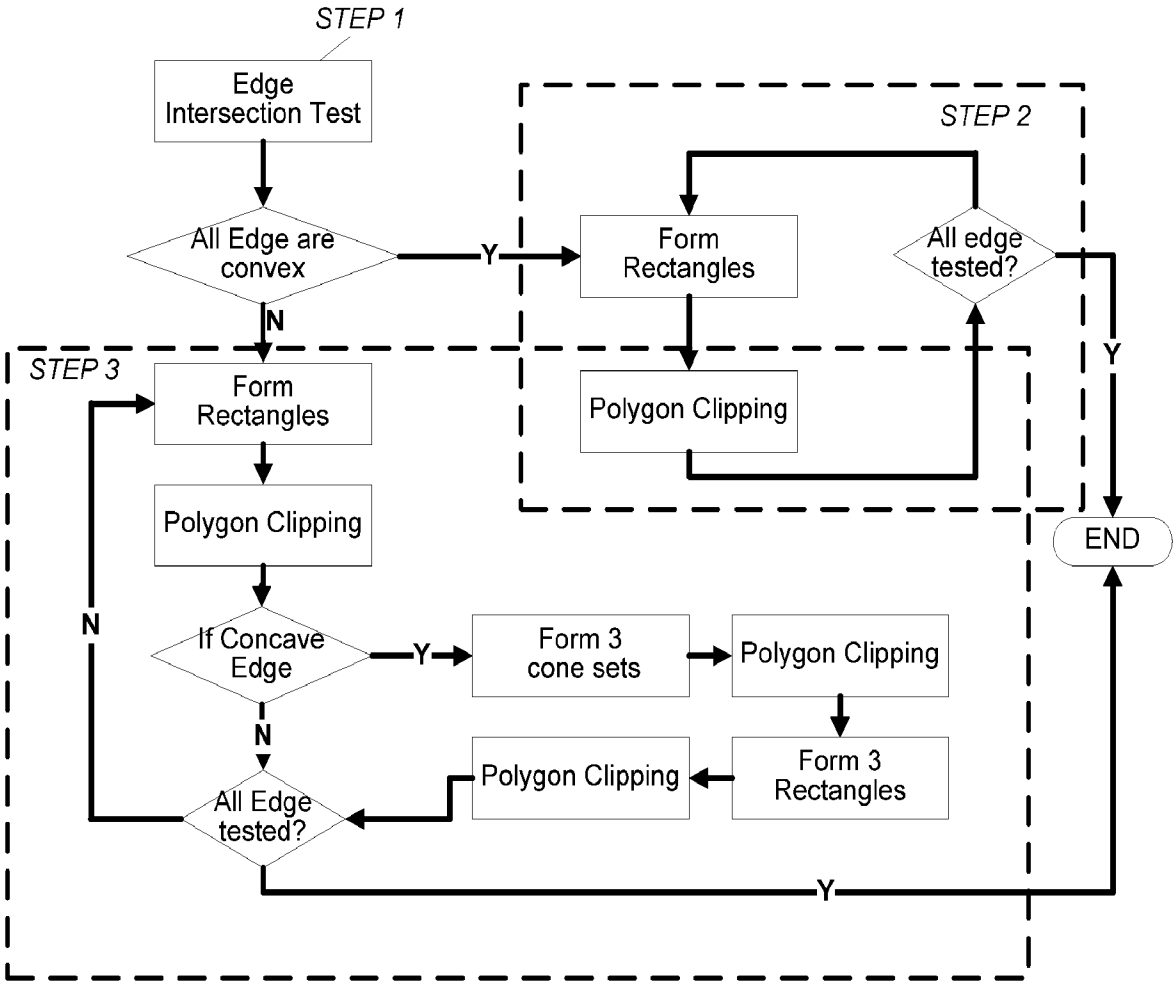
STEP 1
Edge Intersection Test
All Edge are convex
Y
N
STEP 2
Form Rectangles
Polygon Clipping
All edge tested?
Y
END
STEP 3
Form Rectangles
Polygon Clipping
If Concave Edge
Y
Form 3 cone sets
Polygon Clipping
N
Form 3 Rectangles
Polygon Clipping
All Edge tested?
N
Y

FIGURE 23

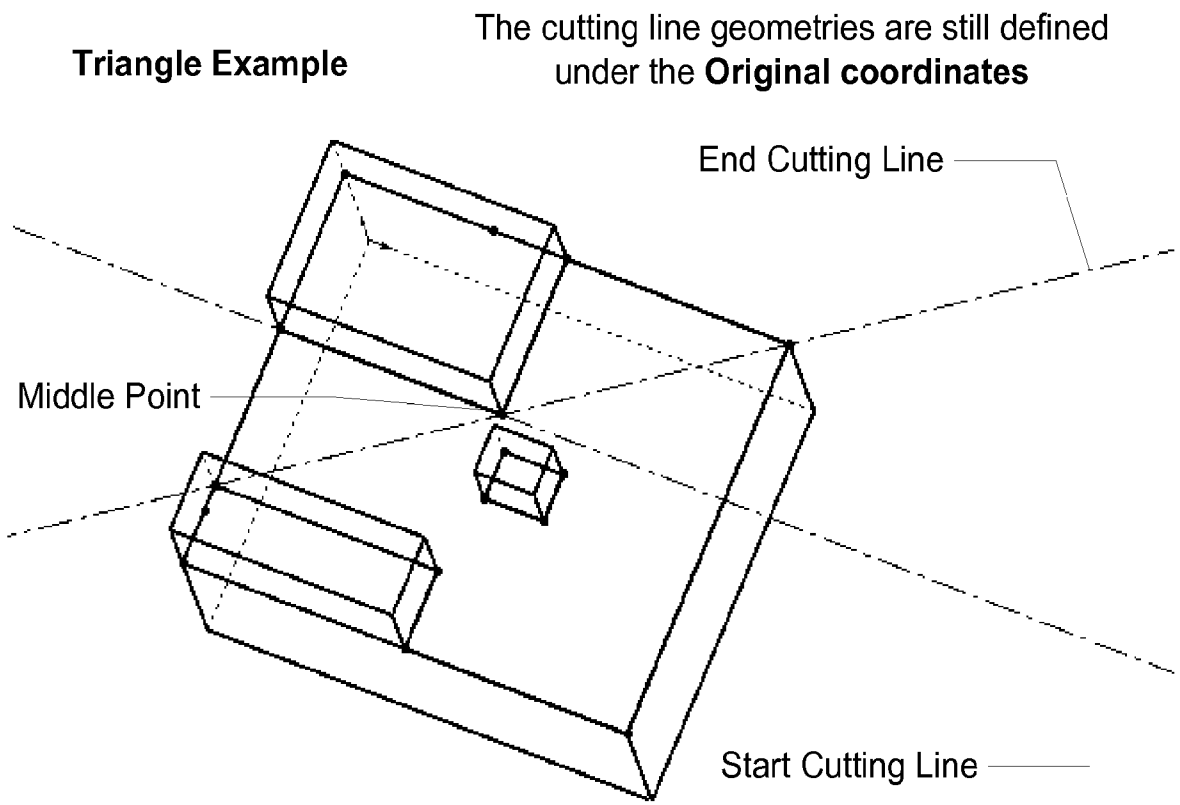
Triangle Example
The cutting line geometries are still defined under the **Original coordinates**
End Cutting Line
Middle Point
Start Cutting Line

FIGURE 24

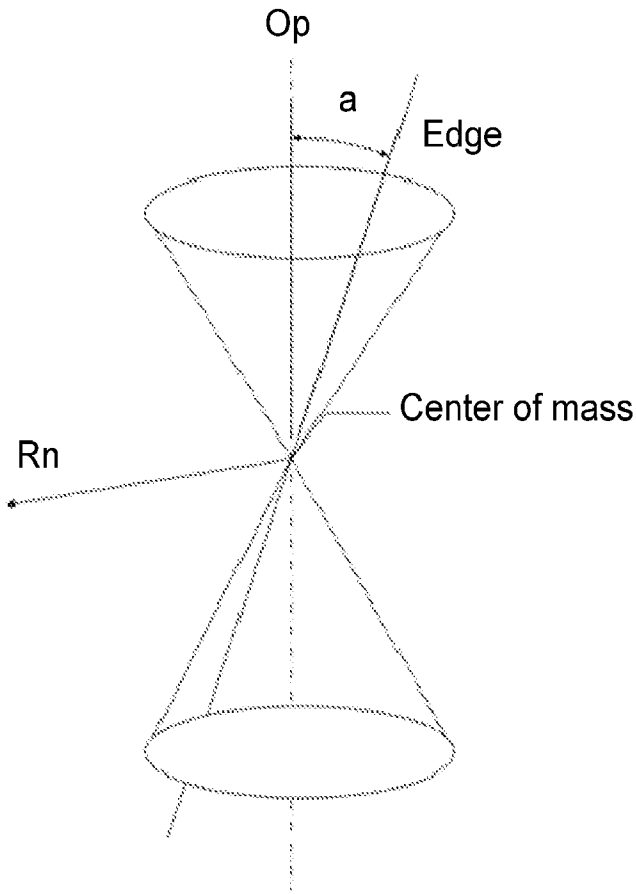

FIGURE 25

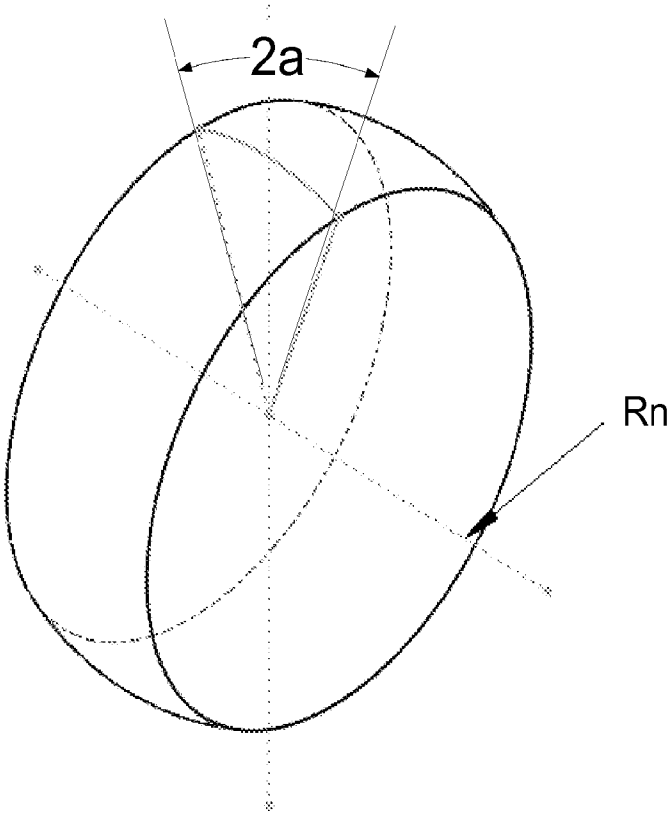

FIGURE 26

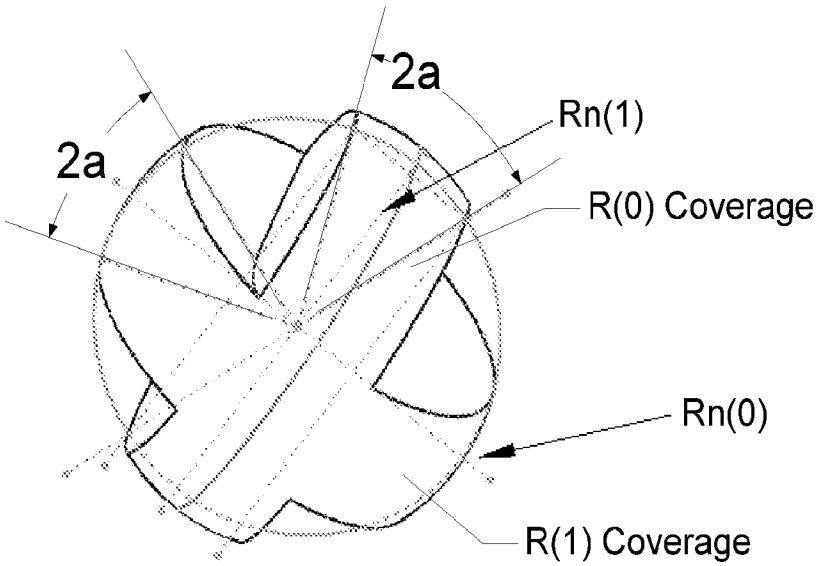

FIGURE 27

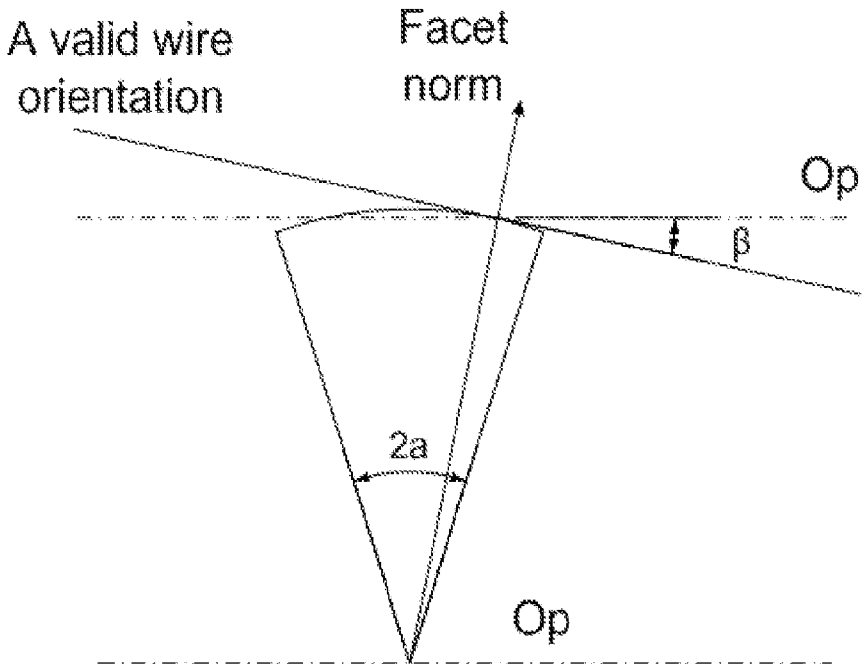

FIGURE 28

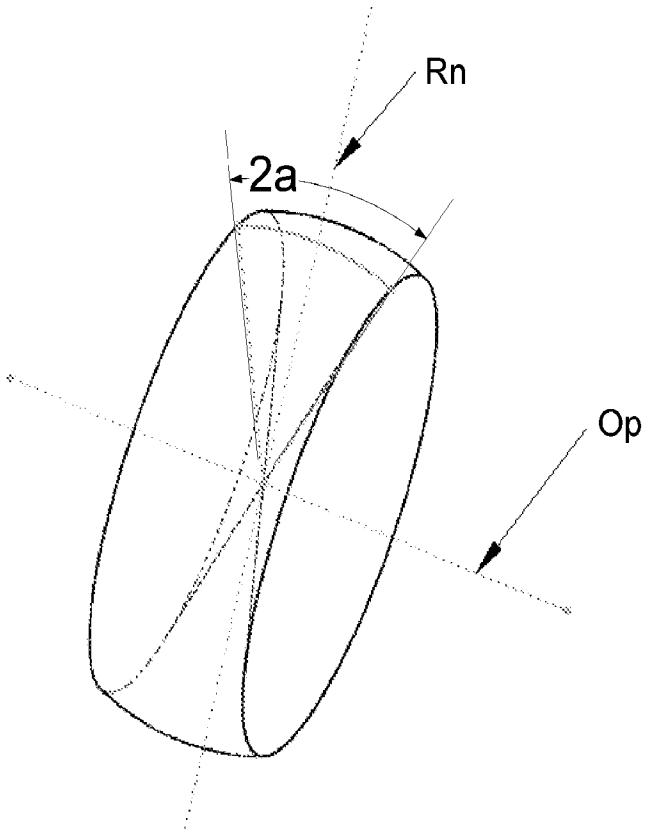

FIGURE 29

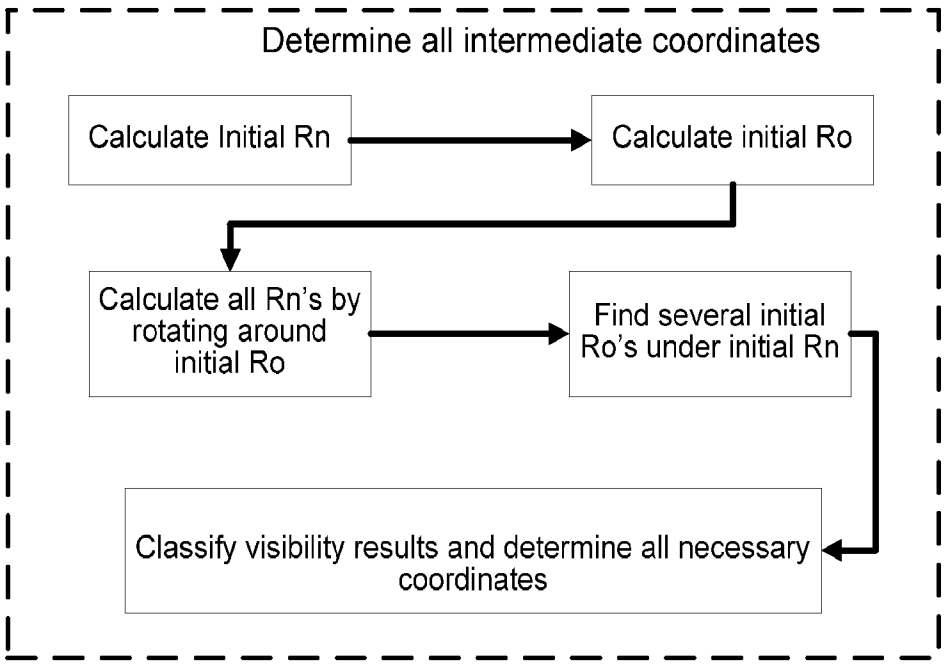

FIGURE 30

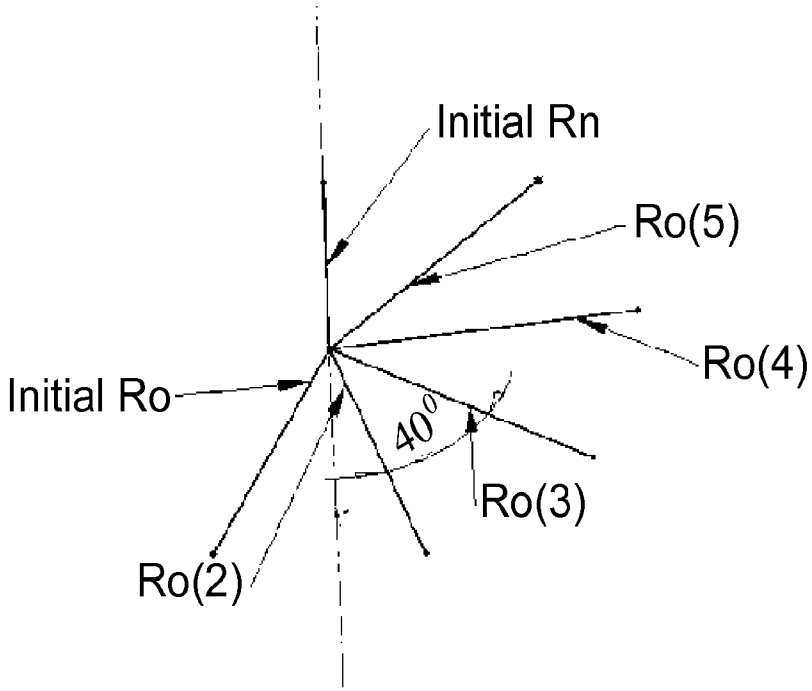

FIGURE 31

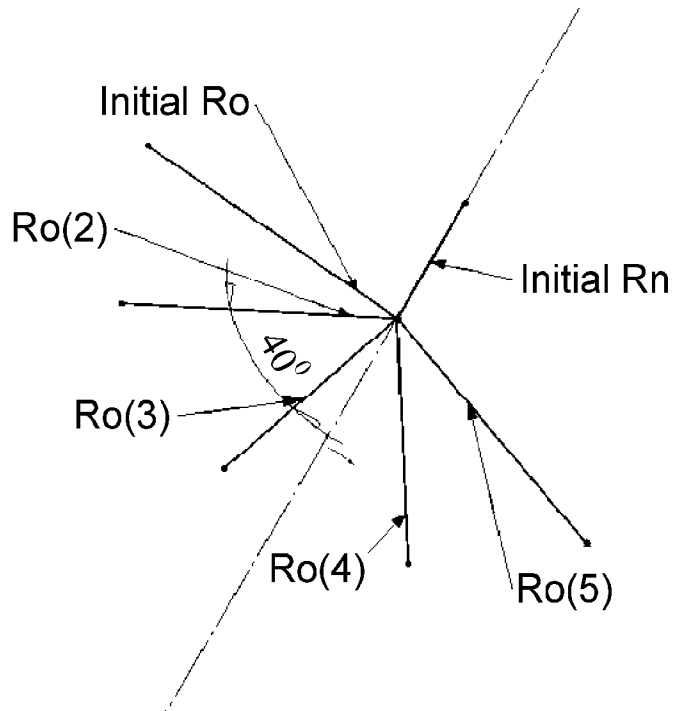

FIGURE 32

Calculate Initial Rn

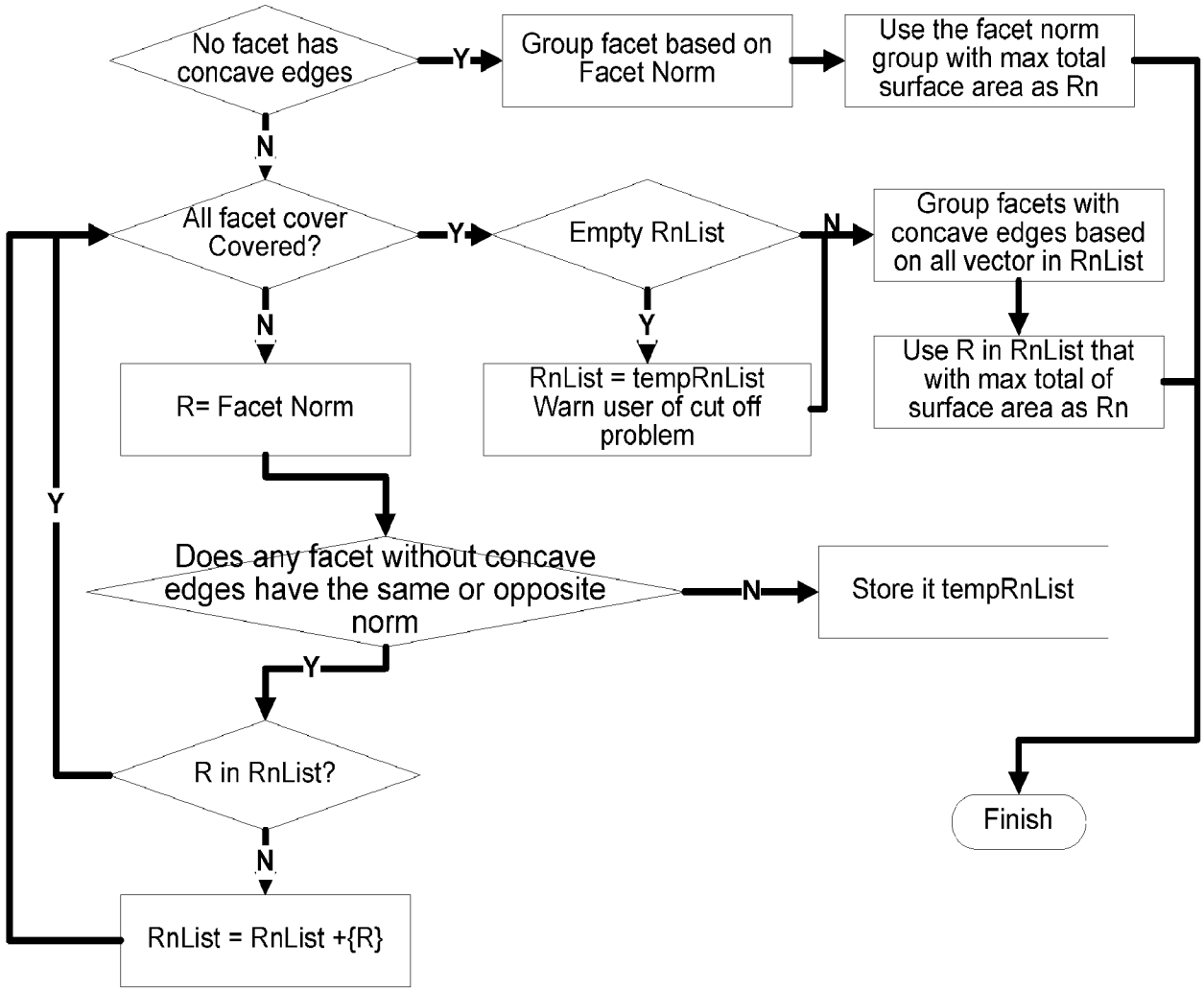

FIGURE 33

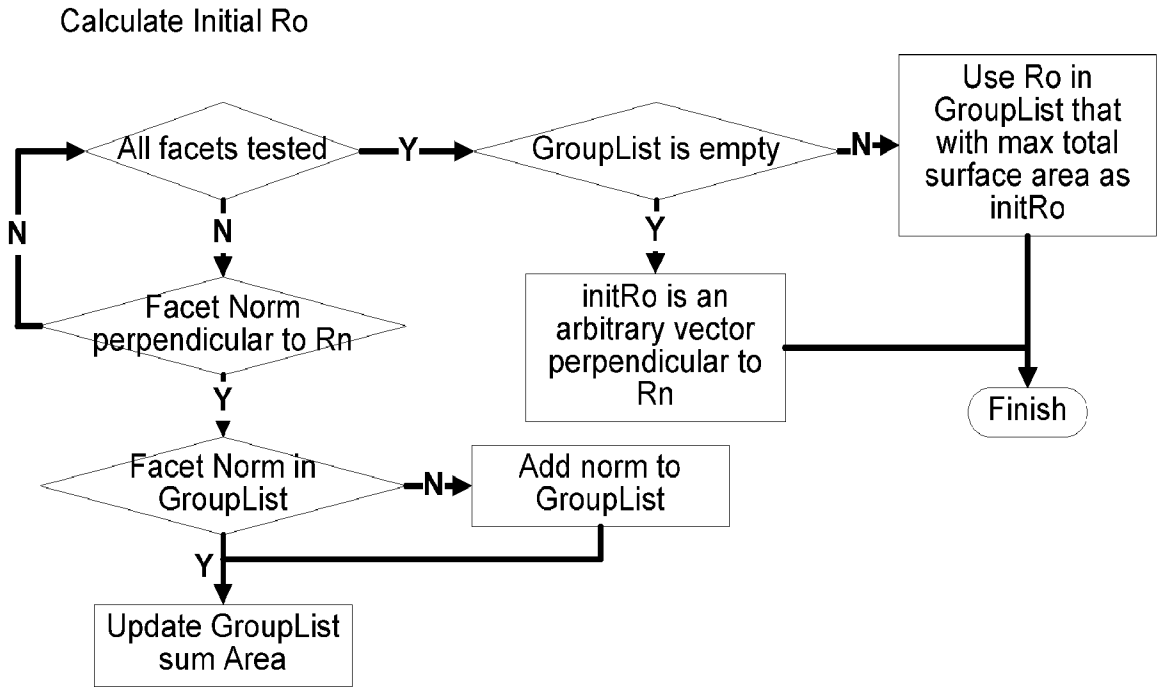
Calculate Initial Ro
All facets tested
Y
GroupList is empty
N
Use Ro in GroupList that with max total surface area as initRo
N
N
Y
Facet Norm perpendicular to Rn
initRo is an arbitrary vector perpendicular to Rn
Finish
Y
Facet Norm in GroupList
N
Add norm to GroupList
Y
Update GroupList sum Area

FIGURE 34

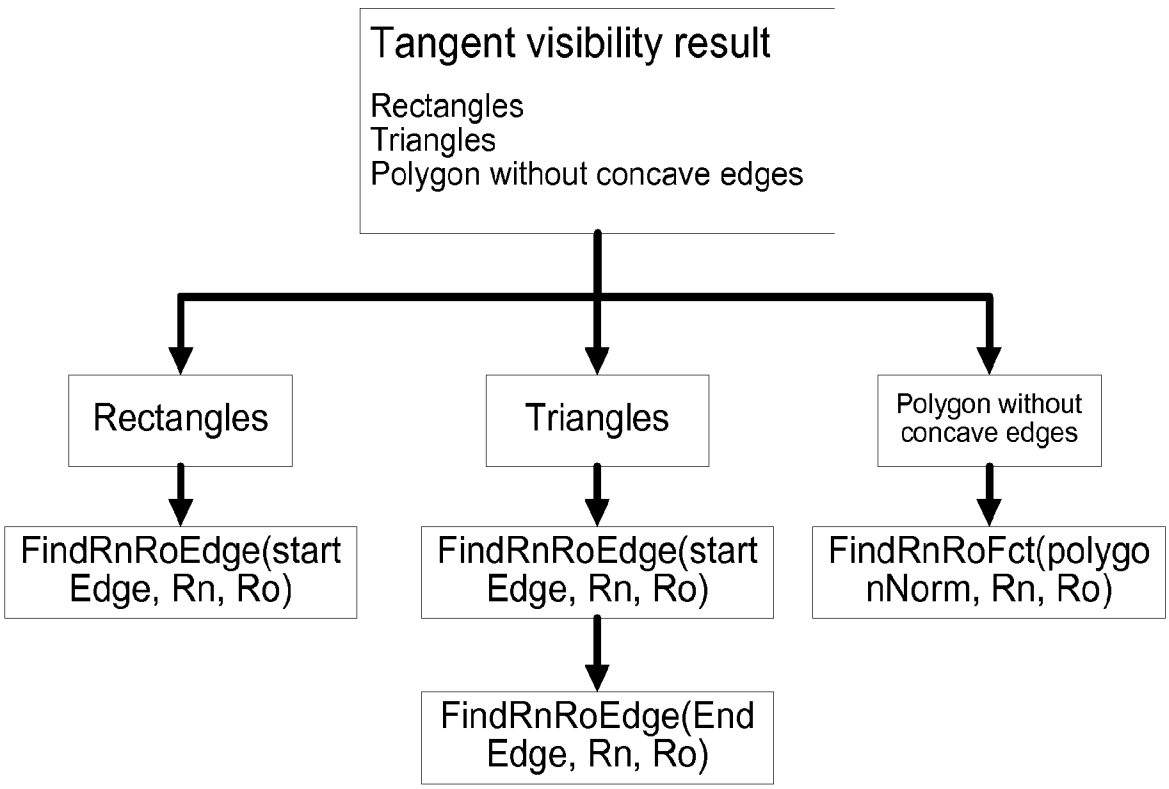
Tangent visibility result
Rectangles
Triangles
Polygon without concave edges
Rectangles
Triangles
Polygon without concave edges
FindRnRoEdge(start Edge, Rn, Ro)
FindRnRoEdge(start Edge, Rn, Ro)
FindRnRoFct(polygonNorm, Rn, Ro)
FindRnRoEdge(End Edge, Rn, Ro)

FIGURE 35

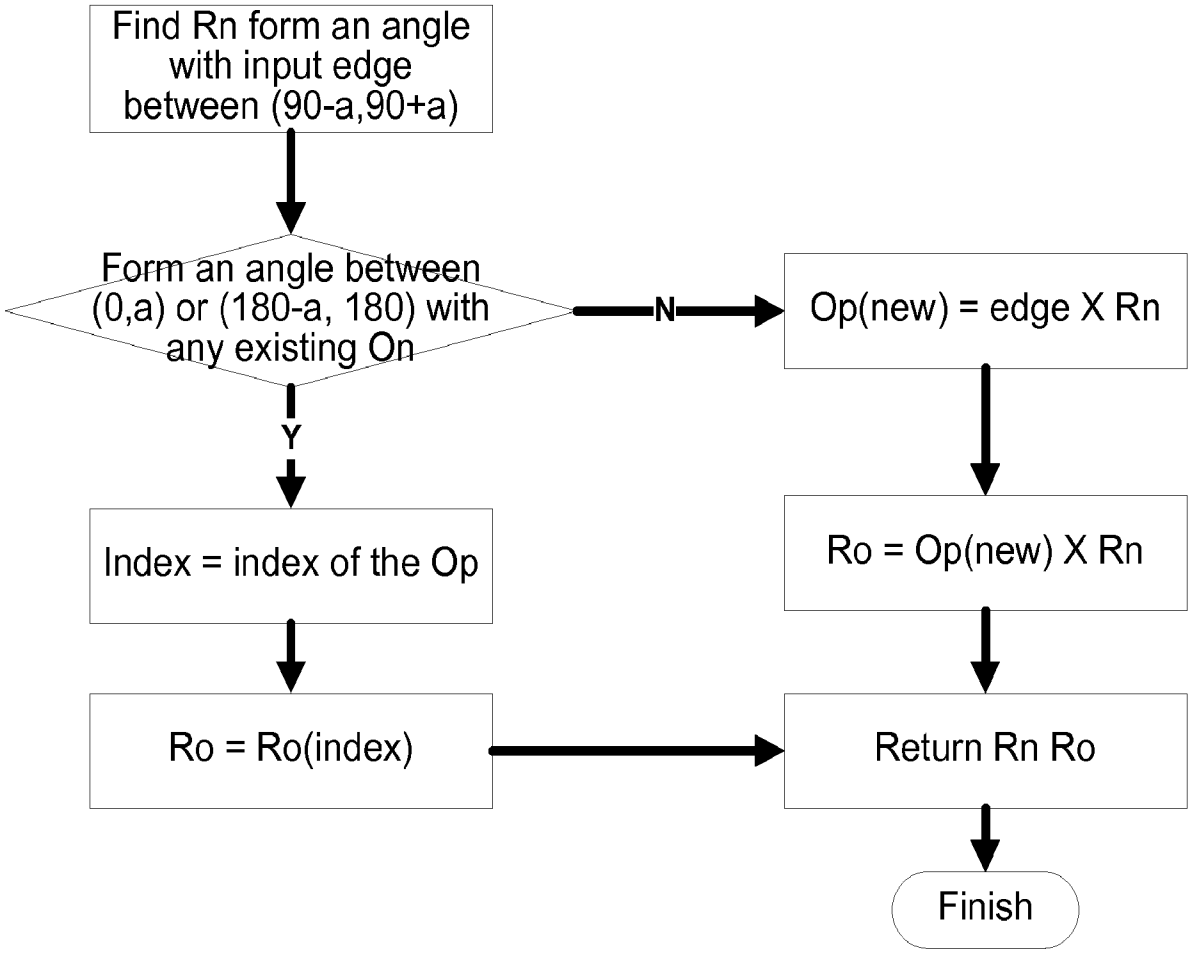

FIGURE 36

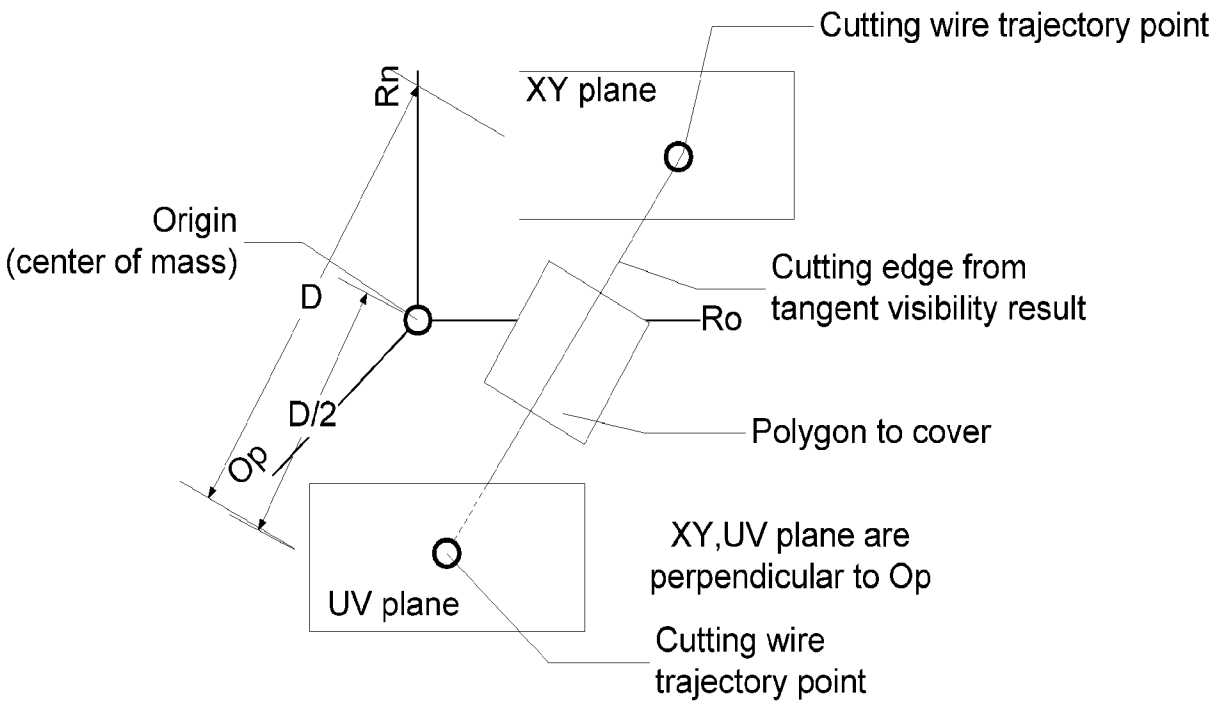
Cutting wire trajectory point
Rn
XY plane
Origin
(center of mass)
D
Cutting edge from
tangent visibility result
Ro
D/2
Op
Polygon to cover
XY,UV plane are
perpendicular to Op
UV plane
Cutting wire
trajectory point

FIGURE 37

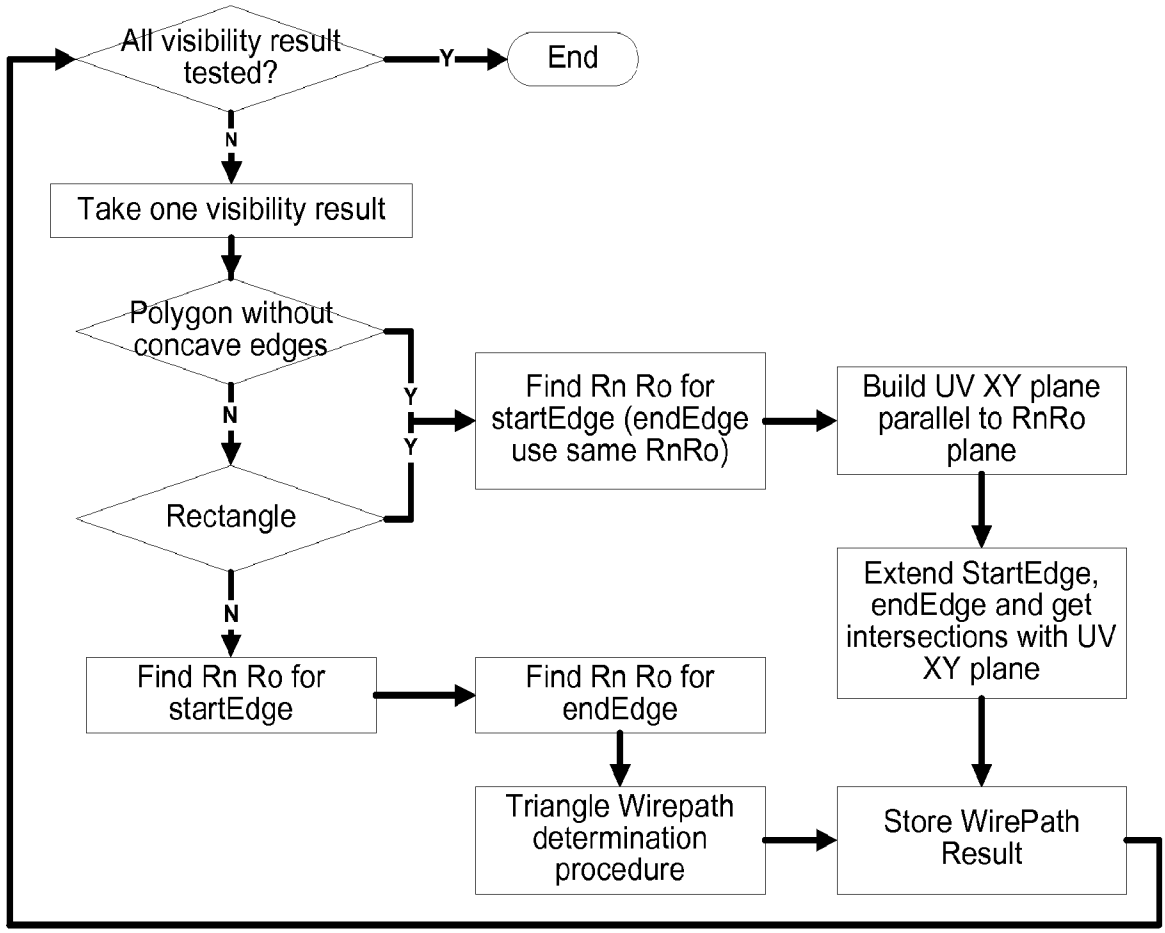
All visibility result tested?
Y
End
N
Take one visibility result
Polygon without concave edges
Y
N
Rectangle
Y
N
Find Rn Ro for startEdge (endEdge use same RnRo)
Build UV XY plane parallel to RnRo plane
Extend StartEdge, endEdge and get intersections with UV XY plane
Find Rn Ro for startEdge
Find Rn Ro for endEdge
Triangle Wirepath determination procedure
Store WirePath Result

FIGURE 38

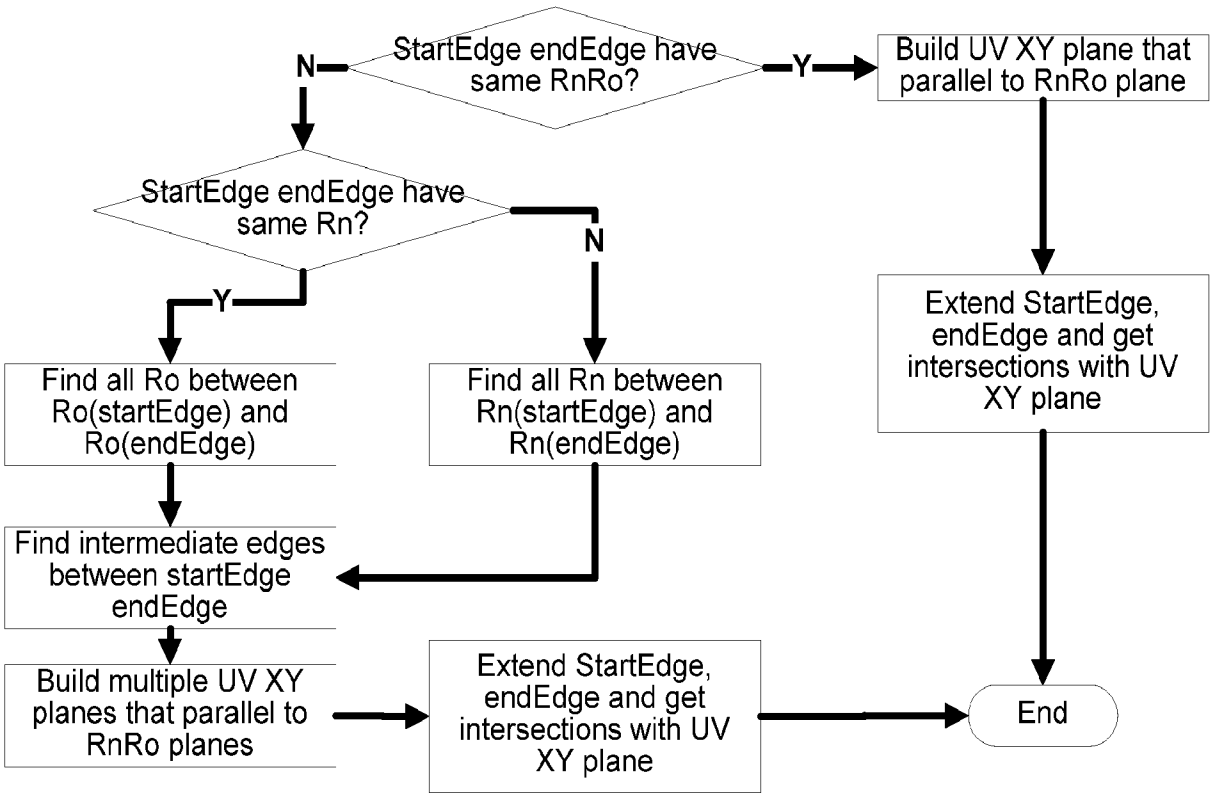
StartEdge endEdge have same RnRo?
N
Y
Build UV XY plane that parallel to RnRo plane
StartEdge endEdge have same Rn?
N
Y
Extend StartEdge, endEdge and get intersections with UV XY plane
Find all Ro between Ro(startEdge) and Ro(endEdge)
Find all Rn between Rn(startEdge) and Rn(endEdge)
Find intermediate edges between startEdge endEdge
Build multiple UV XY planes that parallel to RnRo planes
Extend StartEdge, endEdge and get intersections with UV XY plane
End

FIGURE 39

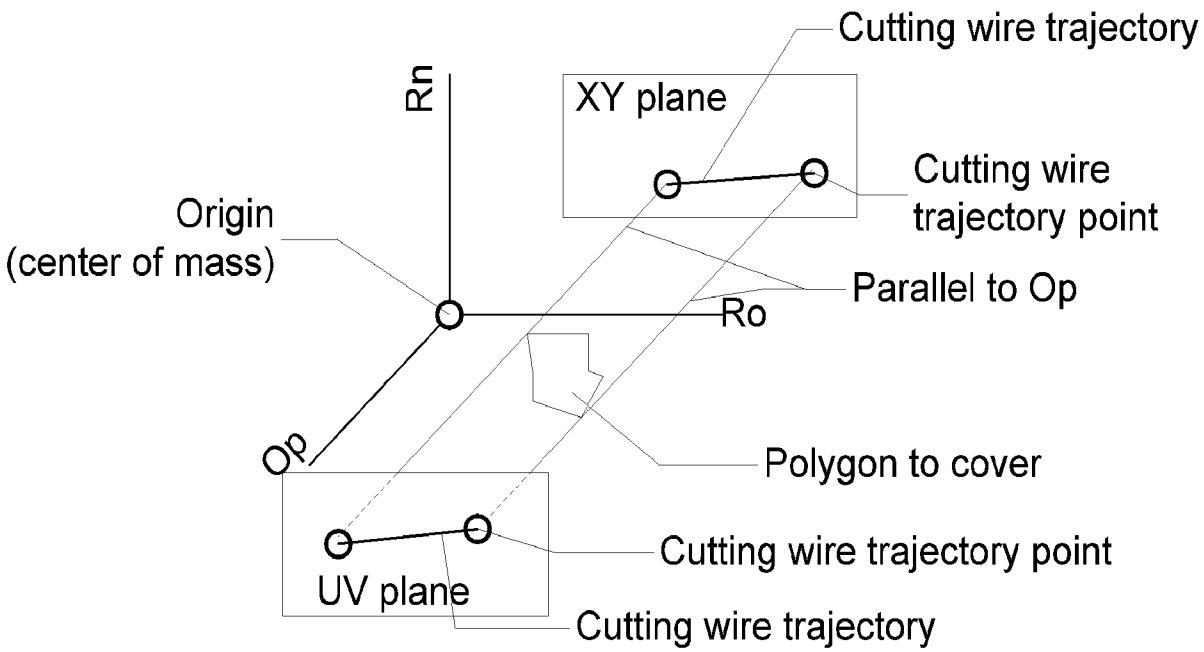
Cutting wire trajectory
Rn
XY plane
Cutting wire trajectory point
Origin (center of mass)
Parallel to Op
Ro
Op
Polygon to cover
Cutting wire trajectory point
UV plane
Cutting wire trajectory

FIGURE 40

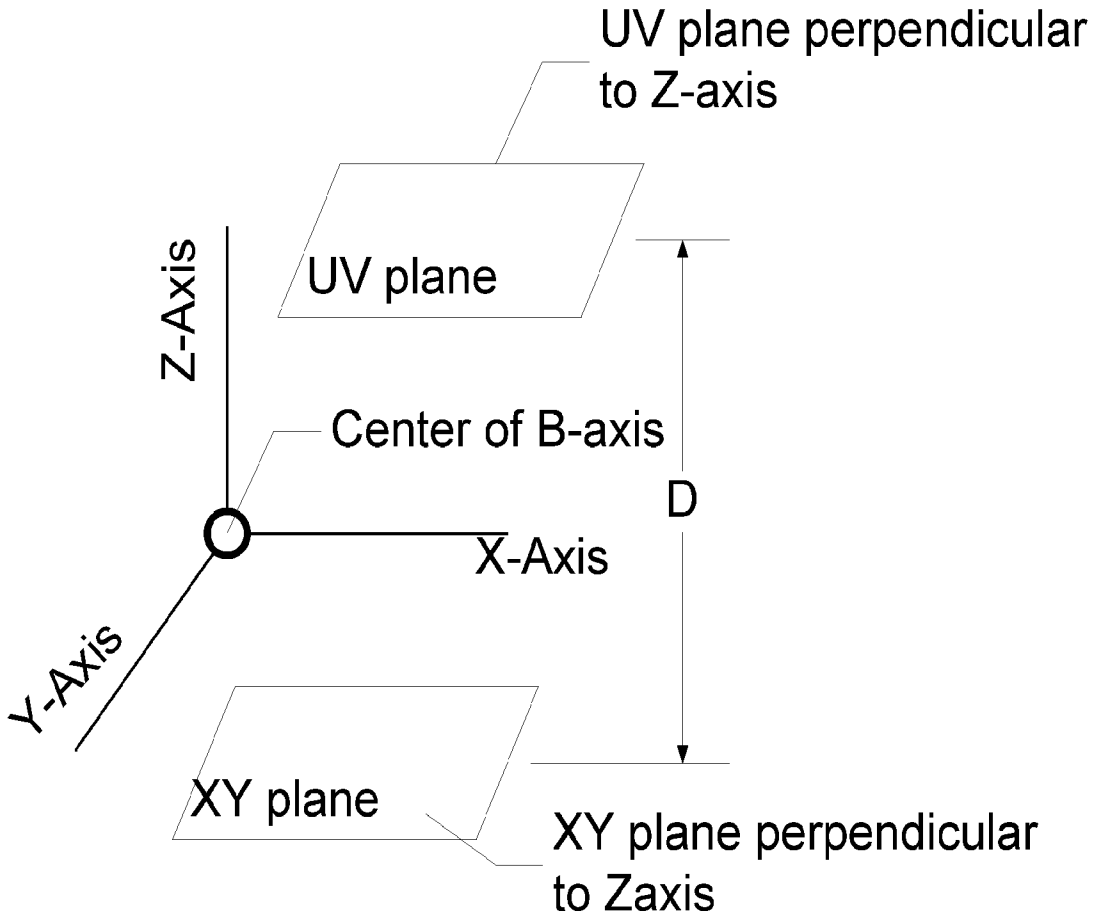

FIGURE 41

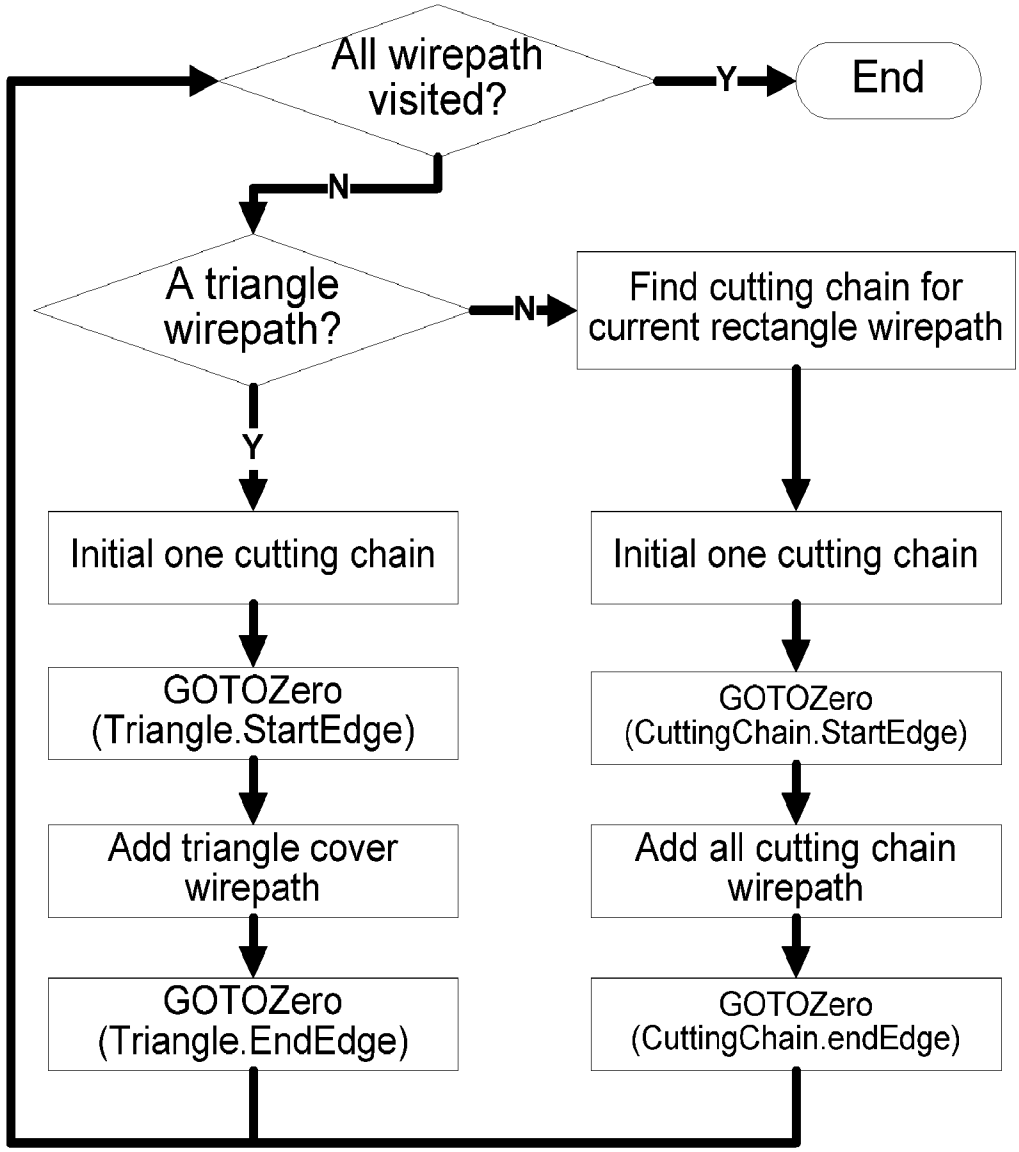
All wirepath visited?
Y
End
N
A triangle wirepath?
N
Find cutting chain for current rectangle wirepath
Y
Initial one cutting chain
Initial one cutting chain
GOTOZero (Triangle.StartEdge)
GOTOZero (CuttingChain.StartEdge)
Add triangle cover wirepath
Add all cutting chain wirepath
GOTOZero (Triangle.EndEdge)
GOTOZero (CuttingChain.endEdge)

FIGURE 42

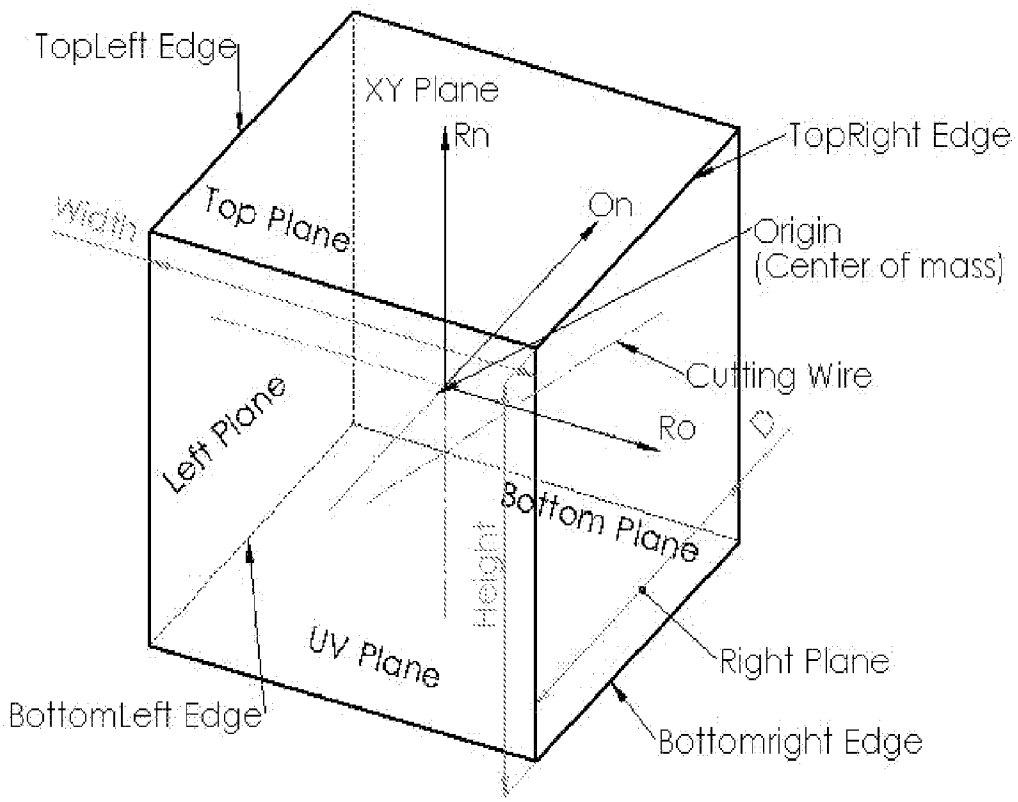
TopLeft Edge
XY Plane
Rn
TopRight Edge
On
Width
Top Plane
Origin
(Center of mass)
Cutting Wire
Ro
Left Plane
Bottom Plane
Height
UV Plane
Right Plane
BottomLeft Edge
Bottomright Edge

FIGURE 43

Input: cutting chain edges
Norm = the norm of the facet that start(end) edge on.
2 types of chains:
1. Chains start and end with convex surface
2. Otherwise.

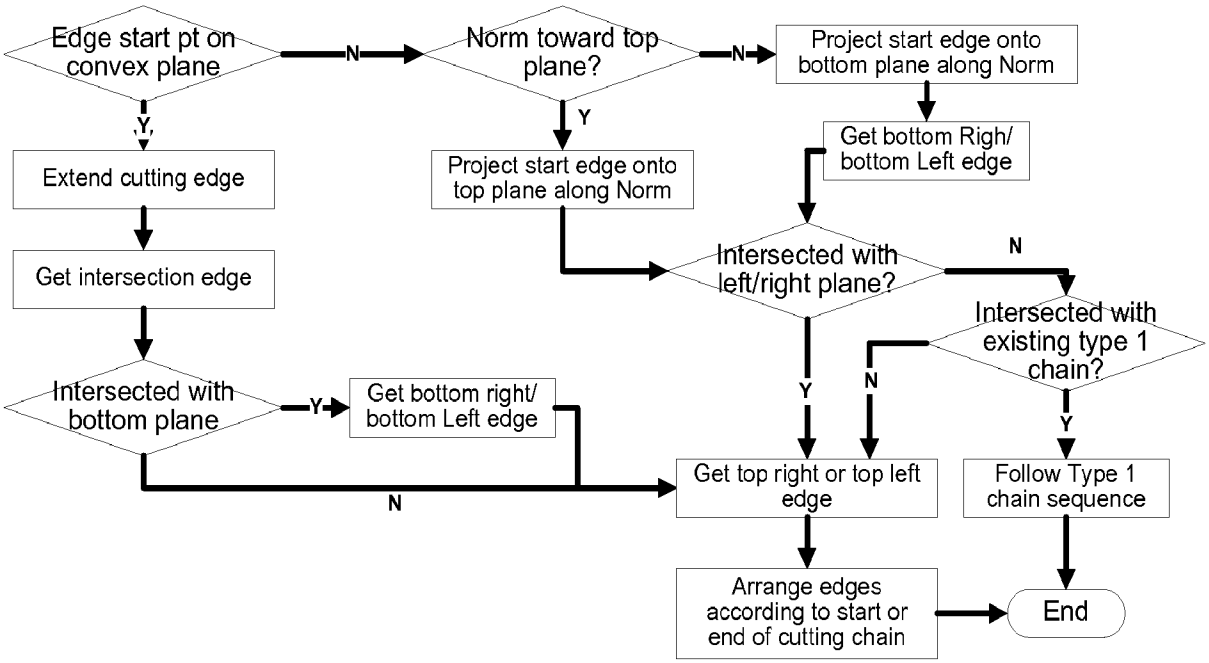

For start of cutting chain, we add the edge sequence:
top right/top left edge →....→start edge
For end of cutting chain, we add the edge sequence
End edge...→ top right/top left edge

FIGURE 44

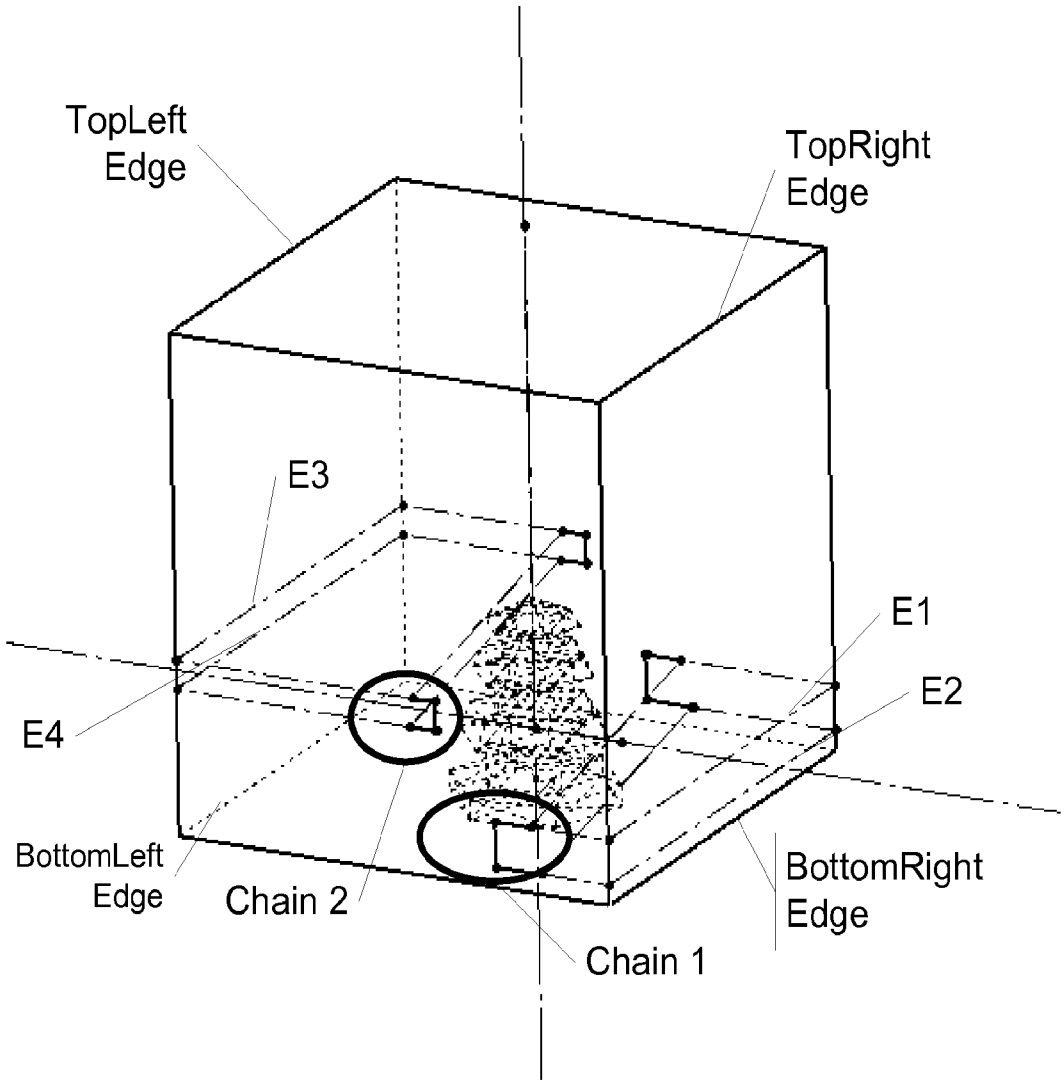
TopLeft
Edge
TopRight
Edge
E3
E1
E2
E4
BottomLeft
Edge
Chain 2
BottomRight
Edge
Chain 1

FIGURE 45

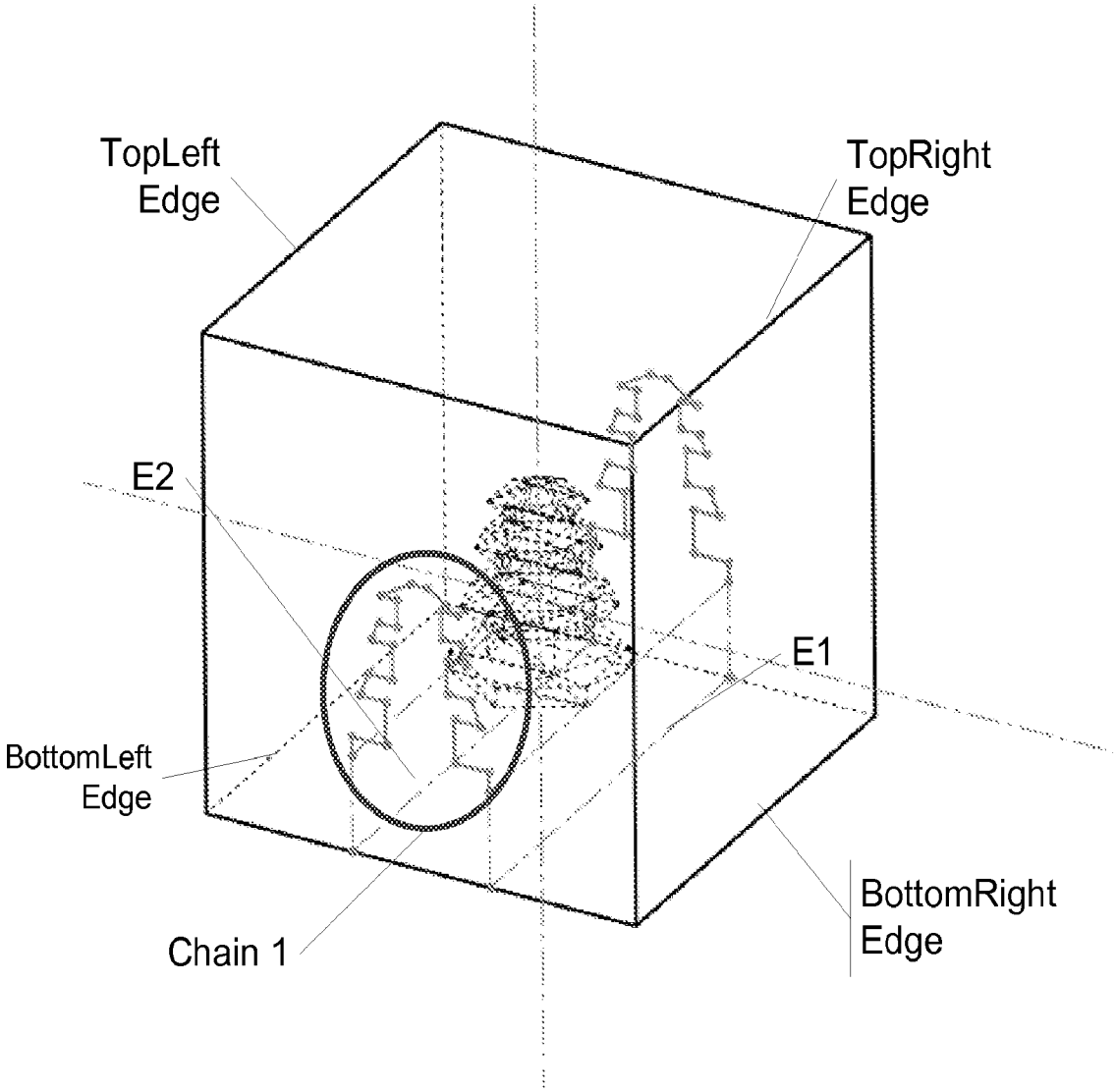
TopLeft
Edge
TopRight
Edge
E2
E1
BottomLeft
Edge
Chain 1
BottomRight
Edge

FIGURE 46

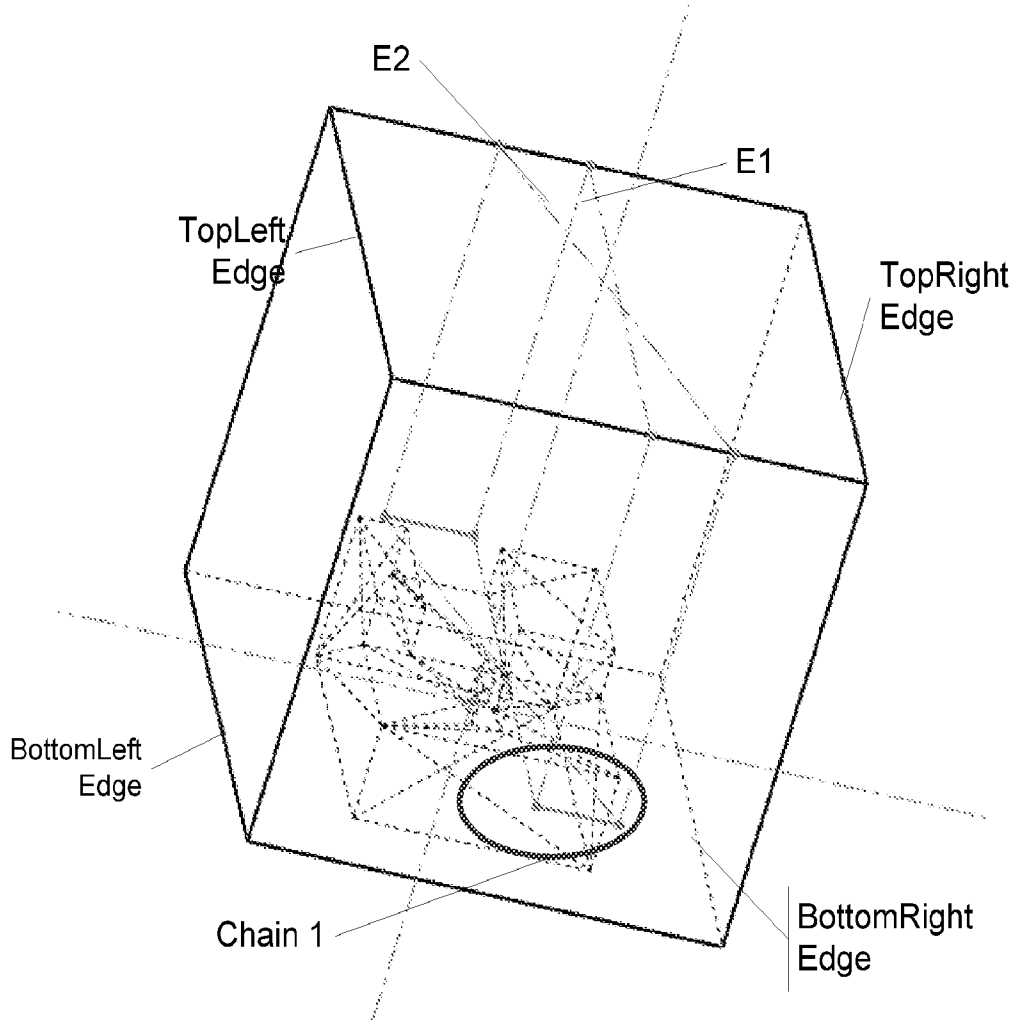
E2
E1
TopLeft Edge
TopRight Edge
BottomLeft Edge
Chain 1
BottomRight Edge

FIGURE 47

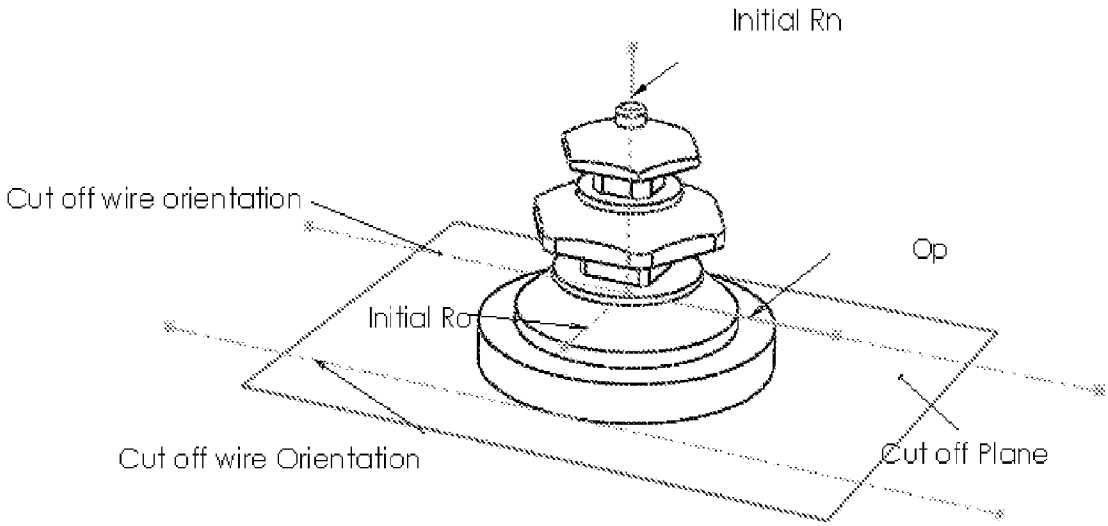

FIGURE 48

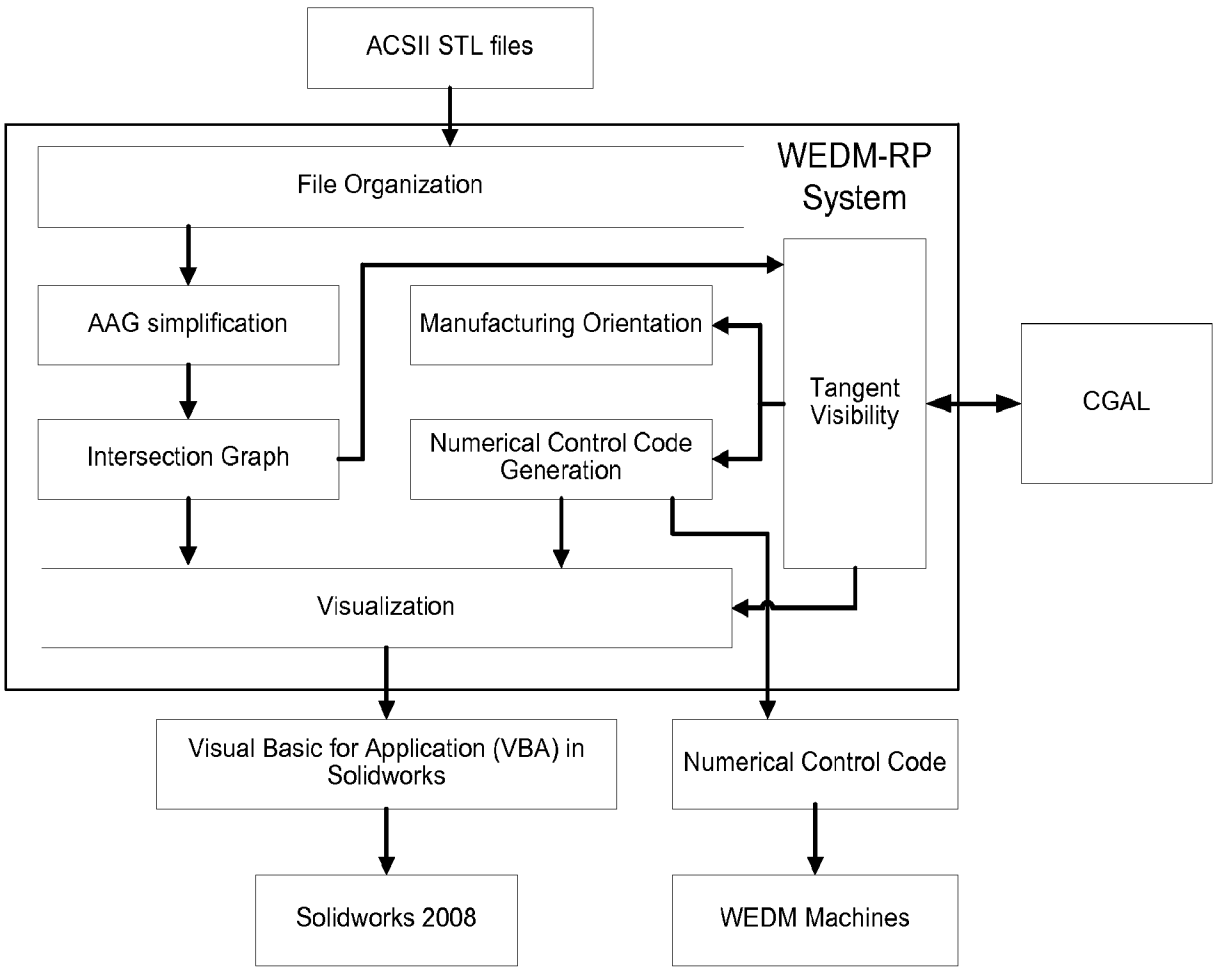

FIGURE 49

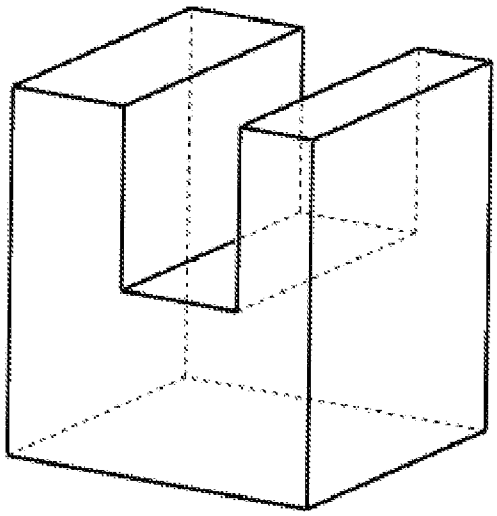

FIGURE 50

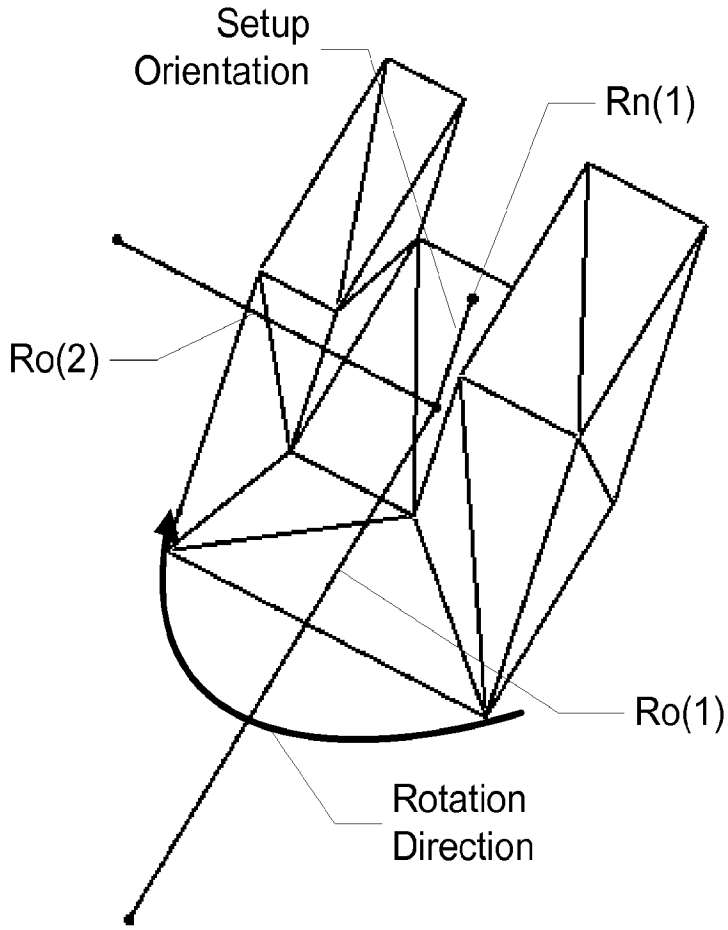

FIGURE 51

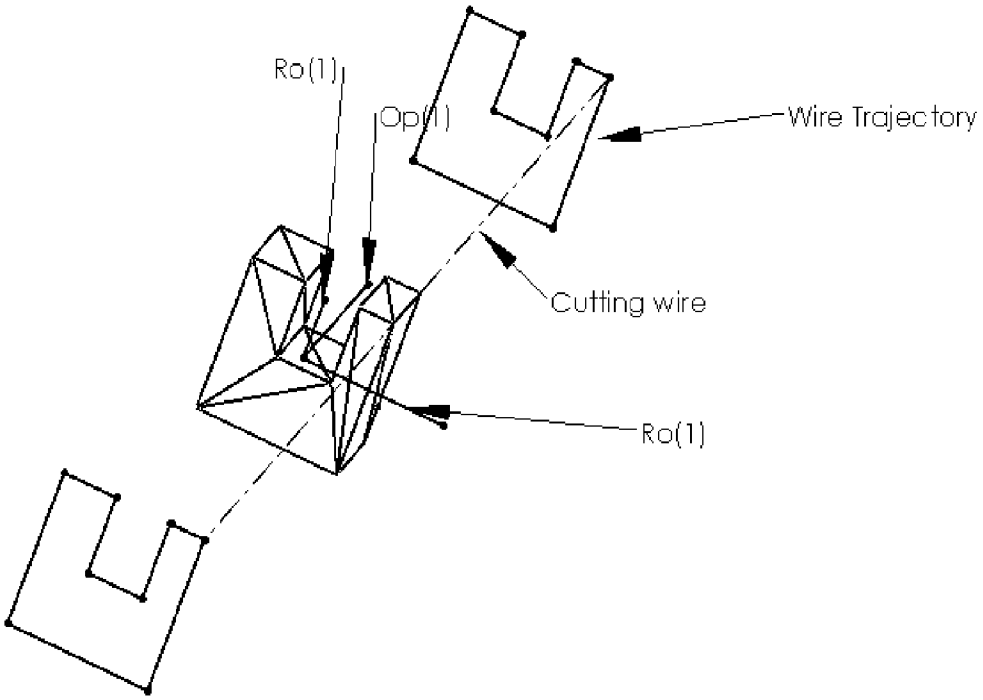

FIGURE 52

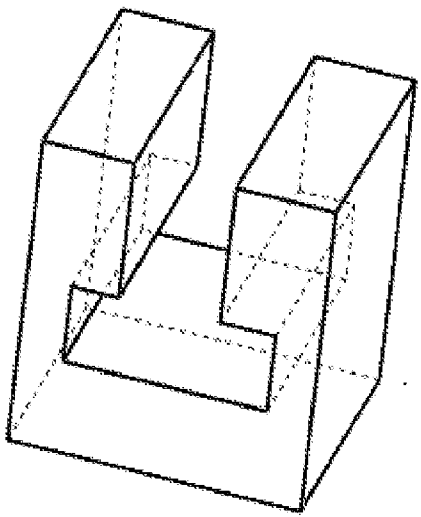

FIGURE 53

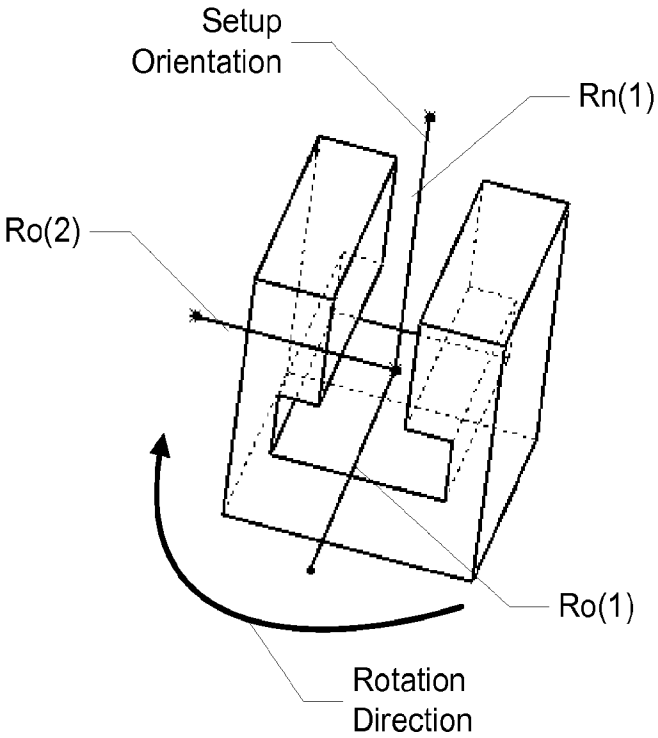

FIGURE 54

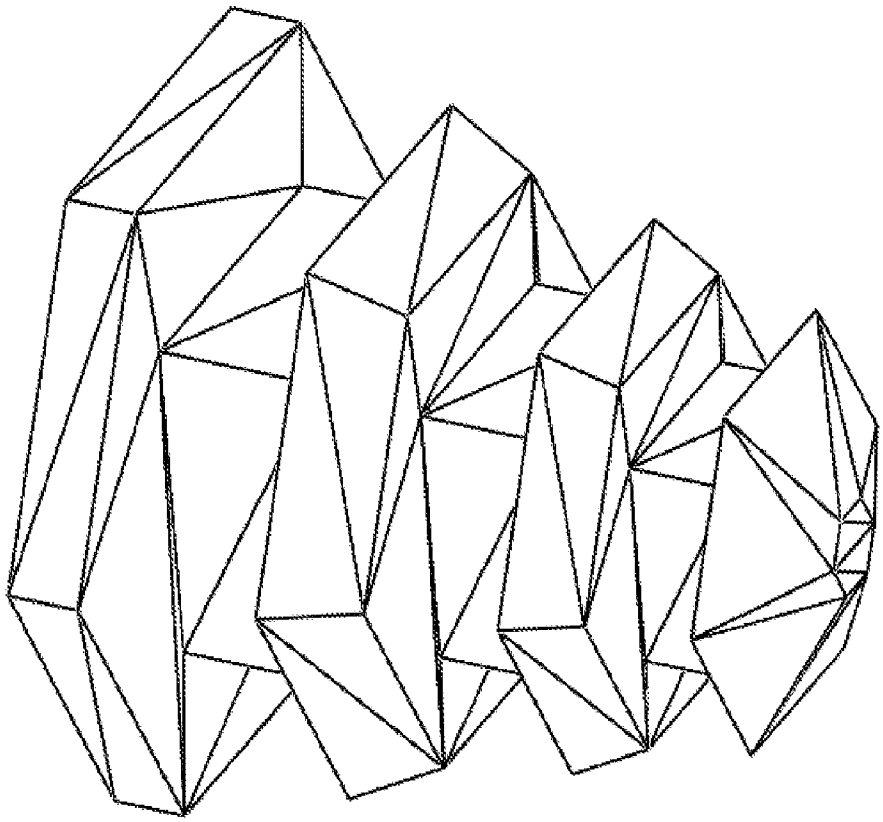

FIGURE 55

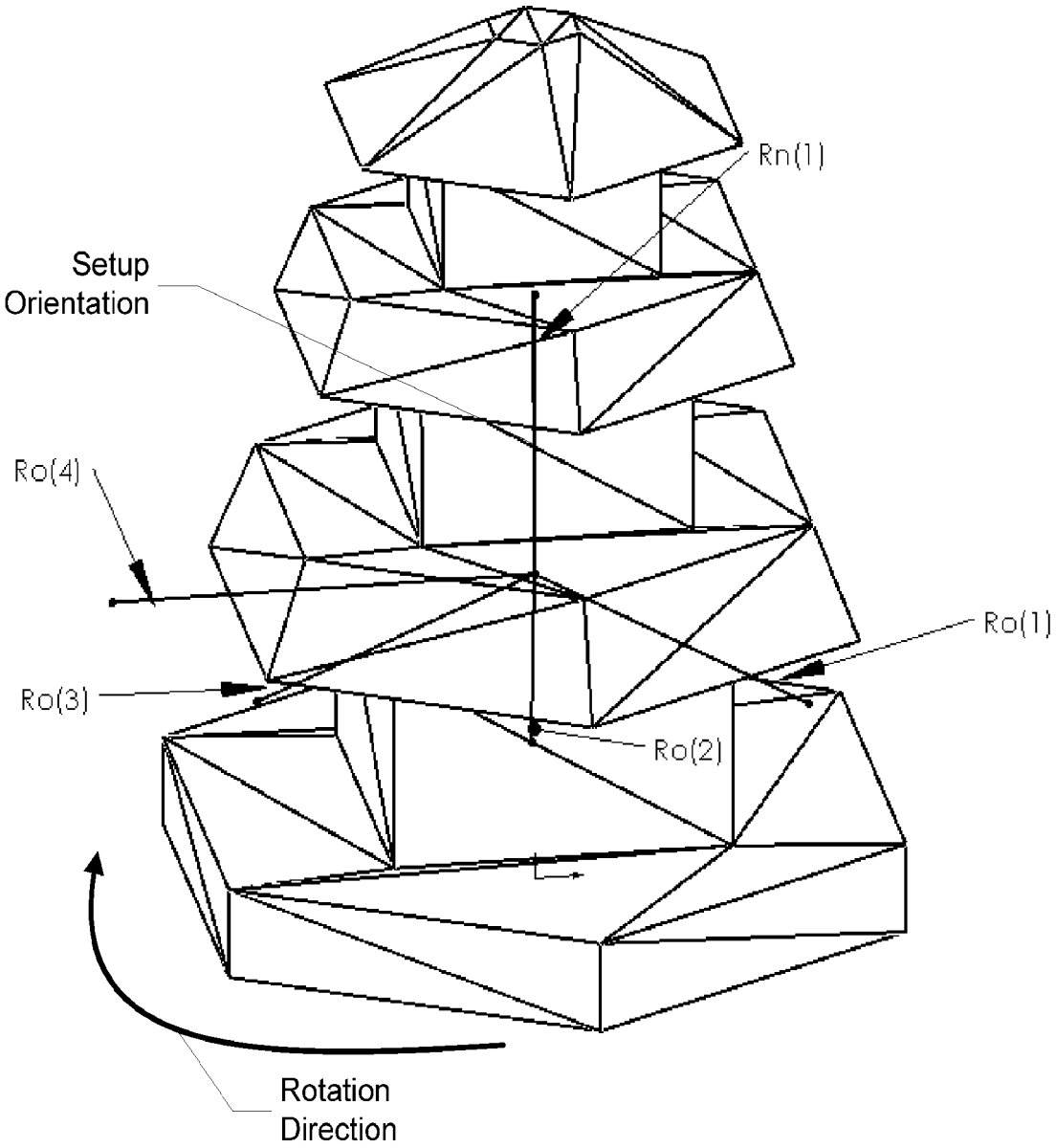

FIGURE 56

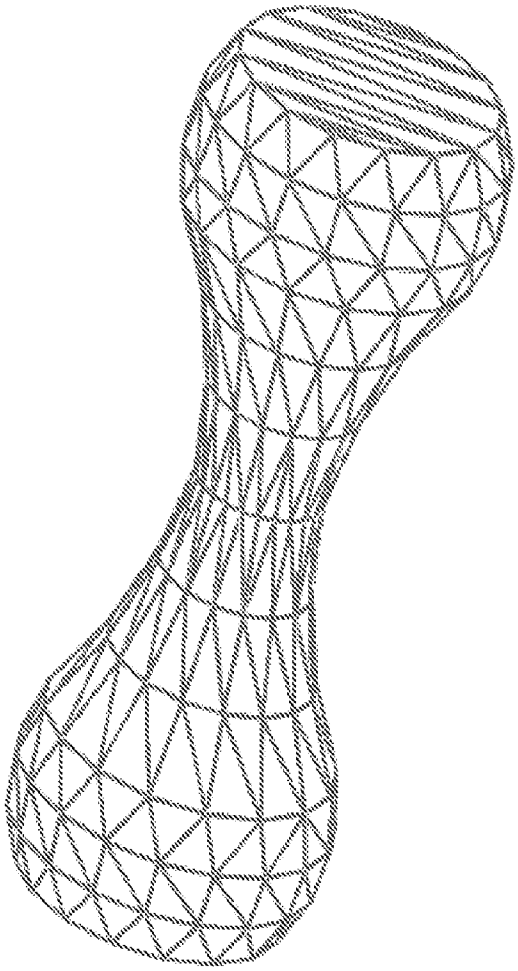

FIGURE 57

INTERNATIONAL SEARCH REPORT

International application No
PCT/US2010/024274

A. CLASSIFICATION OF SUBJECT MATTER
INV. G05B19/4099 B23H7/06
ADD.

According to International Patent Classification (IPC) or to both national classification and IPC

B. FIELDS SEARCHED

Minimum documentation searched (classification system followed by classification symbols)
G05B B23H

Documentation searched other than minimum documentation to the extent that such documents are included in the fields searched

Electronic data base consulted during the international search (name of data base and, where practical, search terms used)
EPO-Internal, WPI Data

C. DOCUMENTS CONSIDERED TO BE RELEVANT

Category*	Citation of document, with indication, where appropriate, of the relevant passages	Relevant to claim No.
X	BOXLER J: "PLATINEN-SCHEIDWERKZEUGE FUER KLEINE STUECKZAHLEN" VDI Z, SPRINGER VDI VERLAG, DE, vol. 132, no. 10, 1 October 1990 (1990-10-01), pages 116,119-122, XP000165981 ISSN: 0042-1766 the whole document	1-3
X	US 6 627 835 B1 (CHUNG CHAN WOO [US] ET AL) 30 September 2003 (2003-09-30)	1-3
Y	column 4, line 60 - column 10, line 40 column 12, line 33 - line 43 figures 3-7	4-21

-/--

[X] Further documents are listed in the continuation of Box C.

[X] See patent family annex.

* Special categories of cited documents :

"A" document defining the general state of the art which is not considered to be of particular relevance

"E" earlier document but published on or after the international filing date

"L" document which may throw doubts on priority claim(s) or which is cited to establish the publication date of another citation or other special reason (as specified)

"O" document referring to an oral disclosure, use, exhibition or other means

"P" document published prior to the international filing date but later than the priority date claimed

"T" later document published after the international filing date or priority date and not in conflict with the application but cited to understand the principle or theory underlying the invention

"X" document of particular relevance; the claimed invention cannot be considered novel or cannot be considered to involve an inventive step when the document is taken alone

"Y" document of particular relevance; the claimed invention cannot be considered to involve an inventive step when the document is combined with one or more other such documents, such combination being obvious to a person skilled in the art.

"&" document member of the same patent family

Date of the actual completion of the international search	Date of mailing of the international search report
11 May 2010	20/05/2010

Name and mailing address of the ISA/	Authorized officer
European Patent Office, P.B. 5818 Patentlaan 2 NL – 2280 HV Rijswijk Tel. (+31-70) 340-2040, Fax: (+31-70) 340-3016	Marrone, Fabrizio

INTERNATIONAL SEARCH REPORT

International application No
PCT/US2010/024274

C(Continuation). DOCUMENTS CONSIDERED TO BE RELEVANT

Category*	Citation of document, with indication, where appropriate, of the relevant passages	Relevant to claim No.
Y	WOO T C: "VISIBILITY MAPS AND SPHERICAL ALGORITHMS" COMPUTER AIDED DESIGN, ELSEVIER PUBLISHERS BV., BARKING, GB LNKD- DOI:10.1016/0010-4485(94)90003-5, vol. 26, no. 1, 1 January 1994 (1994-01-01), pages 6-16, XP000423003 ISSN: 0010-4485 page 7, right-hand column, line 5 - page 8, left-hand column, line 22 page 12, right-hand column, line 1 - page 15, left-hand column, line 6 figures 9-11	4-21

INTERNATIONAL SEARCH REPORT

Information on patent family members

International application No
PCT/US2010/024274

Patent document cited in search report	Publication date	Patent family member(s)	Publication date
US 6627835	B1 30-09-2003	NONE	